Dynamical properties of fractal networks: Scaling, numerical simulations, and physical realizations

Tsuneyoshi Nakayama and Kousuke Yakubo

Department of Applied Physics, Hokkaido University, Sapporo 060, Japan

Raymond L. Orbach

Department of Physics, University of California, Riverside, California 92521

This article describes the advances that have been made over the past ten years on the problem of fracton excitations in fractal structures. The relevant systems to this subject are so numerous that focus is limited to a specific structure, the percolating network. Recent progress has followed three directions: scaling, numerical simulations, and experiment. In a happy coincidence, large-scale computations, especially those involving array processors, have become possible in recent years. Experimental techniques such as light- and neutron-scattering experiments have also been developed. Together, they form the basis for a review article useful as a guide to understanding these developments and for charting future research directions. In addition, new numerical simulation results for the dynamical properties of diluted antiferromagnets are presented and interpreted in terms of scaling arguments. The authors hope this article will bring the major advances and future issues facing this field into clearer focus, and will stimulate further research on the dynamical properties of random systems.

CONTENTS

 0034-6861/94/66(2)/381(63)/$11.30

I. INTRODUCTION

Over the decade a great deal of activity has been concentrated on understanding the nature of quantized excitations in fractal networks, such as their spatial and dynamical properties and their relationship to physical observables. In addition, the dynamics of fractal networks has been used as a model to aid the understanding of thermodynamic and transport properties of random physical systems. Progress has followed three directions: scaling theories, numerical simulations, and physical realizations. The first has proven remarkably useful for the physical interpretation of the dynamics of random systems, the second for dealing with the complexity of random systems, and the third for application of the ideas developed through scaling and numerical simulations. A happy coincidence arose with the possibility of large-scale computations, especially those involving array processors, together with the development of light-scattering and low-energy inelastic neutron-scattering experimental techniques to the point where measurements that elucidate microscopic mechanisms have become possible.

The purpose of this review is to describe the advances that have been made over the past ten years in this field. The relevant systems that have been investigated are so numerous that we shall focus on a specific structure for clarity: the percolating network. This is the random fractal most thoroughly studied, and one for which the most information is currently available. Although some of the physical systems that have been experimentally investigated most certainly do not map onto percolating networks (e.g., the aerogels), some certainly do (e.g., site-diluted antiferromagnets). However, even where the mapping is not technically correct, the insights into the physical properties of random systems afforded by examination of the properties of the percolation network will prove extraordinarily useful.

Work on the dynamics of a percolating network received its most important promotion in the pioneering paper of de Gennes (1976b). He formulated the problem as follows: *an ant parachutes down onto a site on the percolation network and executes random walk. What is the mean-square distance the ant traverses as a function of time?* By applying the scaling theory to this problem, Gefen, Aharony, and Alexander (1983) developed the concept of a range-dependent diffusion constant on the percolation network, introducing an exponent θ so that the diffusion constant, for length scales r less than the percolation correlation length, scales as $r^{-\theta}$.

This insight, together with the realization that solving the problem of diffusion was equivalent to solving the (scalar) elastic vibration problem (Montroll and Potts, 1955; Alexander *et al.*, 1981), led Alexander and Orbach (1982) and Rammal and Toulouse (1983) to evaluate the density of states (DOS) for vibrations of a percolation network with the introduction of the fracton dimension $\tilde{d}$. This quantity was a specific combination of θ and the fractal dimension D_f. It should be noted that the DOS had in fact already been calculated for magnetic systems by Shender (1976a, 1976b) and, independently for deterministic fractals, by Dhar (1977). In particular, they showed that the DOSs are characterized by a new exponent. Alexander and Orbach (1982) determined the DOS and the dispersion relation for vibrational excitations of a fractal lattice, which they termed fractons, in terms of the fracton and fractal dimensions. The concept of crossover was introduced: at long length scales, the vibrational excitations were (softened) phonons with a linear dispersion law; whereas at length scales less than a crossover length scale (the percolation correlation length for percolating networks), corresponding to frequencies greater than an analogous crossover frequency, the vibrational excitations were fractons with their own vibrational dispersion law.

In addition, Alexander and Orbach (1982) noted that the fracton dimension for percolation networks was numerically remarkably close to the mean-field value, 4/3 (exact in Euclidean dimension $d=6$), for all dimensions greater than one, even though θ and the fractal dimension D_f were by no means constant as a function of dimension. This numerical evidence led them to speculate that the fracton dimension might be exactly 4/3 for percolation networks for $d \geq 2$. This has come to be known as the Alexander-Orbach conjecture. It is important because, if true, it would allow the conductivity exponent to be evaluated in terms of static exponents. Recent numerical simulations, considerably more powerful, show that the conjecture is only approximate, though the values found for the fracton dimension continue to be remarkably close to 4/3 for $d \geq 2$.

Immediately after this work appeared, Rammal and Toulouse (1983) developed an analogous scaling method to calculate the vibrational density of states and the mean number of sites visited by de Gennes's "ant" during the random walk on a fractal network. From this result, they were able to use the scaling theory of localization to establish that fractons are localized for fracton dimensions less than two (see Sec. IV.B.1).

Scaling has proven to be a very valuable tool for obtaining insight into the dynamical properties of fractal structures. However, it has its limitations. In particular, it is useful for ensemble averages of a physical quantity. However, when products or matrix elements of physical quantities are involved, it is by no means obvious (and, in general, it is untrue) that the product or matrix element of the individual ensemble average has any relationship to the ensemble average of the product or matrix element. This sharply limits the utility of scaling assumptions, though of course one might hope that any final result would exhibit scaling properties. The problem with random systems is that, without the use of average quantities, fluctuations in general preclude the computation of observables obtainable experimentally, this being the ultimate goal for any microscopic theory. Instead, one must resort to ensemble averages of numerical simulations.

Fortunately, results obtained from such methods do appear to obey scaling. There are two types of scaling arguments: one actually computes critical exponents, and the other can be used to find relations between different exponents. The latter perspective is the one mainly used in the subject related to this review. Again, one must resort to numerical simulations to obtain the values of the critical exponents.

The scaling predictions of Alexander and Orbach (1982) for the vibrational density of states were first subjected to scrutiny numerically by Grest and Webman (1984). They simulated the vibrations of a percolating network for a relatively small number of sites ($N < 2200$). Nonetheless, they were able to establish that the predicted crossover between the phonon and fracton density of states was, in fact, present, and that the latter was, to within their numerical accuracy, in accord with the Alexander-Orbach conjecture. The insights gained from this early work were very important for the direction of further research.

As the size of supercomputers increased, especially with the advent of array processors, the size of the percolating networks that could be simulated grew enormously (Yakubo and Nakayama, 1987a, 1987b). More than 10^6 sites are now possible, yielding a wealth of new results (and insights). Examples are the calculation of the density of states for fractons; the asymptotic form of the fracton wave function; matrix elements for inelastic light scattering in vibrating percolation networks; and the dynamical structure factor (see Secs. V.A and V.B).

Numerical simulations do more than simply verify physical assumptions: they point the way to a new qualitative understanding of the nature of excitations of strongly random structures, ultimately enabling the investigator to develop phenomenological expressions for physical quantities. Soon, these simulations will shed considerable light on the debate over the use of scaling for the interpretation of light-scattering experiments (Alexander, 1989; Alexander, Courtens, and Vacher, 1993), as well as be useful for the calculation of matrix elements for vibrational (hopping) transport processes. A quite natural question to ask is this: *are there physical realizations that justify extensive numerical efforts?* Fortunately, there are a number of physical systems exhibiting measurable dynamical properties that exhibit fractal geometry. Examples are site-diluted magnetic structures (spin-wave or magnon excitations crossing over to fracton magnetic excitations); silica aerogels (phonons, crossing over to fracton vibrational excitations); and glasses and amorphous materials (which, though certainly not fractals, appear to exhibit thermal transport properties that coincide with predictions from phonon-fracton dynamics).

The dynamical properties of these materials have been investigated by the measurement of the thermal conductivity and sound velocity, and by inelastic neutron- and light-scattering experiments. In general, where the connection with a theoretical model has been direct (e.g., the site-diluted antiferromagnet that maps onto the percolation network), detailed numerical agreement between theory and experiment has been found. Where the mapping is less direct (e.g., the silica aerogels), but where the fractal nature of the structure has been unequivocally verified (see Secs. V.C and VI.C), scaling theory seems adequate to represent the experimental data, though, of course, unable to predict the value of the exponents. In the case where the materials are certainly not fractals (e.g., glasses and amorphous materials), the relevance of a scaling model is less direct. Remarkably, a fractal model does appear to generate predictions for the higher temperature thermal transport and velocity of sound which appear to be consistent with experimental observations.

All three of these features—scaling, numerical computations, and physical realizations—are coming together at the present time. They provide a basis for a review article useful as a guide for understanding these developments and for charting future research directions. Our review begins in Sec. II with a detailed introduction to the properties of a percolating network. We study the dynamics of such a structure because it is a random fractal, and because so much analysis and understanding of its properties have been developed over the past few years. An excellent introduction to percolation theory is available (Bunde and Havlin, 1991; Stauffer and Aharony, 1992); so we shall only outline the most important features of this system. In Sec. III, we describe the solution of Gefen, Aharony, and Alexander (1983) for anomalous diffusion on a fractal network, with specific application to percolation. We then introduce the transform of Alexander and Orbach (1982) and develop the concept and application of the fracton dimension. The power and limitations of scaling are developed in Sec. IV, including the characteristic crossover length scale and frequency for sound waves and fractons, the dispersion relation, and the vibrational density of states. Physical realizations for the density of states are introduced in Sec. V.

The dynamical structure factor $S(\mathbf{q},\omega)$ gives rich information on the dynamics of fractal structures. We describe some features of $S(\mathbf{q},\omega)$ for lattice vibrations of fractal networks in Sec. VI, where the results of scattering experiments, scaling arguments, and simulations are given by illustrating silica aerogels. The density of states and the dynamical structure factor for diluted antiferromagnets are exhibited in Sec. VII. Inelastic neutron-scattering measurements of $S(\mathbf{q},\omega)$ by Uemura and Birgeneau (1986, 1987) allow a detailed comparison to be made between experiment and theory. Vibrational anharmonicity is introduced in Sec. VIII as a means for fracton hopping. The associated contribution to thermal transport and to the sound velocity is calculated. Comparison is made with thermal-conductivity measurements for the silica aerogels that exhibit fractal geometry, and for glasses and amorphous materials that do not. It is argued that, above a crossover frequency, all vibrational excitations of glasses or amorphous materials are localized, allowing the use of the hopping model. Comparison is

also made with sound velocity measurements on these materials. A detailed discussion is given of the magnitude of the anharmonic coupling constant extracted from these measurements. Very recent modeling experiments show enhanced anharmonicity in accord with the approach taken here.

Our summary and conclusions constitute Sec. IX. Section IX also outlines some important research opportunities which we feel are available in this field.

We believe that the unusual conjunction of scaling theory, numerical simulations, and physical realizations has created an exciting climate for theoretical and experimental investigation of the dynamics of random structures. We hope that this review will bring the major advances and issues facing this field into clearer focus, and that it will foster further research in the fascinating world of random systems.

II. PERCOLATING NETWORKS AS AN EXAMPLE OF A RANDOM FRACTAL

That the percolating network is a fundamental model for describing geometrical features of random systems and takes *fractal* (self-similar) structure was first noticed by Stanley (1977). The theory of percolation was formulated by Broadbent and Hammersley (1957) in connection with the diffusion of gases through porous media (Hammersley, 1983).[1] They developed the geometrical and probabilistic aspects of percolation. Soon after the paper by Broadbent and Hammersley (1957), Anderson (1958) and de Gennes, Lafore, and Millot (1959a, 1959b) pointed out the physical implications of percolation theory, and Domb and Sykes (1960) provided arguments supporting its critical behaviors. Since these works, it has been widely accepted that percolation theory can be used to interpret an exceptionally wide variety of physical and chemical phenomena. The concept of a fractal (Mandelbrot, 1975, 1977) has contributed significantly to our present understanding of percolation. Percolation theory describes satisfactorily a large number of physical and chemical phenomena, such as gelation processes (de Gennes, 1979), transport in amorphous materials (Zallen, 1983), hopping conduction in doped semiconductors (Shklovskii and Efros, 1984), and many other applications (Harder, Bunde, and Dietrich, 1986; Ingram, 1987). In addition, it forms the basis for studies of the flow of liquids or gases through porous media.

The physical implications of percolation theory have been described in many review articles or books, enlightening both the static and dynamic properties of percolating networks (see, for example, Shante and Kirkpatrick, 1971; Kirkpatrick, 1973a, 1979; Stauffer, 1979, 1985; Thouless, 1979; Essam, 1980; Farmer, Ott, and Yorke, 1983; Stanley and Coniglio, 1983; Zallen, 1983; Shklovskii and Efros, 1984; Aharony, 1986; Efros, 1986; Sokolov, 1986; Deutscher, 1987; Havlin and Ben-Avraham, 1987; Feder, 1988; Bouchaud and Georges, 1990; Clerc *et al.*, 1990; Isichenko, 1992; Odagaki, 1993; Sahimi, 1993), and in many conference proceedings (de Gennes, 1983; Deutscher, Zallen, and Adler, 1983; Goldman and Wolf, 1983; Pynn and Skjeltorp, 1985; Pynn and Riste, 1987). In particular, recent reviews by Bunde and Havlin (1991; see also Havlin and Bunde, 1991) and Stauffer and Aharony (1992) bring the subject to its current state of understanding.

There are two main kinds of percolating networks: *site* and *bond*. To create a site-percolating (SP) network, each intersection (site) of an initially prepared d-dimensional lattice is occupied at random with probability p. Sites are connected if they are adjacent along a principal direction. In a bond-percolation (BP) network, all sites are initially occupied and bonds are occupied randomly with probability p. At a critical (different) concentration $p=p_c$, both site and bond percolation exhibit a single, infinite cluster spanning all space. The difference between the geometrical structure of SP and BP networks is a short-range one, namely, a bond has more nearest neighbors than a site. For example, in a $d=2$ square lattice, a given bond is connected to six nearest-neighbor bonds, whereas a site has only four nearest-neighbor sites. This is the reason why BPs always have smaller p_c than those of SPs (see Table I in which we list the values of p_c for various percolation geometries and dimensions).

A. Nodes-links-blobs model

A very useful model for an infinite network near p_c was first proposed by Skal and Shklovskii (1974) and de Gennes (1976a) and refined by Stanley (1977), Pike and Stanley (1981), and Coniglio (1982b). This model, called the *nodes-links-blobs* model, is quite useful for describing the geometrical features of percolating networks, though it was not evident *a priori* that such a simple picture was mathematically valid.

The *nodes-links-blobs* model is based on the fact that an infinite cluster contains a backbone network with a characteristic length scale $\xi(p)$, defined in Euclidean space, and dead ends attached to the backbone. The backbone comprises the networks made of *links* (quasi-1d strings) and *nodes* (intersection of links). The length of links, i.e., the linear spacing $\xi(p)$ between nearest-neighbor *nodes*, corresponds to the correlation length of the percolating network. This is the original version of the model proposed by Skal and Shklovskii (1974) and de Gennes (1976a), which is called the SSdG model or the *nodes-links* model. This model neglects the strongly bonded (multiconnected) regions in the links. The SSdG model was refined by incorporating these parts, called *blobs*. One imagines for a network at $p>p_c$ in this picture the percolating backbone consisting of a network of

[1]The concept of percolation was introduced rather earlier by Flory (1941a, 1941b, 1941c) and Stockmayer (1943) during their study of the gelation process.

TABLE I. Percolation thresholds p_c for several lattices and the Cayley tree.

Dimension	Lattice	Sites	Bonds
2	Square	0.5927460±0.0000005[a]	1/2[†b]
	Triangle	1/2[†b]	2 sin(π/18) (=0.34729)[†b]
	Honeycomb	0.6962[c]	1−2 sin(π/18) (=0.65271)[†b]
	Kagomé	0.652 704[†d]	0.524 430[†d]
	Penrose	0.5837±0.0003[d]	0.477 0±0.0002[d]
3	Simple cubic (1st nn)	0.311 61[c]	0.248 65±0.0001 3[e]
			0.2488±0.0001[c]
	Simple cubic (2nd nn)	0.137[f]	
	Simple cubic (3rd nn)	0.097[f]	
	Body-centered-cubic	0.245[c]	0.180 25±0.0001 5[g]
			0.1795±0.0003[h]
	Face-centered-cubic	0.198[c]	0.119[c]
	Diamond	0.428[c]	0.388[c]
4		0.197±0.001[i]	0.161±0.0015[j]
			0.160 13±0.000 12[e]
			0.160 05±0.000 15[g]
5		0.141±0.001[i]	0.118±0.01[j]
			0.1182±0.0002[k]
	Simple cubic		0.118 19±0.000 04[g]
6		0.108[l]	0.094 075±0.0001[k]
			0.094 20±0.0001[g]
7		0.085[l]	0.078 62±0.000 03[k]
			0.078 685±0.000 03[g]
$d\to\infty$			$1/(2d-1)$
	Cayley tree		$1/(z-1)$

[a]Ziff (1992).
[b]Sykes and Essam (1963, 1964).
[c]Stauffer (1985) and Stauffer and Aharony (1992).
[d]Sakamoto, Yonezawa, and Hori (1989) and Sakamoto, Yonezawa, Aoki, *et al.* (1989).
[e]Grassberger (1986).
[f]Domb (1966).
[g]Adler *et al.* (1990).
[h]Gaunt and Sykes (1993).
[i]Jan, Hong, and Stanley (1985).
[j]Gaunt and Ruskin (1978).
[k]Adler, Aharony, and Harris (1984).
[l]Nakanishi and Stanley (1980).

quasi-1d string segments (*links*), tying together a set of strongly bonded regions (*blobs*) whose typical separation is of the order of the correlation length $\xi(p)$ [see Fig. 1(a)].

Stanley (1977) called the links *red bonds* and gave the following definition: Consider the situation in which a voltage is applied between two sites at opposite edges of a metallic percolating network at p_c. When the singly connected region (red bonds) is cut, the current flow stops. This bond carries the total current. In this connection, Stanley and Coniglio (1983) introduced the terms *blue* and *yellow* bonds. Blue bonds carry current. But when a blue bond is cut, the resistance of the system increases. Yellow bonds belong to dead ends and can be cut out without changing the resistance.

B. Critical exponents

The occupation probability p of sites or bonds in percolation theory plays the same role as the temperature in thermal critical phenomena. There exists a critical concentration p_c below which ($p<p_c$) only finite clusters exist and above which ($p>p_c$) an infinite cluster is present as well as finite clusters.

Let us define $n_s(p)$ as the average number (per site) of finite clusters with the size (site number) s. The quantity $n_s(p)$ is related to various physical quantities characterizing the network. The scaling theory of percolation is based on the idea that there exists a certain "parameter" characterizing the system, which diverges at $p=p_c$. This allows one to express the scaling Ansatz for $n_s(p)$ by defining a parameter $s(p)$:

$$n_s(p)=s^{-\tau}F[s/s(p)] ,$$

where $F(x)$ is an unknown function. Taking the form of $s(p)$ close to p_c as

$$s(p)\propto|p-p_c|^{-1/\eta} , \tag{2.1}$$

one has an alternative equation for $p\to p_c$ and $s\to\infty$,

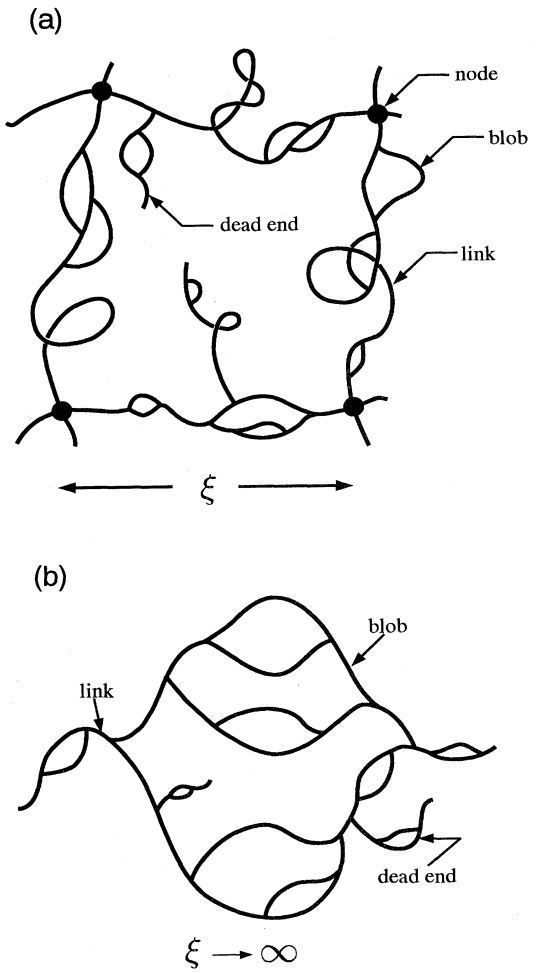

FIG. 1. Schematic of the nodes-links-blobs model. (a) A percolating network above p_c. The solid circles indicate nodes forming the homogeneous network at length scales $L > \xi$. (b) Links-blobs model at $p = p_c$. The hierarchical structure of blobs is stressed here.

$$n_s(p) = s^{-\tau} F[(p - p_c)s^{\eta}] \ . \tag{2.2}$$

Equation (2.2) allows scaling forms to be obtained for various physical quantities around p_c in terms of a set of critical exponents.

The exponent β. The probability that a site belongs to the infinite network, $P(p)$, is associated near p_c with the exponent β. Since an occupied site must be either in a finite cluster or in the infinite cluster, one has the exact relation,

$$P(p) + \sum_s n_s(p)s = p \ .$$

For $p < p_c$, only finite clusters exist and $\sum_s n_s(p)s = p$. When p approaches $p_c (p > p_c)$, the above relation becomes

$$P(p) = \sum_s [n_s(p_c) - n_s(p)]s + (p - p_c) \ .$$

Substituting Eq. (2.2) into the above equation, one finds

$$P(p) = \int s^{1-\tau}[F(0) - F(x)]ds + (p - p_c) \ ,$$

where $x = (p - p_c)s^{\eta}$. Changing the variable s to x gives

$$P(p) = P_0(p - p_c)^{\beta} + (p - p_c) \quad (p > p_c) \tag{2.3}$$

where P_0 is the constant prefactor and the critical exponent β is defined as

$$\beta = \frac{\tau - 2}{\eta} \ . \tag{2.4}$$

Because β is always less than unity, except for the case of the Cayley tree (see Table II), the first term of Eq. (2.3) dominates. Note that $\beta = 1$ for the Cayley tree, and the two terms in Eq. (2.3) are of the same order in $(p - p_c)$. The quantity $P(p)$ was first introduced by Broadbent (1954), corresponding to the order parameter for thermal critical phenomena.

The exponent α. This is the exponent for the total number of *finite* clusters given by

$$M(p) = \sum_s n_s(p) \ . \tag{2.5}$$

The function $M(p)$ consists of the analytic part $M'(p)$ at $p = p_c$ and a singular part $M''(p)$ proportional to $|p - p_c|^{2-\alpha}$, as seen from the same procedure as that in the case of Eq. (2.3). The critical exponent α is given by

$$\alpha = \frac{1 - \tau}{\eta} + 2 \ . \tag{2.6}$$

For a thermal phase transition, the exponent α corresponds to that of specific heat, and $M(p)$ to the free energy.

The exponent γ. The average mass $S(p)$ (number of sites or bonds) of finite clusters is related to $n_s(p)$ by

$$S(p) = \frac{\sum_s n_s(p)s^2}{\sum_s n_s(p)s} \ .$$

Note here that the factor $n_s(p)s / \sum_s n_s(p)s$ is the probability of an occupied site belonging to a cluster of s sites. Because $\sum_s n_s(p)s = p$ when $p < p_c$, one has the equation in the limit of $p \to p_c$

$$S(p) = \frac{\sum_s n_s(p)s^2}{p_c} \ . \tag{2.7}$$

Substituting Eq. (2.2) into (2.7), the critical exponent for the average mass can be given by

$$S(p) = S_0|p - p_c|^{-\gamma} \ ,$$

where S_0 is the constant prefactor and

$$\gamma = \frac{3 - \tau}{\eta} \ . \tag{2.8}$$

For thermal critical phenomena, the analogous quantity is the susceptibility.

TABLE II. Percolation exponents for $d=2$, 3, 4, 5, and $d \geq 6$. Rational numbers give exact results, whereas those with a decimal fraction are numerical estimates.

Exponents	$d=2$	$d=3$	$d=4$	$d=5$	$d \geq 6$
β	5/36[a]	0.463[b]	0.665±0.15[c]	0.83±0.1[c]	1
		0.454±0.008[d]	0.64[e]	0.84[e]	
		0.474±0.014[c]	0.65±0.04[f]	0.835±0.005[h]	
		0.435±0.035[g]	0.64±0.02[h]	0.835±0.005[i]	
		0.43±0.04[f]	0.639±0.020[i]		
		0.405±0.025[i]			
γ	45/18[a]	1.73±0.03[d]	1.41±0.25[j]	1.25±0.15[j]	1
		1.79[c]	1.44±0.05[c]	1.20±0.03[c]	
		1.71±0.06[k]	1.44[h]	1.18[h]	
		1.82±0.04[h]	1.435±0.015[i]	1.185±0.005[i]	
		1.74±0.015[l]			
		1.77±0.02[m]			
		1.805±0.02[i]			
ν	4/3[a]	0.88±0.02[d]	0.68±0.03[f]	0.57[h]	1/2
		0.89±0.01[n]	0.68[h]	0.571±0.003[i]	
		0.88±0.05[f]	0.678±0.050[i]		
		0.90±0.02[k]			
		0.83±0.01[h]			
		0.81[l]			
		0.875±0.008[m]			
		0.872±0.007[i]			
D_f	91/48[a]	2.48±0.09[d]	3.21±0.07[o]	3.74±0.4[o]	4
			3.12±0.02[p]	3.69±0.02[p]	

[a]Nienhuis (1982), den Nijs (1979), Nienhuis, Riedel, and Schick (1980), Pearson (1980).
[b]Gaunt, Whittington, and Sykes (1981).
[c]Adler, Aharony, and Harris (1984) and Adler *et al.* (1986a, 1986b).
[d]Gaunt and Sykes (1983).
[e]Adler *et al.* (1986a, 1986b).
[f]Grassberger (1986).
[g]Adler (1984).
[h]de Alcantara Bonfim, Kirkham, and McKane (1980, 1991).
[i]Adler *et al.* (1990).
[j]Gaunt, Sykes, and Ruskin (1976).
[k]Saleur and Derrida (1985).
[l]Reeve (1982), Reeve, Guttmann, and Keck (1982).
[m]Strenski *et al.* (1988).
[n]Margolina, Herrmann, and Stauffer (1982), Heermann and Stauffer (1981).
[o]Stanley (1977).
[p]Jan, Hong, and Stanley (1985).

C. Correlation length and fractal dimension

The lower cutoff scale characterizing the percolating network is the length a that forms the lattice spacing of the original network. There exists another characteristic length $\xi(p)$, called the correlation length, which was mentioned in Sec. II.A. This length scale exhibits critical behavior in the vicinity of p_c.

The exponent ν. The diameter of finite clusters below p_c is characterized by the correlation length $\xi(p)$, defined as the root-mean-square distance between two sites i and j in the same cluster, averaged over all finite clusters. The average distance between two sites in a given s cluster is written by

$$R_s^2=\frac{1}{2s^2}\sum_{ij}|r_i-r_j|^2 .$$

The number of ways of connecting two sites in a given cluster of size s is s^2, so that $s^2 n_s$ becomes the number of ways of connecting two sites in *clusters* with the same size s. The correlation length $\xi(p)$ is R_s averaged by the probability $s^2 n_s / \sum_s s^2 n_s$. This is expressed by

$$\xi^2(p)=\frac{\sum R_s^2 s^2 n_s}{\sum_s s^2 n_s} . \tag{2.9}$$

We assume the same scaling form for R_s as in Eq. (2.2),

$$R_s = s^{\varpi} H[(p-p_c)s^{\eta}] , \tag{2.10}$$

where ϖ is the new critical exponent. Substituting Eqs. (2.2) and (2.10) into Eq. (2.9), one has, close to p_c,

$$\xi(p)=\Xi_0|p-p_c|^{-\nu}, \tag{2.11}$$

where Ξ_0 is the constant prefactor and

$$\nu=\frac{\varpi}{\eta}.$$

The correlation length $\xi(p)$ represents the characteristic size of the voids in the percolating system when $p>p_c$, and the characteristic size of a finite cluster when $p<p_c$.

The fractal dimension D_f. Stanley (1977) was the first to notice that percolating networks exhibited self-similarity and could be characterized by a noninteger mass dimension, i.e., that they were "fractal." Mandelbrot gave a simple definition of fractals: *A fractal is a shape made of parts similar to the whole in some way* (Feder, 1988). Fractals can be classified as deterministic or random, depending on whether the self-similarity is exact or considered as the average. Percolating networks are a typical example of a random fractal.

From Eq. (2.10), one sees $R_s \propto s^{\varpi}$ at $p=p_c$. This is rewritten as

$$s(R_s)\propto R_s^{1/\varpi}. \tag{2.12}$$

It should be noted that $s(R_s)$ is a measure of the system; i.e., $s(R_s)$ corresponds to the "mass" $M(R_s)$ in our problem. The exponent $D_f=1/\varpi$ is called the fractal dimension or Hausdorff dimension. We can interpret $\xi(p)$ as a length scale up to which the cluster can be regarded as fractal. For the percolating network for $p>p_c$, the structure can be regarded as *homogeneous* for length scales larger than $\xi(p)$. Kapitulnik *et al.* (1983) demonstrated through Monte Carlo simulations that the networks for $p>p_c$ are homogeneous on length scales $L>\xi$ and fractal on scales $L<\xi$. Summarizing,

$$M(L)\propto \begin{cases} L^{D_f}, & L\ll\xi, \\ L^{d}, & L\gg\xi. \end{cases} \tag{2.13}$$

There are many reviews and books concerning the properties and uses of fractals (see, for example, Mandelbrot, 1975, 1977, 1982, 1989; Family and Landau, 1984; Stanley and Ostrowsky, 1986; Barnsley, 1988; Vicsek, 1989; Feder and Aharony, 1990; Sapoval, 1990; Takayasu, 1990; Feder, 1988; Peitgen and Saupe, 1988; Pietronero and Tosatti, 1988; Bunde and Havlin, 1991; Family and Vicsek, 1991).

The shorter limiting length scale l_a, characterizing the underlying components making up the fractal, depends on the type of percolation, i.e., site (SP) or bond (BP). This is because the random filling produces a relatively small number of neighboring sites around an occupied site in SP networks, whereas BP networks have many masses on neighbors that are *not* directly connected. This severely influences the difference in short-range character of these networks. Figure 2 presents results of a calculation by Stoll, Kolb, and Courtens (1992), which

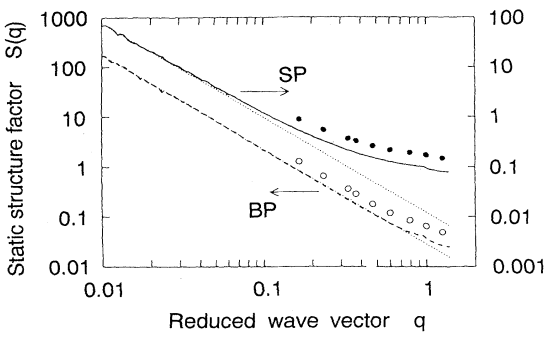

FIG. 2. Structure factor $S(q)$ for SP and BP networks with $d=2$. The dots are for $L=12$ systems (averaged over 20 000 realizations), and the full curves for $L=6800$. The dotted lines have slope $D_f=91/48$. After Stoll, Kolb, and Courtens (1992).

indicates that the lower limiting length scale l_a of BP networks is shorter than that of SP networks by one order of magnitude at $p=p_c$.

The criticality of links. The critical behavior of the links (red bonds) was derived by Coniglio (1982a, 1982b) using renormalization arguments. Coniglio (1982a, 1982b) verified that the number of red bonds varies with p as

$$L_1\propto(p-p_c)^{-1}\propto\xi(p)^{1/\nu}. \tag{2.14}$$

This is rigorous in all dimensions. This relation also indicates that the fractal dimension of the links is $1/\nu$ because L_1 is the measure in this case.

The chemical distance. We should mention that there are exponents, besides those described so far, that are useful for the description of the purely static geometrical properties of fractal networks. An example is the shortest path R_c *along* the percolating network from one site (i) to another (j). We can define the shortest path R_c between the site i and j as the minimum number of steps by which we can reach j from i, with restriction to existing paths between connected sites. This is termed the *chemical distance* R_c (Alexandrowicz, 1980; Middlemiss, Whittingston, and Gaunt, 1980; Pike and Stanley, 1981; Havlin and Nossal, 1984; Cardey and Grassberger, 1985). It is not the same as the linear length R_s measured between the two points (referred to as the "Euclidean distance"). The chemical (or topological) dimension d_c is defined from

$$M(R_c)\propto R_c^{d_c},$$

where $M(R_c)$ is the mass within the chemical distance R_c. From Eqs. (2.13) and (2.14), the chemical distance between two sites that are separated by the Euclidean distance L is given by

$$R_c\propto L^{D_f/d_c}.$$

The ratio of $D_f/d_c=d_{\min}$ is the fractal dimension for the minimum path between two sites (Stanley, 1984; Herrmann and Stanley, 1988). The chemical dimension

d_c has been determined numerically for $d=2$ and $d=3$ percolating networks, and they take the values $d_c=1.678\pm0.005$ and $d_c=1.885\pm0.015$, respectively (Havlin and Nossal, 1984; Havlin *et al.*, 1985, Herrmann and Stanley, 1988; Neumann and Havlin, 1988).

Scaling relations. The relation between D_f and the exponents β and ν can be derived from a simple argument. For percolating networks with $p>p_c$, the correlation length $\xi(p)$ is finite and is the unique length scale describing geometrical features on a scale $L \gg a$. Consider the number of sites $M(\xi)$ within a box of size ξ. From the definition of $P(p)$, $M(\xi)$ is given by

$$M(\xi) \propto \xi^d P(p) \propto \xi^{d-\beta/\nu} ,$$

where $P(p) \propto (p-p_c)^\beta$ is used. Thus the fractal dimension D_f is given by

$$D_f = d - \frac{\beta}{\nu} . \tag{2.15}$$

This relation is called the hyperscaling relation, since it depends on the Euclidean dimension d. The exponents β and ν are universal, so that D_f is also universal. They depend neither on the lattice structure nor on the type of percolation (SP or BP), but are a function only of the dimensionality d.

It is important to note that the critical exponents defined in Eqs. (2.4)–(2.8) are related to each other. Using Eqs. (2.4)–(2.8), one has the scaling relations

$$\alpha = 2 - d\nu = 2 - 2\beta - \gamma , \tag{2.16}$$

$$\eta = \frac{1}{\beta+\gamma} , \tag{2.17}$$

$$\tau = 2 + \frac{\beta}{\beta+\gamma} , \tag{2.18}$$

and

$$d\nu = 2\beta + \gamma . \tag{2.19}$$

All the exponents given above can be found *if the values of two of them are known.*

The values of the exponents have been calculated by various methods: the renormalization-group method (Bernasconi, 1978a, 1978b; Fucito and Marinari, 1981; Derrida and de Seze, 1982; Lobb and Karasek, 1982; Sahimi, 1984), the cluster expansion methods (Sykes, Gaunt, and Glen, 1976a, 1976b; Gaunt, 1977; Nakanishi and Stanley, 1980; Gaunt, Whittington, and Sykes, 1981; Adler *et al.*, 1986a, 1986b; Sykes and Wilkinson, 1986; Harris, Meir, and Aharony, 1987; Takayasu and Takayasu, 1988; Adler *et al.*, 1990; Wada, Watanabe, and Uchida, 1991), Monte Carlo calculations (Margolina *et al.*, 1984; Rapaport, 1985; Kim *et al.*, 1987), and the finite-size scaling method (Chayes *et al.*, 1986; Sakamoto, Yonezawa, Aoki, *et al.*, 1989; Sakamoto, Yonezawa, and Hori, 1989). Table II shows the values of these critical exponents. For $d=2$, the critical exponents are known exactly.

The upper critical dimension above which the mean-field theory is valid is $d=6$. Mean-field percolation can be modeled by percolation on a Cayley tree (Bethe lattice). Hyperscaling relations (2.15) and (2.19) are valid for space dimensions less than the critical value $d=6$. In the classical range $d \geq 6$, the values for all the exponents are given by the relation at $d=6$, namely, $\beta=1$ and $\nu=1/2$, independent of d.

III. RANDOM WALKS ON FRACTAL NETWORKS

The percolation transition has been characterized, in Sec. II, by quantities such as the cluster size $n_s(p)$, the mean size of a finite cluster $S(p)$, the correlation length $\xi(p)$, and the order parameter $P(p)$. These quantities describe the static (geometrical) properties of percolating networks. In this section, we describe the dynamic properties of percolating networks. The first example is diffusion of random *walkers* on a percolating network.

In uniform systems, the mean-square displacement of a random walker, $\langle R^2(t) \rangle$, is proportional to the time t,

$$\langle R^2(t) \rangle \propto t ,$$

for any Euclidean dimension d. In percolating systems, for a length scale $<\xi$, diffusion is anomalous (Gefen, Aharony, and Alexander, 1983). The mean-square displacement is described by the form

$$\langle R^2(t) \rangle \propto t^{2/(2+\theta)} , \tag{3.1}$$

with $\theta>0$. This slowing down of the diffusion is caused by the delay of a diffusing particle because of hierarchically intricate structure and the presence of *dead ends.*

A. Anomalous diffusion

The diffusion coefficient of random walkers is defined by

$$D_\infty = \frac{1}{2} \frac{d\langle R^2(t) \rangle}{dt} ,$$

where $\langle R^2(t) \rangle$ is the mean-square displacement after t-time steps. For $p>p_c$ and the length scale $\langle R^2(t) \rangle^{1/2} \gg \xi(p)$, the system looks homogeneous and normal diffusion holds,

$$\langle R^2(t) \rangle \propto D_\infty t , \tag{3.2}$$

where the diffusion coefficient D_∞ on this cluster is related to the dc conductivity $\sigma_{\rm dc}$ through the Einstein relation

$$\sigma_{\rm dc} = \frac{e^2 n D_\infty}{k_B T} ,$$

where e denotes the carrier charge, n their density, k_B the Boltzmann constant, and T the temperature.

The subscript ∞ of D reflects the fact that, on these scales, the dc conductivity occurs only through the infinite cluster ($p>p_c$). Empirical evidence for power-law behavior was given by Last and Thouless (1971) and

by Watson and Leath (1974). Last and Thouless (1971) measured the current through sheets of graphite paper with randomly punched holes. The exponent μ is defined through the relation

$$\sigma(p)=\Sigma_0(p-p_c)^{\mu} .$$

Noting that the carrier density n is proportional to $P(p)$, we find that

$$D_{\infty} \propto (p-p_c)^{\mu-\beta} . \tag{3.3}$$

We should emphasize that $\mu-\beta$ is always positive because $D_{\infty} \to 0$ with $p_+ \to p_c$ for any Euclidean dimension d.

The mean squared distance $\langle R^2(t)\rangle$ should be linearly proportional to the time t for $p>p_c$ and $\langle R^2(t)\rangle^{1/2} \gg \xi$. One has from Eqs. (3.2) and (3.3)

$$\langle R^2(t)\rangle \propto t(p-p_c)^{\mu-\beta} . \tag{3.4}$$

For finite-size clusters, $\langle R^2(t)\rangle$ becomes independent of time t after a sufficiently long time. One has for $p<p_c$

$$\langle R^2(t)\rangle=\xi^2 \propto |p-p_c|^{-2\nu} . \tag{3.5}$$

Here the relation $\xi \propto |p-p_c|^{-\nu}$ is used. All of these equations can be derived from the dynamic scaling form,

$$\langle R^2(t)\rangle^{1/2}=t^x G[(p-p_c)t^y] . \tag{3.6}$$

When Eq. (3.4) holds for $p>p_c$, Eq. (3.6) leads to the asymptotic form $G(z)_{z\to\infty} \propto z^{(\mu-\beta)/2}$. One can then derive the relation

$$\frac{y(\mu-\beta)}{2}+x=\frac{1}{2} . \tag{3.7}$$

For $p<p_c$, $\langle R^2(t)\rangle$ becomes independent of time t, leading to the form $G(z)_{z\to-\infty} \propto z^{-x/y}$ from Eq. (3.5). One finds the asymptotic form

$$\frac{x}{y}=\nu . \tag{3.8}$$

From Eqs. (3.7) and (3.8), we have the relations

$$x=\frac{\nu}{2\nu+\mu-\beta} , \tag{3.9}$$

$$y=\frac{1}{2\nu+\mu-\beta} . \tag{3.10}$$

Substituting these into Eq. (3.6), one finds at $p=p_c$

$$\langle R^2(t)\rangle \propto t^{2/d_w} , \tag{3.11}$$

where

$$d_w=2+\frac{\mu-\beta}{\nu} . \tag{3.12}$$

This is of the same form as Eq. (3.1), if we define $\theta=(\mu-\beta)/\nu$. The slow process described by Eq. (3.11) is called anomalous diffusion, and d_w is called the diffusion exponent.

From Eq. (3.6) one can estimate the characteristic time τ of the crossover from anomalous diffusion to normal diffusion. Anomalous diffusion occurs when $t \ll \tau$, whereas normal diffusion occurs when $t \gg \tau$. The characteristic time τ can be obtained by setting the argument in the function $G(z)$ in Eq. (3.6) to be of the order of unity:

$$\tau \propto (p-p_c)^{-(2\nu+\mu-\beta)} . \tag{3.13}$$

The value of d_w is obtained by direct numerical calculations of $\langle R^2(t)\rangle$, or from the numbers of sites visited by

TABLE III. Dynamic exponents of percolating networks.

Exponents	$d=2$	$d=3$	$d=4$	$d=5$	$d\geq 6$
d_w	2.69±0.04[a]	3.45±0.1[c]			6
	2.871±0.001[b]	4.00±0.05[d]			
		3.755[b]			
μ	$1.297^{+0.007}_{-0.004}$[e]				3
	1.31[f]	2.04[f]	2.39[f]	2.72[f]	
	1.264±0.054[g]	1.876±0.035[g]			
	$1.303^{+0.004}_{-0.014}$[h]				
	1.315±0.008[i]				
$\tilde{d}$	1.334±0.007[j]	1.14±0.02[c]	1.39[m]	1.44[m]	4/3
	1.323±0.004[a]	1.32±0.06[l]	1.36[n]	1.36[n]	
	1.322±0.003[k]	1.328±0.01[b]	1.31±0.03[o]		
	1.33±0.01[o]	1.31±0.02[o]	1.279±0.07[p]		
	1.325±0.006[p]	1.317±0.03[p]			

[a]Hong *et al.* (1984).
[b]Havlin and Bunde (1991).
[c]Movshovitz and Havlin (1988).
[d]Roman (1990).
[e]Lobb and Frank (1984).
[f]Adler (1985).
[g]Sahimi *et al.* (1983).
[h]Frank and Lobb (1988).
[i]Octavio and Lobb (1991).
[j]Essam and Bhatti (1985).
[k]Zabolitzky (1984).
[l]Argyrakis and Kopelman (1984).
[m]Alexander and Orbach (1982).
[n]Daoud (1983).
[o]See Fig. 5 in Sec. V of this review.
[p]See Fig. 6 in Sec. V of this review.

random walkers within the time t, $V(t) \propto t^{D_f/d_w}$ (Ben-Avraham and Havlin, 1982, 1983; Argyrakis and Kopelman, 1984; Hong *et al.*, 1984; Pandey *et al.*, 1984; Pandey, Stauffer, and Zabolitzky, 1987; Wagner and Balberg, 1987; Movshovitz and Havlin, 1988; Bunde, Havlin, and Roman, 1990; Roman, 1990; Duering and Roman, 1991; Havlin and Bunde, 1991). When calculating these quantities, one must note that Eq. (3.11) represents the diffusion for $t \ll \tau$ on the single *infinite* cluster. Values of d_w, as well as other dynamic exponents, are given in Table III. From Table III, we see that, for any Euclidean dimension d, d_w is larger than the value 2, the value for normal diffusion.

B. Fracton dimension and the Alexander-Orbach conjecture

The linear size of the region of sites visited by the "ant" after t-time steps from Eq. (3.11) is $\langle R^2(t) \rangle^{1/2} \propto t^{1/(2+\theta)}$. Therefore the number of visited sites $V(t)$ becomes

$$V(t) \propto R^{D_f} \propto t^{\tilde{d}/2} , \tag{3.14}$$

where the fracton (or spectral) dimension $\tilde{d}$ is defined by[2]

$$\tilde{d} = \frac{2D_f}{2+\theta} = \frac{2D_f}{d_w} . \tag{3.15}$$

Alexander and Orbach (1982) tabulated the then-known values for the quantities D_f, θ, and $\tilde{d}$ for percolating networks on d-dimensional Euclidean lattices. They pointed out that while D_f and θ change dramatically with d (below $d=6$), $\tilde{d}$ does not. They conjectured from the numerical values for $\tilde{d}$ that for percolation

$$\tilde{d} = 4/3, \quad \text{for } 2 \le d \le 6 . \tag{3.16}$$

The expression "hyper-universal" or "super-universal" was coined to express the possibility that an exponent could be independent not only of the details of the lattice but also of the dimensionality d itself (see Leyvraz and Stanley, 1983). This conjecture is crucial, because, if exact, the dynamic exponent μ can be related to the static ones through the relation

$$\mu = \frac{1}{2}[(3d-4)\nu - \beta] . \tag{3.17}$$

Determining the dynamical exponents, such as $\tilde{d}$, d_w, or μ, has been a challenge in the past decade, and many conjectures have been proposed. The exact values for these exponents are not known, except for the case $d \ge 6$ (footnote 3). Values for μ are usually estimated by numerical methods (Fogelholm, 1980; Derrida and Vannimenus, 1982; Li and Strieder, 1982; Mitescu and Musolf, 1983; Sahimi *et al.*, 1983; Herrman *et al.*, 1984; Lobb and Frank, 1984; Zabolitzky, 1984; Sarychev *et al.*, 1985; Seaton and Glandt, 1987; Frank and Lobb, 1988; Normand *et al.*, 1988; Gingold and Lobb, 1990; Octavio and Lobb, 1991); by analytical approximations such as series expansions (Fisch and Harris, 1978; Adler, 1985; Adler *et al.*, 1990), small cell real-space renormalization technique (Bernasconi, 1978a, 1978b), and the ε-expansion method (Harris *et al.*, 1984; Harris and Lubensky, 1984, 1987; Wang and Lubensky, 1986; Harris, 1987); and from experiment (Song *et al*, 1986; Wodzki, 1986; Domes *et al.*, 1987; Careri *et al.*, 1988; Lin, 1991).

The Alexander-Orbach conjecture leads to a value of the ratio μ/ν equal to $91/96 = 0.948$ for $d=2$ percolating networks. This exponent μ/ν describes how the resistivity R diverges with the linear size L of the system, $R \propto L^{\mu/\nu}$. The value of μ/ν has been studied numerically with the finite-size scaling technique (Hong *et al.*, 1984; Lobb and Frank, 1984; Zabolitzky, 1984; Normand *et al.*, 1988). Gordon and Goldman (1988a, 1988b) tried to obtain the value of μ/ν experimentally for Al thin films of 50 nm thickness. They prepared an 800×800 square lattice by exposing Al thin films to an electron beam. These values for μ/ν previously reported are slightly smaller than the conjectured value 91/96, which means that $\tilde{d}$ is less than 4/3.

The exponent d_w is also related to $\tilde{d}$ by Eq. (3.15). If the Alexander-Orbach conjecture holds, d_w should take the value of $91/32 = 2.844$ for $d=2$ percolating networks.

---

[2]The term "fracton" denotes a localized mode peculiar to fractal structures, coined by Alexander and Orbach (1982). These excitations exist not only for vibrational systems, but also for dilute magnets. This dimension ($\tilde{d}$) plays an important role in describing the dynamical features of percolating networks, such as the density of states, dispersion relation, and localization. This subject is discussed in detail in Sec. IV.

[3]The fracton (or spectral) dimension can be obtained exactly for deterministic fractals (Rammal and Toulouse, 1983; Rammal, 1983, 1984a; Given, 1984; Southern and Douchant, 1985; Yu, 1986; Ashraff and Southern, 1988). In the case of a d-dimensional Sierpinski gasket (Rammal and Toulouse, 1983; Rammal, 1983, 1984a), the fracton dimension is

$$\tilde{d} = 2\frac{\ln(d+1)}{\ln(d+3)} .$$

We see from this that the upper bound for a Sierpinski gasket is $\tilde{d}=2$. Hattori, Hattori, and Watanabe (1986) have noted that this upper bound is a general result for fractal systems in which *coarse-graining* treatments are applicable. It is interesting to note that the fracton dimension for a $d=3$ Sierpinski *carpet* takes the value $\tilde{d}=2.894$ (Hattori, Hattori, and Watanabe, 1985; Hattori and Hattori, 1988). This is because the coarse-graining treatment is not valid for this carpet. Bourbonnais, Maynard, and Benoit (1989) have shown the existence of channeling modes in the $d=2$ Sierpinksi carpet which have large amplitudes along the line of dense matter in the network. Ben-Avraham and Havlin (1983) and Havlin, Ben-Avraham, and Movshovitz (1984) have presented a family of exact fractals with a wide range of fracton dimensions, including the case of $\tilde{d}=2$.

The Monte Carlo method for random walk is useful for estimating the exponent d_w through Eq. (3.11) (Ben-Avraham and Havlin, 1982; Havlin and Ben-Avraham, 1983; Havlin *et al.*, 1983, 1984; Hong *et al.*, 1984; Majid *et al.*, 1984; Pandey *et al.*, 1984, 1987; McCarthy, 1988; Roman, 1990; Duering and Roman, 1991). The calculated values of d_w are somewhat larger than 91/32, which corresponds to $\tilde{d} \lesssim 4/3$.

The fracton dimension $\tilde{d}$ can be evaluated directly by the relation $S_N \sim N^{\tilde{d}/2}$, where S_N is the number of distinct sites visited during an N-step random walk on an infinite percolating network (Rammal and Toulouse, 1983). Using this relation, the value of $\tilde{d}$ has been numerically calculated by random-walk simulations (Ben-Avraham and Havlin, 1982, 1983; Havlin and Ben-Avraham, 1983; Argyrakis *et al.*, 1984; Rammal *et al.*, 1984; Keramiotis *et al.*, 1985). The results indicate that the values of $\tilde{d}$ are quite close, but not equal, to 4/3. The exponent $\tilde{d}$ has also been calculated by series expansion by Essam and Bhatti (1985). Their result is $\tilde{d} = 1.334 \pm 0.007$ for $d = 2$ percolating networks.

Although the value of fracton dimension $\tilde{d}$ is different depending on the method used, it is now accepted that the Alexander-Orbach conjecture is not correct and has really no analytical basis apart from numerical coincidences; the true value of $\tilde{d}$ is slightly smaller than 4/3 for $d < 6$ (see Table III). It remains, nevertheless, a remarkably accurate estimate of $\tilde{d}$ for all $d \geq 2$.

IV. SCALING THEORIES FOR DYNAMICS OF FRACTAL NETWORKS

A. Vibrational density of states and fracton dimension

The fracton dimension $\tilde{d}$ is a key dimension for describing the dynamical properties of fractal networks in addition to the fractal dimension D_f. D_f describes how the mass of the geometrical object depends on its length scale, whereas the fracton dimension $\tilde{d}$ characterizes anomalous diffusion on the fractal system. Alexander and Orbach (1982) mapped the problem of anomalous diffusion onto the vibrational problem with scalar elasticity. They showed that the basic properties of vibrations on fractal networks, such as the density of states (DOS), the dispersion relation, and localization, are characterized by the fracton dimension $\tilde{d}$. Rammal and Toulouse (1983) derived the fracton dimension $\tilde{d}$ via a scaling argument. They showed that various random-walk properties, such as the probability of closed walks and the mean number of visited sites, were governed by the fracton dimension $\tilde{d}$. Feng (1985a, 1985b) included vector displacements in terms of the *nodes-links-blobs* model described in Sec. II. He claimed that the rotationally invariant Hamiltonian having a stretching force constant and an angular force constant required an additional dimensionality $\tilde{d}_b$, which we call the bending-fracton dimension. His theory is discussed in Sec. V.A.3 in connection with the results of computer simulations on the DOS of percolating networks incorporating the vector nature of atomic displacement. In this section we review the works of both Alexander and Orbach (1982) and Rammal and Toulouse (1983).

1. Alexander and Orbach's original version

As noted in Sec. III, de Gennes (1976b) posed the following problem. "*An ant is dropped onto an occupied site of the infinite cluster of a percolating network. The ant at every time unit makes one attempt to jump to one of its adjacent sites. If that site is occupied, it moves to that site. If it is empty, the ant stays at its original site. What is the (ensemble) averaged square distance that the ant travels in a time t?*" The scaling argument to this problem was presented by Gefen, Aharony, and Alexander (1983) as described in Sec. III.A. The solution opened the way for a nearly complete description of the dynamics of fractal networks.

The structure of the diffusion equation is the special case of a master equation, which in turn has the same form as the equation of motion for mechanical vibrations or the linearized equation of motion for ferromagnetic spins (Alexander *et al.*, 1981). This allows the vibrational problem to be mapped onto the diffusion problem.

The master equation of diffusion on a lattice is written as

$$\frac{dP_i}{dt} = \sum_j W_{ij} P_j \ , \tag{4.1}$$

where P_i is the occupation probability of the diffusing particle on site i, and W_{ij} is the probability that a diffusing particle hops from site i to j. If the *diagonal elements* W_{ii} are defined to satisfy the condition $\sum_j W_{ij} = 0$, Eq. (4.1) reduces to the *conventional* maser equation. The equation of motion for lattice vibrations with scalar nearest-neighbor interactions is expressed by

$$m_i \frac{d^2 u_i}{dt^2} = \sum_j K_{ij} u_j \ , \tag{4.2}$$

where m_i and u_i are the mass and the displacement of the atom at site i, and K_{ij} is the spring constant connecting two atoms at sites i and j, respectively. The diagonal elements K_{ii} satisfy the condition $\sum_j K_{ij} = 0$, due to the uniform-translational invariance of the system; i.e., the uniform translation gives rise to no additional energy [this can be derived by putting $u_j = \text{const}$ in Eq. (4.2) for any j]. The only difference between the two equations is the order of the *time derivatives* (Alexander *et al.*, 1981). The spectral DOS can be obtained from the single-site Green's function for the vibrational problem by

$$\mathcal{D}(\varepsilon) = -\left[\frac{1}{\pi}\right] \lim_{\varepsilon \to 0} \mathrm{Im} \langle P_0(-\varepsilon + i0^+) \rangle \ , \tag{4.3}$$

where $\langle \cdots \rangle$ means the ensemble average. The function

$\langle P_0(\varepsilon)\rangle$ is the Green's function. This is defined by

$$\langle P_0(\varepsilon)\rangle = \int_0^\infty \exp(-\varepsilon t)\langle P_0(t)\rangle dt \ , \tag{4.4}$$

where $P_0(t)$ is the autocorrelation function.

The physical meaning of $\langle P_0(t)\rangle$ in the corresponding diffusion problem is the probability of finding the particle at the origin at time t if it were initially at the origin at time $t=0$. For compact diffusion ($\tilde{d} \leq 2$) (Alexander, 1983; Rammal and Toulouse, 1983), we have the relation

$$\langle P_0(t)\rangle \propto [V(t)]^{-1} \ , \tag{4.5}$$

where $V(t)$ is the number of visited sites within time t. From Eq. (3.14), this quantity is written as

$$\langle P_0(t)\rangle \propto t^{-\tilde{d}/2} \ , \tag{4.6}$$

where $\tilde{d}(<2)$ is defined by Eq. (3.15) in the context of the diffusion problem as

$$\tilde{d} = \frac{2D_f}{2+\theta} \ .$$

The substitution of Eq. (4.6) into Eq. (4.4) leads to

$$\langle P_0(\varepsilon)\rangle = \text{const} \times \varepsilon^{\tilde{d}/2-1} \int_0^\infty \exp(-x) x^{-\tilde{d}/2} dx \ . \tag{4.7}$$

Note that the integration takes a real positive value. By letting $\varepsilon \rightarrow -\omega^2 + i0^+$ in Eq. (4.7) and substituting into Eq. (4.3), one has the result

$$\mathcal{D}(\omega^2) \propto \omega^{\tilde{d}-2} \ . \tag{4.8}$$

It should be noted that $\tilde{d}$ must be smaller than 2 due to the condition for convergence of the integral in Eq. (4.7). This conclusion is valid under some conditions (see footnote 3). The DOS is obtained as

$$\mathcal{D}(\omega) \propto \omega^{\tilde{d}-1} \ , \tag{4.9}$$

where the relation $d(\omega^2) = 2\omega\, d\omega$ is used. In analogy to the usual Debye density of states ω^{d-1}, Alexander and Orbach (1982) called the related excitations "fractons," and $\tilde{d}$ the "fracton dimension." It was also called the "spectral dimension" by Rammal and Toulouse (1983) because it represented the DOS for the vibrational excitation spectrum.

2. Finite-size scaling

Rammal and Toulouse (1983) also derived the vibrational DOS of fractals using a finite-size scaling approach.

Consider a fractal structure of size L with fractal dimension D_f. The DOS per one particle at the lowest frequency $\Delta\omega$ for this system is defined by

$$\mathcal{D}(\Delta\omega, L) = \frac{1}{L^{D_f} \Delta\omega} \ . \tag{4.10}$$

Assuming the dispersion relation for $\Delta\omega$ to be

$$\Delta\omega \sim L^{-a} \ , \tag{4.11}$$

one can eliminate the size L from Eq. (4.10):

$$\mathcal{D}(\Delta\omega) \propto \Delta\omega^{D_f/a - 1} \ . \tag{4.12}$$

The explicit expression for the exponent a of the dispersion relation is obtained from the exponent of anomalous diffusion [Eq. (3.11)]; i.e., the corresponding mappings of $t \rightarrow 1/\Delta\omega^2$ and $\langle R^2\rangle^{1/2} \rightarrow L$ yield

$$L \propto \Delta\omega^{-2/d_w} \ .$$

The comparison of the assumed dispersion relation (4.11) with this equation leads to

$$a = \frac{2\nu+\mu-\beta}{2\nu} \quad \left[= \frac{d_w}{2} = \frac{D_f}{\tilde{d}} \right] \ ,$$

where Eq. (3.12) has been used.

Since the structure is fractal (self-similar), $\Delta\omega$ can be replaced by an arbitrary frequency ω. Namely, one has the DOS from Eq. (4.13),

$$\mathcal{D}(\omega) \propto \omega^{\tilde{d}-1} \ , \tag{4.13}$$

and so the "dispersion relation" becomes

$$\omega \propto [L(\omega)]^{-D_f/\tilde{d}} \ , \tag{4.14}$$

where

$$\tilde{d} = \frac{D_f}{a} = \frac{2\nu D_f}{2\nu+\mu-\beta} \quad \left[= \frac{2D_f}{d_w} \right] \ . \tag{4.15}$$

As seen from Eq. (4.15), the fracton dimension $\tilde{d}$ can be obtained knowing the value of the conductivity exponent μ. The fracton dimension $\tilde{d}$ is an intrinsic parameter related to the dynamics of complex systems, and it therefore affects physical properties on a deeper level than any other exponents.

B. Characteristics of fractons

1. Localization

Rammal and Toulouse (1983) showed that fractons are spatially localized at a fracton dimension $\tilde{d} < 2$. They used the so-called β_L function defined by Abrahams *et al.* (1979) in their scaling theory of localization:

$$g(L) \propto L^{\beta_L} \ ,$$

where $g(L)$ is the dimensionless conductance of size L, i.e., a quantity of the order of σL^{d-2}, where σ is the conductivity. It is presumed that $g(L)$ follows a power-law relation on L in the above relation. It is clear that the wave functions are localized when β_L is zero or negative. In the case of percolating networks, $\sigma \propto (p - p_c)^\mu$. This leads to $\sigma \propto L^{-\mu/\nu}$ for a correlation length $\xi(p)$ larger than the size L. The conductance becomes

$$g(L) \propto L^{-\mu/\nu+d-2} \propto L^{D_f(\tilde{d}-2)/\tilde{d}} \ ,$$

where the scaling relation for fractal dimension

$D_f = d - \nu/\beta$ and the definition $\tilde{d} = 2D_f/[2+(\mu-\beta)/\nu]$ have been used. From the above relation, one finds $\beta_L = D_f(\tilde{d}-2)/\tilde{d}$. For $\tilde{d} \cong 4/3$, the β_L function is negative independent of Euclidean dimension d. It is interesting to note that for length scales greater than ξ, $\tilde{d} \to d$. Thus, for $d=3$, for example, β_L may well be positive, indicating delocalized vibrations (phonons). As the length scale shortens to less than ξ, $\tilde{d} \approx 4/3$ leads negative β_L and localization. Hence the crossover can be thought of as a dimensionality change in so far as localization is concerned: passing through ξ, $\tilde{d}$ crosses over from d to 4/3, causing localization (β_L changes sign).

2. Dispersion relation

Alexander (1989) gave a simple derivation of the dispersion law from the given form of the DOS such as that of Eq. (4.9). Consider the vibrations of an *isolated* fractal blob of size L. Though high-frequency modes will not be affected by the change in the boundary conditions, the low-frequency modes will disappear from the spectrum. The crossover occurs at some frequency ω_L such that

$$L \approx \Lambda(\omega_L) ,$$

where $\Lambda(\omega)$ is the wavelength. The integrated spectral weight of the missing low-frequency modes is lumped together in the center-of-mass degrees of freedom of the disconnected blob (e.g., the rotational and translational modes). This is a number that cannot depend on L and ω. Therefore, using Eq. (4.9), one has

$$[\Lambda(\omega_L)]^{D_f} \int_0^{\omega_L} \omega^{\tilde{d}-1} d\omega \propto \Lambda^{D_f} \omega_L^{\tilde{d}} = \text{const} .$$

This relation holds for any length scale L, and one has the dispersion relation for an arbitrary frequency ω:

$$\omega \propto \Lambda(\omega)^{-D_f/\tilde{d}} . \tag{4.16}$$

Applying the argument of a frequency-dependent length scale $\Lambda(\omega)$ to waves in a finite *homogeneous* system ($D_f = \tilde{d} = d$), one obtains the length scale $\Lambda = 2v\pi/\omega = \lambda$ (where v is the sound velocity), because the lowest frequency of a blob of size Λ is $\omega(\Lambda) = 2v\pi/\Lambda$.

3. Crossover from phonons to fractons: Characteristic frequency

If the wavelengths λ of excited modes on percolating networks $p > p_c$ are larger than the characteristic length scale $\xi(p)$, the system is homogeneous on this scale, and vibrational excitations are weakly localized phonons. This is because the scattering is determined by the square of the mass-density fluctuation averaged over regions of volume λ^d. Hence, even if the short-range disorder is strong, the effective strength of the disorder for phonons with $\lambda \gg \xi$ is very weak. If the characteristic length λ of waves becomes of the order of or shorter than $\xi(p)$, fractal structures become relevant. Thus there is a crossover in the nature of the vibrational excitations when $\lambda(\omega_c) \sim \xi(p)$. One has from Eq. (4.14) or (4.16) the crossover frequency of the form

$$\omega_c \propto (p - p_c)^{\nu D_f/\tilde{d}} . \tag{4.17}$$

By putting $\omega_c = v(p)k$ at $k \sim 1/\xi(p)$ in Eq. (4.17), the concentration (p) dependence of the phonon velocity becomes

$$v(p) \propto (p-p_c)^{\nu D_f/\tilde{d} - \nu} \propto (p-p_c)^{(\mu-\beta)/2} . \tag{4.18}$$

Because the value $\mu - \beta$ is always positive, we have $v(p) \to 0$ when $p \to p_c$. The results for the DOS are summarized as

$$\mathcal{D}(\omega) \propto \begin{cases} \dfrac{\omega^{d-1}}{[v(p)]^d}, & \omega \ll \omega_c , \\ \omega^{\tilde{d}-1}, & \omega \gg \omega_c . \end{cases}$$

The dispersion relations become

$$\omega \propto \begin{cases} v(p)k, & \omega \ll \omega_c , \\ k^{D_f/\tilde{d}}, & \omega \gg \omega_c , \end{cases}$$

where k for $\omega \gg \omega_c$ does not mean wave number due to the lack of the translational symmetry of the system, but rather it describes the inverse of the characteristic length Λ^{-1} [see Eq. (4.16)]. It should be noted that fractons reflect two features of fractal structures, namely, the fractality and the lack of the translational symmetry. The latter leads the localization of fractons.

V. LARGE-SCALE SIMULATIONS AND PHYSICAL REALIZATIONS

In this section, we first present results of simulation for the vibrational DOS for very large percolating networks with scalar interactions. These data provide rich information about the fracton dynamics. The characteristic properties of fracton wave functions themselves are also described. We also show the results for the model taking account of the vector nature of interactions and displacements. In addition, experimental results for the DOS measured in real materials—aerogels—are discussed using the concept of fractons.

A. Vibrations of a percolating network

1. Density of states: Site percolation with scalar elasticity

Computer simulations can provide deep insight into the eigenstates of random systems. Grest and Webman (1984) have calculated the DOS of $d=3$ percolating networks, using the standard diagonalization routine for

$d=3$ systems of size $L=18$. For larger systems, they used a recursive technique to calculate the eigenfunctions and eigenvalues in the low-frequency region. The standard diagonalization routines were sufficiently accurate, except at low frequencies. They averaged over three samples to obtain the DOS. Although there are obvious difficulties in the treatment of large-scale systems, the situation is changing as array-processing supercomputers become available. Many numerical methods have been reported to overcome these difficulties and have been applied to the investigation of fracton dynamics (Lam *et al.*, 1985; Yakubo and Nakayama, 1987a, 1987b, 1989a, 1989b, 1989c; Nakayama, 1990, 1992; Nakayama *et al.*, 1989; Russ *et al.*, 1989, 1991; Böttger *et al.*, 1990; Li *et al.*, 1990; Montagna *et al.*, 1990; Stoll and Courtens, 1990; Yakubo, Courtens, and Nakayama, 1990; Yakubo, Takasugi, and Nakayama, 1990; Lambert and Hughes, 1991; Roman *et al.*, 1991; Royer *et al.*, 1991, 1992; Mazzacurati *et al.*, 1992; Russ, 1992; Stoll *et al.*, 1992; Nakayama and Yakubo, 1992a, 1992b). Li, Soukoulis, and Grest (1990) used the Sturm sequence method to calculate the integrated DOS and treated $d=2$ systems of 160×640. Royer, Benoit, and Poussigue (1991, 1992) used the spectral moment method, which allowed them to work with a very large percolating network consisting of a square lattice of size $L=1415$.

Yakubo and Nakayama (1987a, 1987b, 1989a, 1989b), Yakubo, Courtens, and Nakayama (1990), and Yakubo, Takasugi, and Nakayama (1990) succeeded in treating systems with size number $N\sim10^6$ by applying the forced oscillator method of Williams and Maris (1985). Russ, Roman, and Bunde (1989, 1991), Russ (1992), and Bourbonnais, Maynard, and Benit (1989) have also used this method to calculate the DOS and the localization behavior of fractons. This algorithm is based on the principle that a complex mechanical system, when driven by a periodic external force of frequency Ω, will respond with a large amplitude in those eigenmodes close to this frequency. Yakubo, Nakayama, and Maris (1991) have formulated a method for judging the accuracy of the calculated eigenmodes and eigenfrequencies, and this method is now used in many different fields. This algorithm can be readily vectorized for use on an array-processing supercomputer (Yakubo and Nakayama, 1987a, 1987b). It should be noted that, for the calculation of the DOS, the algorithm becomes more accurate with increasing site number.

a. Two-dimensional case

Consider a site-percolating network consisting of N particles with unit mass and linear springs connecting nearest-neighbor atoms. The equation of motion of the atoms is given by

$$m\ddot{u}_i(t)=\sum_j K_{ij}u_j(t)\ , \tag{5.1}$$

where u_i is the scalar displacement of the atom with unit mass ($m=1$) on the ith site. The force constant is taken as $K_{ij}=0$ if either site i or j is unoccupied, and as $K_{ij}=1$ otherwise.[4] The displacement u_i has only one component.

The calculations for the DOS for $d=2$ percolating networks with the site number $N\sim10^5$ have been performed by Yakubo and Nakayama (1987a, 1987b, 1989a). Figure 3(a) shows the DOS at the percolation threshold p_c ($=0.593$). This network, formed on a 700×700 square lattice, has 116 991 atoms. The line through the solid circles has a slope of 1/3. It should be emphasized that the $\omega^{1/3}$ law holds even in the low-frequency region, because the lower cutoff frequency ω_L is determined from the finite size of the clusters. One can estimate the cutoff frequency to be $\omega_L\sim10^{-5}$ for the present case, using the relation $\omega_L\sim\omega_D/N$ where $\omega_D=2\sqrt{2}$. The correlation length $\xi(p)$ diverges at $p=p_c$, and the network has a fractal structure at longer length scales.

The DOS of a $d=2$ site-percolating cluster with $p=0.67$ is shown in Fig. 3(b). This percolating cluster is formed on a 700×700 square lattice with the cluster size $N=317\,672$. The results show that the frequency dependence of the DOS is characterized by two regimes. In the frequency region $\omega_c\ll\omega\ll1$, the DOS is closely proportional to $\omega^{1/3}$. The crossover frequency ω_c corresponds to the mode of wavelength λ equal to the percolation correlation length $\xi(p)$. Therefore the DOS in the frequency regime lower than ω_c should be given by the conventional Debye law $\mathcal{D}(\omega)\propto\omega^{d-1}$, where d is the Euclidean dimension and $\mathcal{D}(\omega)\propto\omega^{\tilde{d}-1}$ for $\omega\gg\omega_c$. The simulated result is consistent with this view because the frequency dependence of the DOS for lower frequencies ($\omega\ll\omega_c$) clearly obeys the law $\mathcal{D}(\omega)\propto\omega$, as discussed in Sec. IV.B.3. Vibrational excitations in this frequency regime behave as *phonons*.[5]

The region in the vicinity of ω_c is the crossover region between *phonons* and *fractons* [Fig. 3(b)]. It should be stressed that the DOS is smoothly connected in this region, exhibiting neither a notable steepness nor a hump in the vicinity of ω_c. It is remarkable that the DOS does not follow the $\omega^{1/3}$ dependence above $\omega\simeq1$. The interpretation on this is given in Sec. V.A.4 in connection with the discussion of the missing modes.

b. Three-dimensional case

The absence of the hump in the crossover region has also been demonstrated in the case of $d=3$ percolating

[4]The force constants K_{ij} have a different sign from the definition of the dynamical matrix elements Φ_i^j normally used in the field of lattice dynamics. See Chap. IV of the book by Born and Huang (1954).

[5]It is known that excitations in disordered systems with the Euclidean dimension $d\leq2$ should be localized (Abrahams *et al.*, 1979). In this sense, phonons mentioned here are localized, but weakly, whereas fractons are strongly localized in the sense of the Ioffe-Regel criterion (see Sec. V.B.2).

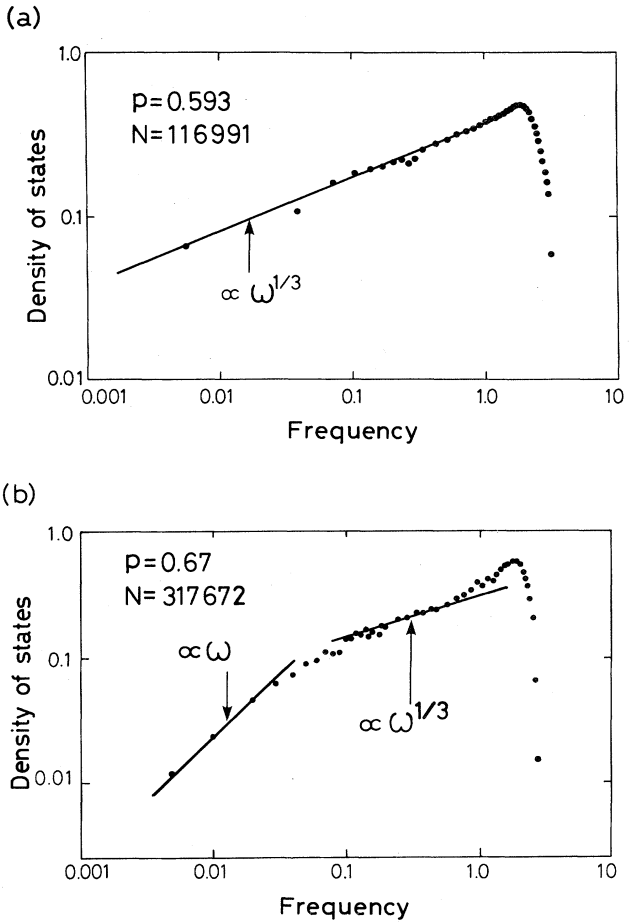

FIG. 3. Density of states for $d=2$ site-percolating networks at two different concentrations: (a) The density of states per site at the percolation threshold $p_c=0.593$. The network is formed on a 700×700 square lattice and contains 116,991 atoms. (b) The density of states per site at $p=0.67$ formed on a 700×700 square lattice. The network size is 317 672. Solid circles indicate the numerical results. The straight lines are only meant as a guide to the eye. After Yakubo and Nakayama (1989a).

networks (Yakubo and Nakayama, 1989a). The DOS of a percolating network at $p=0.4$ ($p_c=0.312$) formed on a $70\times70\times70$ simple cubic lattice is shown in Fig. 4. The network size is $N=122\,448$. The DOS in the frequency region $0.1<\omega<1$ is proportional to $\omega^{1/3}$, as was found in $d=2$. The DOS in the low-frequency regime ($\omega\ll0.1$) obeys the Debye law $\mathcal{D}(\omega)\propto\omega^2$, where at this concentration the phonon-fracton crossover frequency ω_c is close to 0.1. A *sharp* peak at $\omega=1$ in Fig. 4 is attributed to vibrational modes of a single site connected by a single bond to a relatively rigid part of the network.

It is clear that no steepness or hump of the DOS exists in the crossover region in the vicinity of ω_c. This feature is also found in the results by Grest and Webman (1984) for $d=3$ percolating networks. They found that the phonon-fracton crossover clearly exists for their systems. The behavior of the DOS at the phonon-fracton crossover has been determined from mean-field treatments

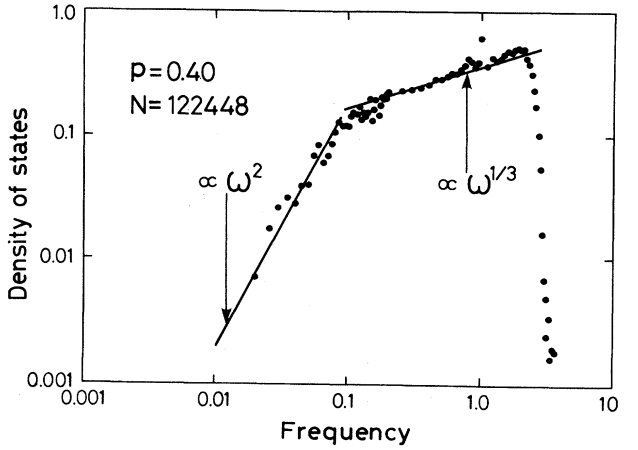

FIG. 4. Density of states per site for a $d=3$ site-percolating network at $p=0.4$ formed on a $70\times70\times70$ simple cubic lattice. The network size is $N=122\,488$. After Yakubo and Nakayama (1989a).

(Loring and Mukamel, 1986; Korzhenevskii and Luzhkov, 1991). In particular, Loring and Mukamel (1986) suggested a smooth transition of the DOS at the phonon-fracton crossover, in contrast to the prediction of the effective-medium theory (Tua *et al.*, 1983; Derrida *et al.*, 1984; Entin-Wohlman *et al.*, 1984; Tua and Putterman, 1986) or the scaling theory (Aharony *et al.*, 1985a, 1985b, 1987b).

2. Density of states: Bond percolation with scalar elasticity

The other percolating network, bond percolation (BP), shows some interesting differences from site percolation (SP) networks. The difference in geometrical structure between SP and BP is short range, as mentioned in Sec. II.C. As shown in Fig. 2, the fractal nature of the network extends to very short ranges for BP. The DOS and the integrated DOS have been computed for large-scale ($d=2$, 3, and 4) BP networks (Nakayama, 1992).

In Figs. 5 and 6, the DOS and the integrated DOS per atom are shown by the solid squares for a $d=2$ BP network at $p_c=0.5$ formed on a 1100×1100 square lattice ($N=657\,426$) with periodic boundary conditions. The fracton dimension $\tilde{d}$ is obtained as $\tilde{d}=1.33\pm0.01$ from Fig. 5, whereas the data in Fig. 6 indicate the value $\tilde{d}=1.325\pm0.002$. The DOS and the integrated DOS for $d=3$ BP networks are also computed, with results exhibited in Figs. 5 and 6 by the solid triangles (middle). These data show the averaged DOS and DOS integrated over three samples at the percolation threshold $p_c(=0.249)$. The networks, formed on $100\times100\times100$ cubic lattices, have 155 385, 114 303, and 143 026 atoms. The fracton dimension $\tilde{d}$ is obtained as $\tilde{d}=1.31\pm0.02$ from a least-squares fit, using the data of Fig. 5. It should be mentioned that $\tilde{d}$ takes the value $\tilde{d}=1.317\pm0.003$ when using the data of Fig. 6.

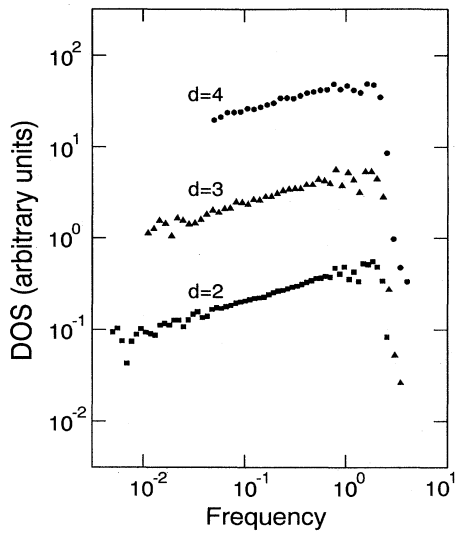

FIG. 5. DOSs per atom for $d=2$, $d=3$, and $d=4$ bond-percolating networks at $p=p_c$. The angular frequency ω is obtained in units of mass $m=1$ and force constant $K=1$. The networks are formed on 1100×1100 ($d=2$), $100\times100\times100$ ($d=3$), and $30\times30\times30\times30$ ($d=4$) lattices with periodic boundary conditions, respectively. After Nakayama (1992).

The DOS and the integrated DOS of $d=4$ BP networks at $p_c=0.160$, formed on $30\times30\times30\times30$ quartic lattices, are shown, respectively, in Figs. 5 and 6 by the solid circles, obtained by averaging over 15 samples. The network sizes are $N=8410\sim64\,648$. The DOS in the frequency region $0.12<\omega<0.9$ clearly shows a power law, as was found in the $d=3$ case. The fracton dimension $\tilde{d}$ is estimated to be $\tilde{d}=1.31\pm0.03$ from the least-squares fitting using the data of Fig. 5.

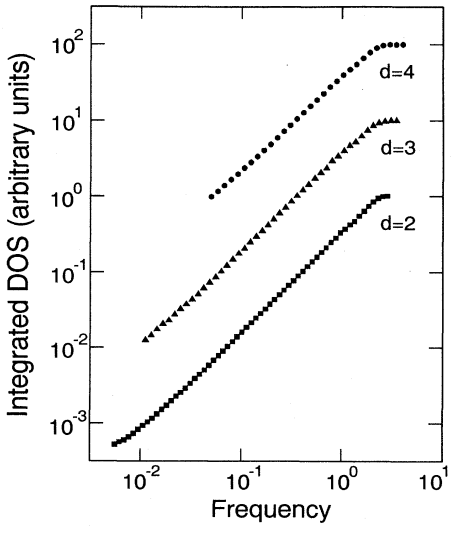

FIG. 6. Integrated DOSs per atom at $p=p_c$ for $d=2$, $d=3$, and $d=4$ bond-percolating networks. The symbols correspond to those in Fig. 5. After Nakayama (1992).

It should be noted that, from these values of $\tilde{d}$, the conductivity exponents μ can be determined using Eq. (4.15) as $\mu=1.288$ for $d=2$, $\mu=2.02$ for $d=3$, and $\mu=2.45$ for $d=4$. The value μ for $d=2$ is obtained using the exact values for β and ν in Eq. (4.15). The values of μ for $d=3$ and $d=4$ are calculated by substituting the values obtained by Monte Carlo calculations (Grassberger, 1986) into Eq. (4.15), namely, $\beta=0.43$ and $\nu=0.88$ for $d=3$, and $\beta=0.65$ and $\nu=0.68$ for $d=4$.

3. Density of states: Vector elasticity

We have discussed the dynamical properties of percolating networks with scalar displacements in Sec. V.A.1 and V.A.2. In most vibrational systems under the conditions set forth by Feng (1985a, 1985b), the vector nature of atomic displacements becomes crucial. Percolating networks with rotationally invariant vector elastic forces have different critical exponents for elastic moduli from those of the scalar forces (Benguigui, 1984; Feng and Sen, 1984; Feng *et al.*, 1984; Kantor and Webman, 1984; Bergman, 1985; Deptuck *et al.*, 1985; Feng, 1985a, 1985b; Feng and Sahimi, 1985; Roux, 1986; Sahimi, 1986; Arbabi and Sahimi, 1988; Sahimi and Arbabi, 1991). The same corresponding relation as that for the scalar displacement (the mapping of the diffusion problem onto the vibrational problem) is more difficult to express because of the significant additional complication of the vector nature of the displacements. The Hamiltonian taking vector displacements into account is given by (Keating, 1966)

$$H=\frac{1}{2}\sum_i m\dot{\mathbf{u}}_i^2+\frac{1}{2}\alpha\sum_{ij}K_{ij}[(\mathbf{u}_i-\mathbf{u}_j)\cdot\mathbf{r}_{ij}]^2 + \frac{1}{2}\beta\sum_{ijk}K_{ij}K_{ik}(\Delta\theta_{jik})^2 . \tag{5.2}$$

Here $\mathbf{u}_i$ is the vector displacement of the ith atom with unit mass ($m=1$); $\mathbf{r}_{ij}$, the unit vector between nearest neighbors $\langle ij\rangle$; and $\Delta\theta_{ijk}$, the small change in angle between bonds $\langle ij\rangle$ and $\langle ik\rangle$ due to the displacements of atoms.[6] The parameter K_{ij} takes the value unity if both sites i and j are occupied by atoms; otherwise, $K_{ij}=0$ and α and β are the bond-stretching and the bond-bending force constants, respectively. The rigidity threshold of this system is identical to the percolating threshold p_c.

Kantor and Webman (1984), Feng (1985a, 1985b), and Webman and Grest (1985) have applied the *nodes-links-blobs* model (described in Sec. II.A) to predict the dy-

[6]It should be emphasized that, for square or cubic lattices, both the equilibrium angles $\theta_{ijk}=\pi/2$ and π should be involved in this Hamiltonian. From the model taking into account only $\theta_{ijk}=\pi/2$, the angular force along linear links becomes irrelevant, so that the rigidity threshold becomes larger than the percolation threshold.

namic properties of percolating networks with bond-bending force constants. That model describes well the features of percolating networks in which the backbone consists of a network of quasi-one-dimensional strings (*links*), tying together a set of more strongly bonded regions (*blobs*). The typical separation of the *nodes* forming the macroscopically homogeneous network is equal to the correlation length $\xi(p)$ (see Fig. 1).

There exist two kinds of characteristic length, $\xi(p)$ and l_c, for percolation networks with *vector* elasticity. The length $\xi(p)$ scaling as $|p-p_c|^{-\nu}$ is the correlation length, the crossover length scale from a homogeneous to a fractal structure. The mechanical length l_c determines the crossover length scale *below* which bond-stretching motion is energetically favorable and *above* which the bond bending becomes dominant. This crossover length l_c depends only on the force constants α and β, namely, $l_c \propto \sqrt{\beta/\alpha}$, as shown below. One can connect the characteristic lengths $\xi(p)$ and l_c with two characteristic frequencies, ω_ξ and ω_{l_c}, respectively.

a. Theoretical prediction based on the nodes-links-blobs model

Kantor and Webman (1984) claimed that the effective spring constant K of a *blob* of size $\xi(p)$ is given by

$$K^{-1} \propto \left[\frac{\alpha}{L_1}\right]^{-1} + \left[\frac{\beta}{L_1 \xi(p)^2}\right]^{-1}, \tag{5.3}$$

where the blobs are assumed to be perfectly *rigid* and L_1 denotes the number of links (red bonds). The critical behavior of the links (red bonds) was described by Coniglio (1982a, 1982b) using a renormalization-group argument. The mean number of red bonds varies with p as [see Eq. (2.13)]

$$L_1 \propto (p-p_c)^{-1} \propto \xi(p)^{1/\nu}. \tag{5.4}$$

If $\xi(p) \ll l_c$, where l_c is proportional to $\sqrt{\beta/\alpha}$, the first term of the effective spring constant Eq. (5.3) (stretching motions) dominates. One has

$$K \propto \frac{\alpha}{L_1}. \tag{5.5a}$$

This implies that the elastic energy of the system is primarily associated with the stretching force constant. For the case of $l_c \ll \xi(p)$, the bond-bending spring constant becomes dominant, and the effective force constant is

$$K \propto \frac{\beta}{L_1 \xi(p)^2}. \tag{5.5b}$$

Let us derive the formula for the DOS of "stretching" fractons according to the theories of Kantor and Webman (1984) and Feng (1985a, 1985b) for a system of size $L \ll \xi$. The DOS at the lowest finite frequency ω_L for this system takes the form

$$\mathcal{D}(\omega_L) = \frac{1}{L^{D_f} \Delta\omega},$$

where the level spacing $\Delta\omega$ is taken to be equal to the lowest finite frequency ω_L of a fractal structure with finite size L. This is expressed by

$$\Delta\omega = \omega_L \propto \left[\frac{K(L)}{M(L)}\right]^{1/2},$$

where $M(L)$ and $K(L)$ are the mass and the effective spring constant of the system at length scale L. The effective spring constant is obtained for $L \ll \xi \ll l_c$ from Eq. (5.5a),

$$K(L) \propto \frac{\alpha}{L_1} \propto L^{-1/\nu}, \tag{5.6}$$

where Eq. (5.4) is used, replacing $\xi(p)$ by L. Using the relation $M(L) \propto L^{D_f}$, the lowest frequency ω_L is expressed in terms of the length scale L as

$$\omega_L \propto L^{-(D_f+1/\nu)/2}.$$

By using this dispersion relation and replacing ω_L by an arbitrary frequency ω, we obtain the DOS for *stretching* fractons,

$$\mathcal{D}(\omega) \propto \omega^{2\nu D_f/(\nu D_f+1)-1}. \tag{5.7}$$

Note that the exponent is determined only through the *static* exponents D_f and ν. This is due to the assumption that one-dimensional links dominate the elastic properties, and that the blobs are assumed to be "rigid" (or *superconducting*[7]) [see Eq. (5.6)].

The nodes-links-blobs model predicts a direct relationship between the dynamic exponent μ and the static exponents. The conductance G of this model is given by

$$G \propto \frac{1}{L_1},$$

when the blobs are assumed to be superconducting. Using the relation between the conductivity σ and G, $G \propto \sigma L^{d-2}$ (see Sec. IV.B.1), the conductivity can be expressed as

$$\sigma \propto L^{2-d-1/\nu}.$$

This is written as a function of p, for L large (p close to p_c),

$$\sigma \propto (p-p_c)^{\nu(d-2)+1}.$$

As a result, one has[8]

---

[7]The conductivity σ_{ij} between site i and j corresponds to the elastic force constant K_{ij} in Eq. (5.2), as seen from the mapping relation between the resistive and elastic networks (de Gennes, 1976a).

[8]The value of μ given by Eq. (5.8) constitutes a lower bound for the conductivity exponent, except at $d=6$ (where it is exact). This is because blobs are assumed to be superconductors in this model, and the actual conductivity of the network is necessarily smaller than that predicted by the relation (5.8).

$$\mu=\nu(d-2)+1 . \tag{5.8}$$

By using Eq. (5.8) and the hyperscaling relation $D_f=d-\beta/\nu$, one can obtain the relation between D_f and μ. This yields, using Eq. (5.7) for stretching fractons,

$$\mathcal{D}(\omega)\propto\omega^{\tilde{d}_s-1} ,$$

where

$$\tilde{d}_s=\frac{2D_f}{2+(\mu-\beta)/\nu} . \tag{5.9}$$

Note that the exponent $\tilde{d}_s$ takes the same form as $\tilde{d}$ given in Eq. (3.15). Thus the nodes-links-blobs model for vector elasticity predicts that *stretching fractons* belong to the same universality class as scalar fractons. It should also be noted that the stretching elasticity is, in general, different from scalar because the stretching force constant becomes relevant only along the bond connection, whereas scalar displacements respond to any deformation. Nevertheless, under the condition $L\gg l_c$, they both belong to the same universality class.

Consider now the opposite case, $l_c\ll L\ll\xi(p)$. The effective spring constant K is given by Eq. (5.5), and bending motions become relevant. The equation corresponding to Eq. (5.6) becomes

$$K(L)\propto L^{-(1/\nu)-2} . \tag{5.10}$$

Using Eq. (5.10), we see that $\Delta\omega$ becomes

$$\Delta\omega\propto L^{-[D_f+(1/\nu)+2]/2} .$$

As a result, one has

$$\mathcal{D}(\omega)\propto\omega^{[2\nu D_f/(\nu D_f+2\nu+1)]-1} . \tag{5.11}$$

The elasticity exponent f for the Young's modulus Y is defined as

$$Y\sim(p-p_c)^f .$$

The critical exponent f can be derived in terms of the nodes-links-blobs model as follows: Because one has the relation between Y and K as $K\propto YL^{d-2}$ (this is analogous with the relation between the conductance and the conductivity), using Eq. (5.10) for the case $l_c\ll L\ll\xi$, one has the relation

$$Y\propto L^{-d-1/\nu} .$$

This implies that

$$f=\nu d+1 . \tag{5.12}$$

We should note that this relation also gives a lower bound for the dynamic exponent f, as explained in footnote 8. The rigorous bound is expressed through $\nu d+1\le f\le\nu d+\nu d_{\min}$ (Havlin and Bunde, 1991).

Inserting Eq. (5.12) into Eq. (5.11), we see that the DOS for *bending* fractons becomes

$$\mathcal{D}(\omega)\propto\omega^{\tilde{d}_b-1} ,$$

where

$$\tilde{d}_b=\frac{2D_f}{2+(f-\beta)/\nu} . \tag{5.13}$$

The dispersion relation for bending fractons is given by

$$\Lambda(\omega)\propto\omega^{-\tilde{d}_b/D_f} .$$

Comparing Eqs. (5.8) and (5.12), one has the relation between μ and f in the nodes-links-blobs model,

$$f=\mu+2\nu . \tag{5.14}$$

Because $\nu>0$, one has $f>\mu$ (Kantor and Webman, 1984; Webman and Kantor, 1984). This implies that $\tilde{d}_b<\tilde{d}_s$ $(=\tilde{d})$. The bending-fracton dimension $\tilde{d}_b$ for $2d$ percolating networks, using the known values $f=3.96$ (Sahimi, 1986), $\nu=4/3$, $\beta=5/36$, and $D_f=91/48$, is estimated to be ~0.78. This indicates that the DOS weakly diverges at very low frequencies. The value of the exponent f has been evaluated numerically (Feng and Sen, 1984; Feng and Sahimi, 1985; Arbabi and Sahimi, 1988) and experimentally (Benguigui, 1984; Deptuck *et al.*, 1985; Benguigui *et al.*, 1987; Forsman *et al.*, 1987; Sofo *et al.*, 1987). The upper/lower bounds for f, $3.67\le f\le4.17$ for $d=2$ and $3.625\le f\le3.795$ for $d=3$ percolating networks (Havlin and Bunde, 1991), provide bounds for $\tilde{d}_b$.

The vibrational correlation between blobs connected by zigzag chains longer than l_c becomes irrelevant for the stretching modes, as seen from Fig. 7. This implies that stretching fractons with very low eigenfrequencies do not exist, but bending fractons can (see footnote 6). This is the reason bending fractons become dominant in the regime below ω_{l_c}.

Liu and Liu (1985) have found for the Sierpinski gasket that bending fractons do not dominate over stretching fractons, in contrast with the case for percolating networks. They suggest that the disagreement is purely a result of geometry, namely, the Sierpinski gasket is stabilized by central forces alone, but percolating networks are not. In this connection, it is interesting to note the work by Garcia-Molina, Guinea, and Louis (1988) and succeeding comments by Tyc (1988), Roux, Hansen, and

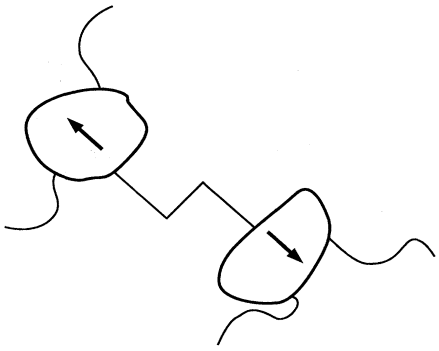

FIG. 7. Blobs connected by zigzag links.

Guyon (1988), and Day and Thorpe (1988), who consider triangular networks connected by central forces.

Alexander (1984) claimed theoretically that an elastic network with rotationally invariant elastic force constants is not the only approach for describing the elasticity of tenuous objects and amorphous materials. He showed that there are scalar contributions to the elastic energy in *stressed* systems, noting that real materials always have internal stresses.

This section can be summarized in the following manner.

(i) *Percolating networks with* $p > p_c$ *and* $\xi > l_c$. As shown in Fig. 8(a), fractons are excited in the frequency range $\omega_c \ll \omega$, whereas the vibrational excitations in the low-frequency regime ($\omega_c \gg \omega$) are phonons. There are two classes of localized modes, depending on the frequency regimes: $\omega_c \ll \omega \ll \omega_{l_c}$ and $\omega_{l_c} \ll \omega$. We call the former excitations "bending" fractons and the latter "stretching" fractons. Stretching fractons belong to the same universality class as fractons with scalar displacements under the nodes-links-blobs model (Feng, 1985b). This result holds only under the assumption of perfectly rigid blobs.

(ii) *The case of* $\xi(p) < l_c$. As illustrated in Fig. 8(b), phonons directly crossover to stretching fractons at ω_c, and bending fractons are not observed.

b. Simulated results for vector displacements

The first attempt to calculate the DOS for the vector displacement model was made by Webman and Grest (1985). They focused on the limit $\Lambda(\omega) \gg l_c$ when the bending fractons dominated, and treated a system with $N \sim 10^3$. They found that the DOS was weakly divergent at low frequencies. The DOS of excitations for $\Lambda(\omega) \gg l_c$ showed no crossover from bending to stretching fractons because ω_{l_c} is a high frequency. Lam and Bao (1985) used a recursion method to calculate the vibrational DOS of a site-diluted central-force elastic percolating network on a triangular lattice. They found the DOS in the fracton regime to be proportional to $\omega^{\tilde{d}_b - 1}$ with $\tilde{d}_b = 0.625$. This estimate should be regarded with caution because of the very narrow frequency interval in the fracton regime from which they estimated the value of $\tilde{d}_b$. Day, Tremblay, and Tremblay (1985) calculated the DOS of percolating networks formed on a triangular lattice with central forces and 60° bond-bending forces. They found values for the rigidity percolation threshold p_r and the fracton dimension $\tilde{d}_b$ in the ranges $0.4 \le p_r \le 0.405$ and $1.25 \le \tilde{d}_b \le 1.3$, respectively. The result suggests that the 60° bond-bending model does not fall into the same universality class as a full bond-bending model. In order to calculate the DOS for triangular elastic BP networks with central forces and full bond-bending forces, Böttger, Freyberg, and Wegener (1990) performed a homeomorphic coherent-potential approximation (HCPA), a recursion technique, and a replica trick calculation. They obtained $\tilde{d}_b = 1.0$ from the recursion method and the HCPA, whereas the replica method did not show fracton behavior. Liu (1984) calculated the fracton dimension of an elastic Sierpinski gasket using the relation $f/\nu = d - 1$ (Bergman and Kantor, 1984) and found $\tilde{d}_b = 2D_f/(D_f + 1)$. Arbabi and Sahimi (1988) performed numerical simulations for the elastic properties of $d = 3$ percolating networks in which both central and bond-bending forces were taken into account. Rahmani *et al.* (1993) considered the model incorporating the nearest- and next-nearest-neighbor interactions.

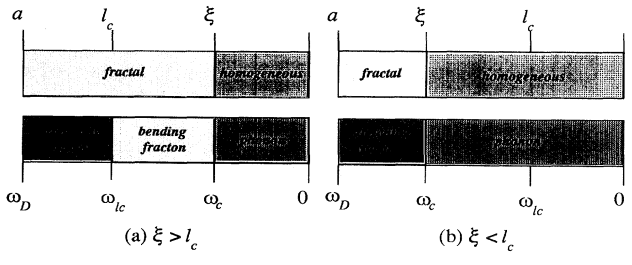

FIG. 8. Schematics illustrating the correspondence between length scale and frequency. The upper line is for the length scale where a is the lattice constant, and the lower one shows the corresponding frequency region.

In this subsection, we present simulation results for the DOS of large-scale percolating networks with vector displacements by Yakubo, Takasugi, and Nakayama (1990; see also Nakayama and Yakubo, 1990). We discuss first the crossover behavior of the DOS from bending to stretching fractons. For this purpose, Yakubo, Takasugi, and Nakayama considered the situation in which the bond-bending force constant β is larger than the stretching one α, so that the characteristic frequency ω_{l_c} is much smaller than the Debye cutoff frequency ω_D. The network was prepared at $p = p_c$, so that the condition $l_c < \xi$ always held. The calculated DOS is shown in Fig. 9, where the percolating network formed on a 500×500 square lattice has 53 673 occupied sites, and the set of the force constants $[\alpha, \beta]$ in Eq. (5.2) was chosen as [0.0133,0.133]. This network had a cutoff frequency $\omega_D = 2.0784$. The steplike decrease of the states in the high-frequency regime in Fig. 9 indicates that the stretching motions are not excited above some frequency ω_0, whose value is determined by the force constants α. For $\alpha = 0.0133$, this frequency ω_0 is estimated to be 0.2309 from the relation $\omega_0 = 2\sqrt{\alpha}$. This value coincides with the observed value in Fig. 9.

In order to clarify the individual contributions from the bending or stretching motions, the ratio of the potential energies [Eq. (5.2)] was calculated as a function of frequency ω. The solid curve in Fig. 9 shows the ratio between the potential energy attributed to the stretching motion ($E_{\rm st}$) and the total potential energy ($E_{\rm tot}$) obtained by substituting the displacements of calculated eigenmodes into the potential-energy expression of Eq.

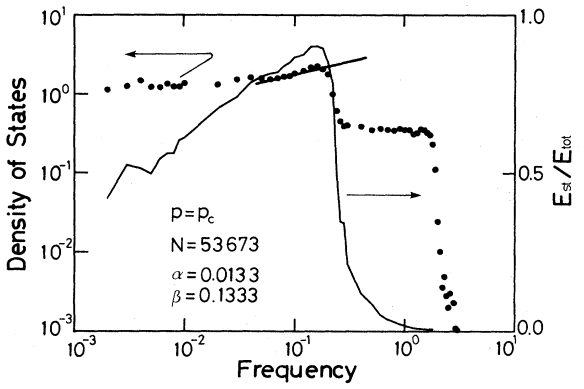

FIG. 9. Calculated density of states, shown by the solid circles. The network is formed on a 500×500 square lattice at the percolation threshold p_c with 53 673 sites. Force constants α and β are taken as 0.0133 and 0.1333, respectively. The straight line through solid circles is only a guide to the eye for the law $\mathcal{D}(\omega) \propto \omega^{1/3}$. The solid curve indicates the ratio of potential energy E_{st}/E_{tot} as a function of frequency. After Yakubo, Takasugi, Nakayama (1990).

(5.2). The crossover frequency ω_{l_c} is estimated from the condition $E_{st}(\omega)/E_{tot}(\omega)=\frac{1}{2}$, leading to $\omega_{l_c} \simeq 0.005$. The DOS in the vicinity of ω_{l_c} is independent of frequency. The crossover region from bending to stretching fractons extends over at least two orders of magnitude in frequency. This is because the ratio $E_{st}(\omega)/E_{tot}(\omega)$ increases logarithmically, as shown in Fig. 9. This observation is in contrast with the sharp crossover from phonons to fractons for scalar displacements described in Sec. V.A.1.

The straight line through the solid circles in Fig. 9 is drawn according to the law $\mathcal{D}(\omega) \propto \omega^{1/3}$ [see Eq. (5.9)]. It is not clear from the data of Fig. 9 in the frequency region between ω_{l_c} and ω_0 that the $\omega^{1/3}$ law holds. This is crucial for decreasing frequencies. A physical interpretation of this discrepancy has been given in Sec. V.A.3.a.

In order to clarify the contribution of bending fractons, the DOS for the case $\beta/\alpha=0.01$ and 1.0 has been calculated. These sets of force constants allow exclusive examination of the DOS for the bending-fracton regime because the stretching-fracton regime is shifted into the high-frequency region. Figures 10(a) and 10(b) show the results for the DOS and the integrated DOS, respectively, for percolating networks at $p=p_c$ for the same network as that of Fig. 9. The sets of force constants $[\alpha,\beta]$ in Eq. (5.2) were taken as [1.0,0.01] (solid circles) and [0.12,0.12] (open circles), respectively [see Fig. 10(a)]. The cutoff frequencies are the same as the previous cutoff frequency, $\omega_D=0.2784$, by virtue of the above choice of force constants. The DOS, given by solid circles in Fig. 10(a), weakly diverges as $\omega \to 0$, in accord with the theory by Feng (1985b). The value of the bending-fracton dimension $\tilde{d}_b$ obtained by a least-squares fitting from Fig. 10 is $\tilde{d}_b=0.79$. The straight lines on the left-hand side through the solid and open circles in Fig. 10(a) [Fig. 10(b)] are drawn according to $\omega^{\tilde{d}_b-1}$ ($\omega^{\tilde{d}_b}$) with $\tilde{d}_b=0.79$. This value agrees well with the predicted value ($\tilde{d}_b \simeq 0.78$), in contrast with the case of stretching fractons.

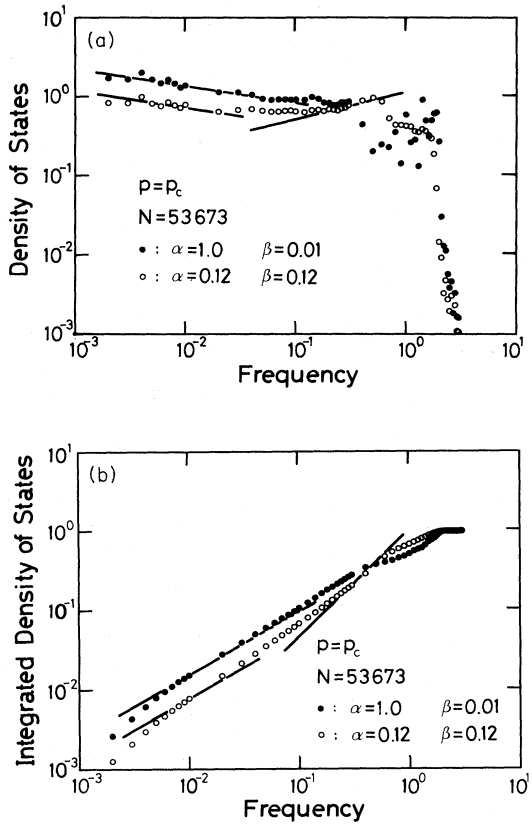

FIG. 10. Density of states (a) and the integrated density of states (b) of percolating networks with vector displacements. Networks have the same structure as that of Fig. 9. Solid circles indicate the result for the net with stretching force constant $\alpha=1.0$ and bending force constant $\beta=0.01$. Open circles are for $\alpha=\beta=0.12$. The straight lines on the left-hand side of (a) and (b) are drawn by least-squares fitting, indicating a law proportional to $\omega^{\tilde{d}_b-1}$ and $\omega^{\tilde{d}_b}$ with $\tilde{d}_b=0.79$, respectively. The straight lines on the right-hand side indicate a density of states proportional to $\omega^{1/3}$ and $\omega^{4/3}$, respectively. After Yakubo, Takasugi, and Nakayama (1990).

In the case of $\beta/\alpha=0.01$ (solid circles in Fig. 10), the mechanical length scale l_c becomes close to the lattice constant, resulting in the crossover frequency ω_{l_c}'s becoming too large to distinguish the crossover frequency region. For the case of $\beta/\alpha=1.0$ (open circles in Fig. 10), the crossover frequency can be estimated from the evaluation of E_{st}/E_{tot} as in the case of Fig. 9. The crossover frequency ω_{l_c} from bending to stretching fractons becomes close to $\omega \simeq 0.1$. Note that the simulation does not exhibit any noticeable change in frequency dependence of the DOS around crossover, as shown by the open circles in the vicinity of $\omega \simeq 0.1$. The DOS for the case $\beta/\alpha=1.0$ does not exhibit a distinct crossover to stretching fractons at ω_{l_c}. Similar behavior is found for

the case $\beta/\alpha=10.0$ in Fig. 9. For comparison, the lines on the right-hand side are proportional to $\omega^{1/3}$ ($\omega^{4/3}$). Note that the agreement with the data is unsatisfactory. Furthermore, it should be emphasized that the magnitudes of the DOS in the bending-fracton regimes are different for the two sets of force constants (see the difference between solid and open circles in Fig. 10). We shall show that this implies that the missing modes tend to accumulate in the high-frequency region ($\omega>\omega_0$) (see the next subsection).

In this subsection, simulated results for the DOS with vector displacements have been presented. In the case $\beta\gg\alpha$ (strong bending force), stretching fractons are excited in the high-frequency regime. It has been shown that the crossover region from bending to stretching fractons is rather broad. The opposite choice of force constants, such as the case of open circles shown in Fig. 10, makes it difficult to clarify the bending-to-stretching crossover in the DOS. It has been shown that the bending-fracton dimension takes a value $\tilde{d}_b\simeq 0.79$ for $d=2$ percolating networks. This is close to the predicted value from scaling theory. However, the calculated DOS for stretching fractons is not in accord with the value $\tilde{d}_s=4/3$. The results given in this section will be useful in discussing the characteristics of the DOS for real disordered materials in which the vector nature of displacements is crucial.

4. Missing modes in the density of states

a. Missing modes at low frequencies: scaling arguments

The simulation results for the DOS for scalar displacements confirmed that the crossover between the phonon and fracton regimes is smooth, with no visible accumulation of modes or a "hump" in the DOS around the crossover frequency ω_c (Yakubo and Nakayama, 1987a, 1989a, 1989b; Russ *et al.*, 1989; Li *et al.*, 1990; Royer *et al.*, 1992). This is in accord neither with earlier predictions based on scaling considerations (Alexander *et al.*, 1983; Aharony *et al.*, 1985a, 1985b, 1987b), nor with arguments based on the effective-medium approximation (Derrida, 1984; Derrida *et al.*, 1984; Sahimi, 1984), nor with the results given by a recursion technique (Lam *et al.*, 1985). The scaling considerations attributed the origin of this hump to the fact that the crossover from fractons to phonons is accompanied by "missing modes" in the normalized DOS. In this subsection, the whereabouts of these missing modes are discussed according to the work of Yakubo, Courtens, and Nakayama (1990).

The early scaling arguments about missing modes should first be recalled. The DOS of a percolating network above threshold ($p>p_c$) was characterized by two regimes: the fracton DOS, $\mathcal{D}_{\rm fr}(\omega,p)\propto\omega^{\tilde{d}-1}$, for high frequencies ($\omega>\omega_c$), and the phonon DOS, $\mathcal{D}_{\rm ph}(\omega,p)\propto\omega^{d-1}$, for low frequencies ($\omega<\omega_c$). Assuming *strict* similarity in the fractal regime, one expects $\mathcal{D}_{\rm fr}(\omega,p)=\mathcal{D}_{\rm fr}(\omega,p_c)$, where the DOS per particle is normalized by $\int_0^\infty\mathcal{D}(\omega)d\omega=1$. Because d is always larger than $\tilde{d}$, $\mathcal{D}_{\rm ph}$ is smaller than $\mathcal{D}_{\rm fr}$ when the latter is extrapolated to phonon frequencies. As the integration of $\mathcal{D}_{\rm fr}(\omega,p_c)$ is normalized to unity, some modes must be missing for $\mathcal{D}(\omega,p>p_c)$ in view of the existence of the phonon regime. Their spectral weight must be recovered somewhere, and it was argued that the most reasonable place for accumulation is near ω_c, leading to a hump in the DOS and to a corresponding hump in the low-temperature specific heat (see Fig. 11). The main point is that a hump is seen neither in simulations of the phonon-fracton crossover nor in actual experiments on silica aerogels (Courtens *et al.*, 1987a, 1987b, 1988; Courtens, Pelous, Vacher, and Woignier, 1987; Courtens and Vacher, 1988; Conrad *et al.*, 1990; Buchenau, Morkenbusch, *et al.*, 1992), the latter to be presented in Sec. V.C.2.

b. The hump at high frequencies: geometrical interpretation

To explain the absence of a hump in the crossover region, we write the scaling form for the DOS of a percolating network for $p>p_c$:

$$\mathcal{D}(\omega,p)=A(p)\omega^{\tilde{d}-1}F(\omega/\omega_c)\ . \tag{5.15}$$

For an infinite percolating network, the phonon-fracton crossover frequency scales as $\omega_c=\Omega(p-p_c)^{\nu D_f/\tilde{d}}$. The crossover frequency ω_c is defined as the intercept of the asymptotic phonon and fracton lines in a double-logarithmic presentation of the DOS vs ω (Alexander *et al.*, 1983). The scaling function takes the forms $F(x)=1$ for $x\gg 1$ and $F(x)=x^{d-\tilde{d}}$ for $x\ll 1$. Equation (5.15) yields a prediction for the p dependence of $\mathcal{D}(\omega,p)$ in the phonon regime,

$$\mathcal{D}(\omega)\propto A(p)(p-p_c)^{\nu D_f(\tilde{d}-d)/\tilde{d}}\omega^{d-1}\ .$$

Simulation results are illustrated in Fig. 12, which exhibits the validity of Eq. (5.15) in the phonon-fracton crossover region. Because the ordinate in Fig. 12 is the

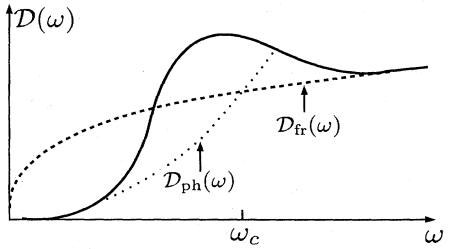

FIG. 11. Crossover of the DOS (solid line). The dotted (dashed) lines represent the continuation of the phonon (fracton) asymptotic behavior into the crossover regime.

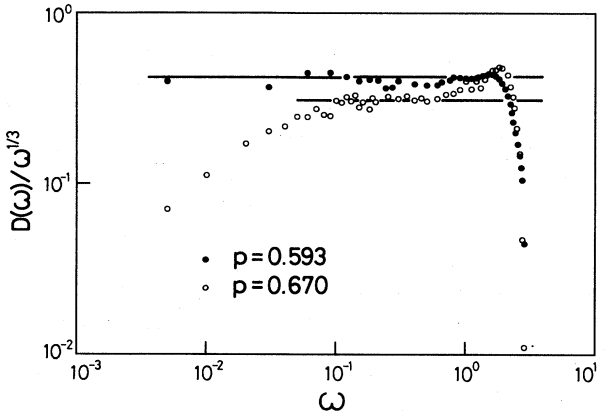

FIG. 12. Calculated density of states, normalized to one particle, divided by $\omega^{1/3}$, and plotted as a function of the frequency ω. The solid circles correspond to the critical percolation density p_c. The open ones are for $p=0.67$. The horizontal lines are meant as guides to the eye. After Yakubo, Courtens, and Nakayama (1990).

quantity $\mathcal{D}(\omega)/\omega^{1/3}$, the fracton regime corresponds to a horizontal line of height $A(p)$. Data at $p_c=0.593$ are plotted as solid circles, where the network was prepared on a 700×700 lattice with $N=116{,}991$. The data for the DOS for a network with $p=0.67$ ($N=317{,}672$) are plotted as open circles. One can clearly discern the two regimes in Fig. 12, with a crossover frequency $\omega_c\simeq0.1$. It is clear that this simulation does not exhibit any noticeable hump near ω_c. Further, the magnitude of the DOS in the fracton regime is *different* in the two simulations, invalidating the equality $\mathcal{D}_{\rm fr}(\omega,p)=\mathcal{D}_{\rm fr}(\omega,p_c)$ assumed by Aharony *et al.* (1985a, 1985b, 1987b). This justifies a nontrivial dependence of $A(p)$ on p in Eq. (5.15). Finally, one notices that the two curves of Fig. 12 could not possibly be made to scale towards the upper end of the fracton range. This is the region where modes "missing" from the low-frequency regime have accumulated, exhibiting the violation of the scaling hypothesis of Eq. (5.15).

To understand these observations, it is helpful to consider the simple models illustrated in Fig. 13. From the Sierpinski gasket of Fig. 13(a), one can construct large-scale homogeneous systems in different ways. A first example, illustrated in Fig. 13(b), is the carpet treated by Southern and Douchant (1985). The modes of the simple gasket, Fig. 13(a), have been investigated in considerable detail by Rammal (1984a). They can be classified into "hierarchical" modes, where the density at $d=2$ peaks at $\omega=\sqrt{5}$, and into "molecular," or strongly localized, modes with a highest density near the upper cutoff at $\omega=\sqrt{6}$. These modes are only slightly modified by the higher coordination of a few sites ($z=6$) in Fig. 13(b). The higher z simply produces a few modes at frequencies above the Sierpinski gasket "band" in the region $\sqrt{6}<\omega<3$. One notes that $\omega=3$ is the upper cutoff of the $d=2$ triangular lattice. An alternative way to construct a large-scale homogeneous system is illustrated in Fig. 13(c). That model corresponds more closely to the intuitive picture of fractal networks that reach their correlation length by "growing into each other." In that case, the whole region $\sqrt{6}<\omega<3$ becomes rather densely populated with modes, at the expense of the DOS in the fracton regime. The corresponding "missing" spectral weight is rather uniformly distributed over the low-frequency region.

The above considerations can now be extended to percolation with a correlation length $\xi(p)$. The discussion is facilitated by adopting the *nodes-links-blobs* picture as illustrated in Fig. 1. The typical separation of the nodes forming the macroscopically homogeneous network equals the correlation length $\xi(p)$. With $\mathcal{D}_{\rm ph}=A(p)\omega/\omega_c^{2/3}$, and $\mathcal{D}_{\rm fr}=A(p)\omega^{1/3}$, one calculates the number of "missing modes" associated with the phonon regime, $M_{\rm ph}$, as

$$M_{\rm ph}\simeq\int_0^{\omega_c}(\mathcal{D}_{\rm fr}-\mathcal{D}_{\rm ph})d\omega$$
$$=\frac{1}{4}A(p)\omega_c^{\bar{d}}$$
$$=\frac{1}{4}A(p)\Omega^{\bar{d}}(p-p_c)^{\nu D_f}\ . \tag{5.16}$$

With $A(p)\simeq A(p_c)=0.4$ and $\Omega\simeq13$ from Fig. 12, one estimates $M_{\rm ph}\simeq3(p-p_c)^{\nu D_f}$. The number of occupied sites on the infinite network in the correlation volume for $d=2$, ξ^2, is ξ^2P_∞, where $P_\infty=P_0(p-p_c)^\beta$, with $\beta=5/36$ and $P_0\simeq1.53$. Hence the actual number of missing modes within the correlation area is $\simeq\xi^2P_\infty M_{\rm ph}\simeq3\Xi_0^2P_0$. Here Ξ_0 is defined by $\xi=\Xi_0|p-p_c|^{-\nu}$, independent of $p-p_c$ because the exponent $-2\nu+\beta+\nu D_f$ is identically zero. Using $\Xi_0=0.95$, we find the number of missing modes to be of the order of unity.[9] Thus there is one missing mode per area ξ^2. One should also note that, for any non-negligible ξ, the number $M_{\rm ph}$ relative to the total number of modes with $\omega<\omega_c$ is very small compared to one, the corresponding area in Fig. 12 being overemphasized by the logarithmic presentation.

Numerically more important is the number of missing modes $M_{\rm fr}$ produced by the depression of the fracton density from $A(p_c)$ to $A(p)$. Ignoring the hump near the high-frequency cutoff, this number is

$$M_{\rm fr}=\int_0^{\omega_D}[\mathcal{D}_{\rm fr}(\omega,p_c)-\mathcal{D}_{\rm fr}(\omega,p)]d\omega=1-\frac{A(p)}{A(p_c)}\ . \tag{5.17}$$

[9]There is a certain degree of arbitrariness in the absolute definition of $\xi(p)$, as illustrated, for example, in the work of Kapitulnik *et al.* (1983), where two rather different values are found (one in their Fig. 2, and another further in the text). The value of Ξ we derived was taken from the mean-square size of the fracton. The value of P_0 is taken from a series analysis using Padé approximants, by Sykes, Gaunt, and Glen (1976a).

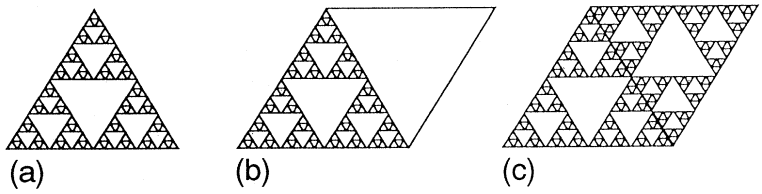

FIG. 13. Lattice models based on the Sierpinski gasket: (a) a gasket up to the fourth level of hierarchy; (b) a unit cell made of such a gasket and an empty triangle; (c) a denser unit cell, possibly more representative of real fractal objects, obtained by the junction of two gaskets, such as in (a).

For the second equality, use was made of Eq. (5.15) and of the fact that the integral of $\mathcal{D}_{\rm fr}(\omega,p_c)$ over the full frequency range is normalized to unity. The simulated values of $M_{\rm fr}$ for several values of p are shown in Fig. 14, demonstrating a critical behavior, $M_{\rm fr}=M_0(p-p_c)^m$. The solid line, drawn with $m=\frac{4}{3}$, gives $M_0\simeq 4.1$.

This behavior can be explained as follows. Within the area ξ^2, a number of sites have higher coordination than in the network at p_c. The number of these sites is much larger than the small number of nodes that eventually form the homogeneous system and whose relative density is $1/(\xi^2 P_\infty)\simeq M_{\rm ph}$. Based on the naive picture of Fig. 13(c), one could expect that the number of these sites is proportional to the length of the perimeter, i.e., $\propto \xi^{d-1}$. In the case of the percolation cluster, the perimeter at ξ is a fractal of dimension D_f-1, and its length is ξ^{D_f-1}. The total number of occupied sites within this perimeter being ξ^{D_f}, the relative number of modes rejected to high frequency is then $M_{\rm fr}\simeq \xi^{D_f-1}/\xi^{D_f}\propto (p-p_c)^\nu$. In fact, taking a square of side ξ, the ratio of occupied perimeter sites to occupied area is $M_{\rm fr}=4/\xi\simeq 4.2(p-p_c)^\nu$; and one notices that $\nu=4/3$ for the $d=2$ case. Both the exponent and the amplitude agree well with the simulated values (Fig. 14). This supports the validity of this interpretation. Although there is, strictly speaking, no well-defined "perimeter" at ξ for which the connectivity of all sites increases, the concept appears to remain well defined from an average point of view. The effect of the higher connectivity is to depress the number of modes throughout the fracton regime.

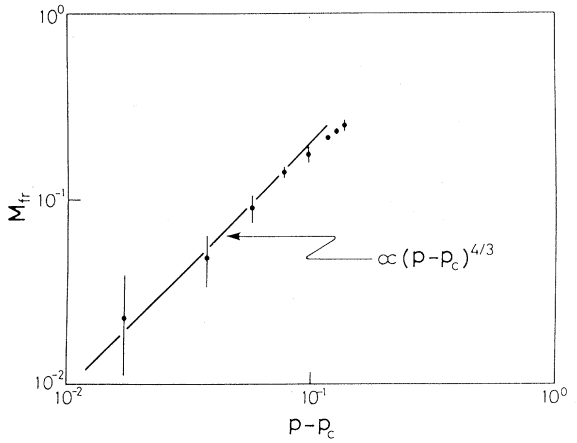

FIG. 14. Relative number of missing modes, $M_{\rm fr}$, produced by the depression in the fracton DOS, presented vs $p-p_c$. The error bars are standard deviations. The straight line of slope $\nu=\frac{4}{3}$ is shown to agree with the asymptotic behavior for $p\to p_c$. After Yakubo, Courtens, and Nakayama (1990).

B. Localized properties of fractons

1. Mode patterns of fractons

The first realization of mode patterns of large-scale fractons was obtained by applying the numerical method mentioned in Sec. V.A (Yakubo and Nakayama, 1987a, 1989b). The network at $p_c=0.593$ was formed on a 700×700 square lattice with the number of occupied sites $N=169\,576$. The magnified color picture of the mode pattern of a fracton (snaphot) on a $d=2$ network is shown in Fig. 1 in the paper by Yakubo and Nakayama (1989b), where the eigenmode belongs to an angular frequency $\omega=0.01$. To clarify the details more directly, the cross section of amplitudes of the mode pattern is shown in Fig. 15. Figure 15 exhibits this cross section of the vibrational amplitudes for the fracton mode along the lines A and B drawn in Fig. 1 in the paper by Yakubo and Nakayama (1989b). The solid circles and the open circles represent the occupied sites and the vacant sites in the percolating network, respectively. One sees that the fracton core (the blue part with the largest amplitude) possesses very clear boundaries for the edges of the excitation, almost of steplike character, with a long tail in the direction of the weak segments. This is in contrast with the case of homogeneously extended modes (phonons) in which the change of their amplitudes is correlated smoothly over a long distance. It should be noted that displacements of atoms in "dead ends" (weakly connected portions in the percolating network) move in phase, and the vibrational amplitudes fall off sharply at their edges. In addition, it is interesting to note that the tail (the portion spreading from the center of the figure in the upper-right direction) extends over a very large distance with many phases changes.[10]

[10]This is a natural consequence of the orthogonality condition of eigenmodes, since vibrational modes belonging to eigenfrequencies $\omega^2\neq 0$ must be orthogonal to the mode of $\omega^2=0$ (uniform displacement).

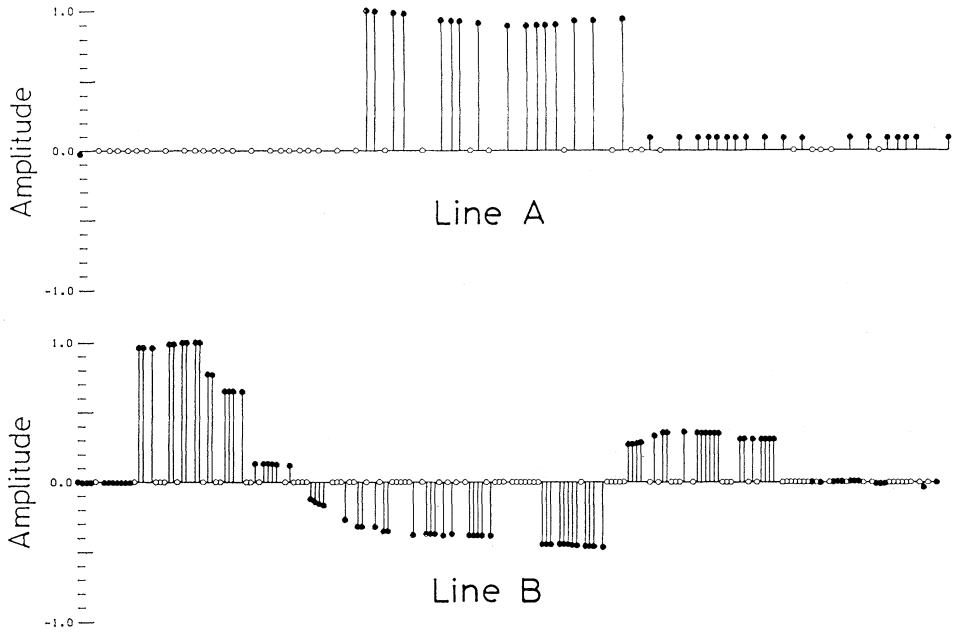

FIG. 15. Cross sections of a single fracton shown in Fig. 1 in the paper by Yakubo and Nakayama (1989b). The upper figure corresponds to line A in Fig. 1 in the paper and the lower one to line B. The signs of the amplitudes (plus and minus) are switched for convenience. After Yakubo and Nakayama (1989b).

2. Ensemble-averaged fractons

Localization of waves in disordered systems has received much attention since the work of Anderson (1958). The progress made in understanding electron localization (Mott, 1967; Thouless, 1974; Abrahams *et al.*, 1979) has had implications for other excitations in disordered media such as phonons, photons, and spin waves (John *et al.*, 1983; Akkermans and Maynard, 1985). In particular, it was predicted by John, Sompolinsky, and Stephen (1983) that the vibrational excitations on $d \leq 2$ disordered systems would always be localized, and the localization length Λ would behave as $\Lambda \propto \exp(1/\omega^2)$ for $d=2$ and as $\Lambda \propto \omega^{-2}$ for $d=1$.

Rammal and Toulouse (1983) applies the scaling theory of localization (Abrahams *et al.*, 1979) to fracton excitations on a percolating network. The key parameter in the scaling theory, as described in Sec. IV.B.1, is the exponent β_L, which they expressed in terms of the fractal and fracton dimensions D_f and $\tilde{d}$ as

$$\beta_L = \frac{D_f}{\tilde{d}}(\tilde{d}-2) .$$

Because $\tilde{d} \approx \frac{4}{3}$ for percolation in any Euclidean dimension d, it is clear that fractons are always localized. In this context, Entin-Wohlman, Alexander, and Orbach (1985; see also Alexander, Entin-Wohlman, and Orbach, 1985a, 1985b, 1985c, 1986a, 1986b, 1987) supposed that the ensemble average of the fracton wave function on percolating networks was localized with the form

$$\langle \phi_{\rm fr} \rangle \propto \exp\left[-\left[\frac{r}{\Lambda(\omega)} \right]^{d_\phi} \right] , \tag{5.18}$$

where $\Lambda(\omega)$ is the frequency-dependent fracton length scale (dispersion or localization), and r a radial distance from the center. The exponent d_ϕ denotes the strength of localization. Note that this is an ensemble-averaged *envelope* function. Many studies of the value of d_ϕ have been performed: theoretical (Aharony *et al.*, 1987b; Harris and Aharony, 1987; Levy and Souillard, 1987; Bunde *et al.*, 1990; Aharony and Harris, 1992; Bunde and Roman, 1992), experimental (Tsujimi *et al.*, 1988), and numerical (de Vries *et al.*, 1989; Nakayama *et al.*, 1989; Li *et al.*, 1990; Lambert and Hughes, 1991; Roman *et al.*, 1991; Terao *et al.*, 1992). Levy and Souillard (1987) suggested that $d_\phi = D_f/\tilde{d}$. For $d=2$, because $D_f = 91/48 \sim 1.896$, this gives $d_\phi = 1.42$. Localized states with $d_\phi > 1$ are called superlocalized modes. Harris and Aharony (1987) found that averaged fracton excitations decay exponentially ($d_\phi = 1$).

Van der Putten *et al.* (1992) have experimentally estimated the superlocalization exponent d_ϕ from measurements of the d_c conductivity of carbon-black-polymer composites. They obtained the value of the exponent $d_\phi = 1.94 \pm 0.06$ as well as the value of the conductivity exponent $\mu = 2.0 \pm 0.2$.

a. Shape of core region

The localized nature of fractons, focusing on the value of the exponent d_ϕ for the *core* region of fractons, has been numerically investigated by Nakayama, Yakubo, and Orbach (1989; see also Yakubo and Nakayama, 1990). They performed numerical simulations on $d=2$ percolation networks to determine d_ϕ for the cores of $2d$ fractons. The core has a large amplitude around the

center of a localized fraction ($r \lesssim \Lambda$), as described in Sec. V.B.1. They prepared nine $2d$ site-percolating networks at p_c formed on 700×700 square lattices in order to take an ensemble average. The maximum network size was $N = 171\,306$ and the minimum size was $N = 76\,665$. Smoothly varying ensemble-averaged mode patterns were obtained. The ensemble-averaged shape of the fracton core was calculated by averaging over 129 fractons at $\omega = 0.01$. They obtained $d_\phi = 2.3$.

In addition, d_ϕ and $\Lambda(\omega)$ were calculated for four different eigenfrequencies, $\omega = 0.005$, 0.006, 0.007, and 0.008, excited on five percolating networks. As seen from Fig. 16, the localization length $\Lambda(\omega)$ depended on frequency. The straight line drawn using least-squares fitting indicates that $\Lambda(\omega) \propto \omega^{-0.71}$, showing good agreement with the theoretical dispersion law $\Lambda(\omega) \propto \omega^{-\bar{d}/D_f}$ with $\bar{d}/D_f = 0.705$. For all those frequencies, they found $d_\phi = 2.3 \pm 0.1$, independent of ω. It is now understood that this large value of $d_\phi = 2.3$ applies only to the *core* region of fractons, and that two exponents are required to characterize the localized nature of fractons, namely, for the core and for the tail (Roman *et al.*, 1991).

b. Asymptotic behavior

The averaged profile of tails (asymptotic behavior) of fractons has been numerically investigated by de Vries, de Raedt, and Lagendijk (1989), Li, Soukoulis, and Grest (1990), Lambert and Hughes (1991), Roman, Russ, and Bunde (1991), and Terao, Yakubo, and Nakayama (1992). Roman, Russ, and Bunde (1991) have solved the vibrational equations for large percolation clusters (300 sheets) with $d = 2$, and have averaged over ten individual fracton modes for each frequency. The amplitudes $|\phi(r,\omega)|$ for typical fracton modes are exhibited in Fig. 17. The data

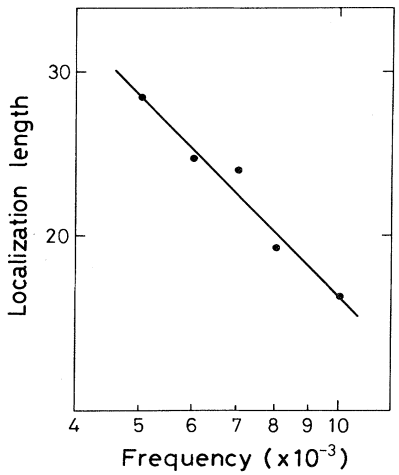

FIG. 16. Values of localization length $\Lambda(\omega)$ plotted as a function of frequency on a log-log scale. The straight line $[\Lambda(\omega) \propto \omega^{-0.71}]$ drawn using least-squares fitting shows that fractons in the ensemble follow the correct fracton dispersion law. After Yakubo and Nakayama (1989a).

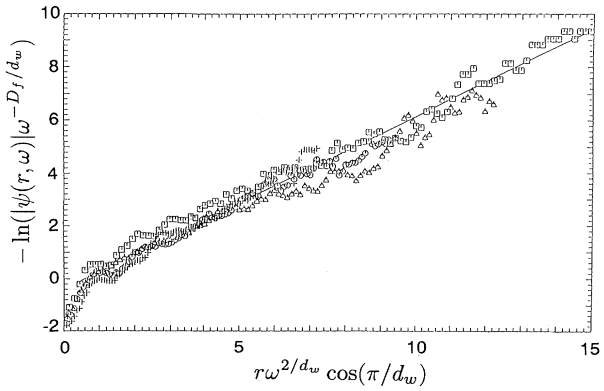

FIG. 17. Plot of $-\ln[|\phi(r,\omega)|\omega^{-D_f/d_w}]$ vs $r\omega^{2/d_w}\cos(\pi/d_w)$, with $D_f \cong 1.896$ and $d_w \cong 2.87$, for frequencies $\omega = 0.20$ (squares), 0.15 (triangles), 0.10 (circles), and 0.07 (crosses). After Roman, Russ, and Bunde (1991).

strongly support the value $d_\phi = 1$ and the expected frequency dependence of Λ. Note that a large crossover regime exists when $r \lesssim \Lambda$, with an effective exponent $d_\phi > 1$ which coincides numerically with the result of Nakayama, Yakubo, and Orbach (1989). Asymptotically, for $r \gg \Lambda$, the curves approach a straight line in a semilogarithmic plot, and hence $d_\phi = 1$.

Bunde and Roman (1992) have given an analytic explanation for the asymptotic behavior of fractons. For scalar vibrations, the envelope function of the fracton, $|\phi(r,\omega)|$, is related to the probability density $P(r,t)$ the probability of finding the random walker after time t at a site a distance r from its starting point:

$$P(r,t) = \int_0^\infty d\omega\, \mathcal{D}(\omega)|\phi(r,\omega)|\exp(-\omega^2 t) , \qquad (5.19)$$

where $\mathcal{D}(\omega)$ is the DOS normalized to unity. For a large class of networks, including percolating networks at p_c, $P(r,t)$ decays, upon averaging over typical configurations, as (Havlin and Bunde, 1989)

$$\ln P(r,t) \sim -[r/R(t)]^u, \quad u = \frac{d_w}{d_w - 1} , \qquad (5.20)$$

where d_w is the diffusion exponent defined in Eq. (3.12). Using the asymptotic result Eq. (5.20), one obtains $d_\phi = 1$ upon taking the inverse Laplace transform of Eq. (5.19) using the method of steepest descent, with $\Lambda(\omega)^{-1} \simeq a\cos(\pi/d_w)\omega^{2/d_w}$ and a a constant of order unity (Roman, Russ, and Bunde, 1991).

We warn the reader that the ensemble average of *matrix elements* will be very different, in general, from the matrix element using ensemble averages for the fracton functions (Nakayama, Yakubo, and Orbach, 1989). For example, the Raman-scattering intensity is proportional to the square of the elastic strain induced by fracton excitations. For this case, the ensemble average of the matrix element for *individual* fractons should be taken into account [see Eq. (6.5)].

c. Multifractal behavior

A multifractal analysis (see, for example, Paladin and Vulpiani, 1987), which originated from the study of turbulence (Mandelbrot, 1978), is useful for the analysis of the distribution of various physical quantities (measures) on fractal supports such as the voltage drop distribution on a random resistor network (Rammal, Tannous, Breton, and Tremblay, 1985; Rammal, Tannous, and Tremblay, 1985; de Arcangelis, Redner, and Coniglio, 1985, 1986; Coniglio, 1987), the growth probability of a diffusion-limited aggregate (DLA; see Meakin, 1986; Blumenfeld and Aharony, 1990; Mandelbrot and Evertsz, 1990; Schwarzer *et al.*, 1990), and the spatial profile of a localized excitation (Castellani and Peliti, 1986; Bunde, Havlin, and Roman, 1990; Evangelou, 1990; Evangelou, 1991; Schreiber and Grussbach, 1991, 1992; Bunde and Roman, 1992; Roman, 1992a). Such analyses give information about the distribution of physical quantities (measures) on a fractal support.

Consider a measure f_i on the ith site of a fractal structure of size L. The multifractal nature arises when the qth order moments of f_i, averaged by the distribution function $n(f,L)$, scale as

$$\langle f^q \rangle = \left\langle \sum_i^{L^{D_f}} f_i^q \right\rangle \sim L^{-\tau(q)}$$

with a *nonlinear* function $\tau(q)$. Typical examples of multifractal distributions are growth probabilities $\{p_i\}$ for DLA and voltage drops $\{V_i\}$ on percolating resistor networks. In many cases, the multifractal properties are related to a very broad distribution function $n(f,L)$, so that different moments of f are dominated by different parts of the distribution function.[11]

As mentioned in Sec. V.B.1, the profile of a fracton eigenfunction $\phi_{\rm fr}$ is extremely complicated, and the distribution function $n(|\phi_{\rm fr}|^2)$ of amplitudes should be very broad. It is natural to consider the possibility that such large fluctuations may show multifractal properties. Petri and Pietronero (1992; see also Petri, 1991) have performed a multifractal analysis for fracton wave functions on $d=2$ percolating networks. They calculated fracton eigenfunctions using a direct diagonalization technique and obtained the (Euclidean) length-scale dependence of the qth moments of the measures $|\phi_{\rm fr}^i|^2$, which are the squared amplitudes at the ith sites. Their results suggest that the function $\tau(q)$ is nonlinear with respect to q (see Fig. 18), showing multifractal behavior.

We note here that an exponentially decaying averaged wave function does not recover multifractal behavior for a Euclidean length scale. The distribution of $|\phi_{\rm fr}^i|^2$ does not exhibit multifractality, at least for $r \gg \Lambda$, where Λ is the localization length. Therefore the observed multifractality must arise from the core region $r \lesssim \Lambda$, as in the case of Anderson localization, for which localized wave functions within $r \lesssim \Lambda$ do have multifractal properties (Wegner, 1980). Since Petri and Pietronero (1992) chose relatively high frequency modes, the fracton cores handled by them are very small (of the order of a lattice constant).

Another kind of multifractal property for fracton wave functions was proposed by Aharony and Harris (1992), Bunde and Roman (1992), and Bunde *et al.*, (1992) that does not conflict with an exponentially decaying ensemble-averaged wave function. They introduced r-dependent moments $\langle |\phi_{\rm fr}(r,\omega)|^{2q} \rangle$, where $\phi_{\rm fr}(r,\omega)$ represents the amplitude of a fracton with frequency ω at a distance r from the center of the fracton mode. The angular bracket $\langle \cdots \rangle$ denotes the average over all fracton states with frequency ω and all possible realizations. An exponentially decaying wave function leads to the moment $\langle |\phi_{\rm fr}(r,\omega)|^{2q} \rangle$ decaying exponentially with r. This is not multifractal *in the usual sense.* However, if the moments take the form

$$\langle |\phi_{\rm fr}(r,\omega)|^{2q} \rangle \propto \exp\left[-y(q) \left[\frac{r}{\Lambda} \right]^{\zeta} \right], \tag{5.21}$$

where $y(q)$ is a nonlinear function with respect to q, the wave function $|\phi_{\rm fr}^i|$ can be regarded as multifractal under a *new definition* in which $\exp[-(r/\Lambda)^{\zeta}]$ is considered as the scale for fracton modes, instead of L.

Assuming that the moments of $\phi_{\rm fr}^i$ at a fixed chemical distance l from the center of a fracton are expressed as $\phi_q(l,\omega) \sim \exp[-ql/\Lambda]$, which holds for deep impurity states with energies far from the band edge (Harris and Aharony, 1987; Aharony and Harris, 1992), Bunde *et al.*

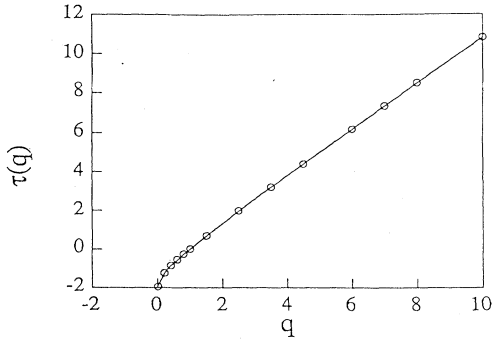

FIG. 18. Simulated results of $\tau(q)$ for a fracton at the band center ($\omega=0.5107$). After Petri and Pietronero (1992).

[11] In multifractal analyses, measures are usually normalized as $\sum_i f_i = 1$. For example, choosing the mass m_i of the ith site in a fractal network as the measure f_i, one should take $\langle m_i \rangle = L^{-D_f}$. The moments $\langle m_i^q \rangle$ are calculated as $\langle m_i^q \rangle = \sum_i^{L^{D_f}} m_i^q = L^{D_f} \cdot L^{-qD_f}$. Therefore the exponent $\tau(q)$ becomes $\tau(q) = D_f(q-1)$, namely, $\tau(q)$ is a linear function with respect to q. In this case the distribution is called unifractal. In general, the distribution function $n(f,L)$ can be expressed by a simple scaling form as $n(f,L) = f^x F(f^y/L)$ for unifractals.

(1992) have suggested that the moments of the fracton wave function obey the form Eq. (5.21). They have also predicted a critical value q_c below which, $q < q_c$, the moments $\langle |\phi_{\rm fr}(r,\omega)|^{2q} \rangle$ exhibit multifractal behavior for $r > r^*(q)$. Here, $r^*(q) \propto q^{-1/d_{\rm min}}$, where $d_{\rm min}$ describes the average chemical distance as $\langle l \rangle \propto r^{d_{\rm min}}$. For $q > q_c$, $\langle |\phi_{\rm fr}(r,\omega)|^{2q} \rangle$ has the simple *unifractal* exponential behavior $e^{-2qr/\Lambda}$. For multifractal fracton wave functions, the exponent $y(q)$ becomes proportional to $q^{1/d_{\rm min}}$ in the theory of Bunde *et al.* (1992). They have estimated a value for q_c from their numerical simulations using 50 fractons with frequencies $\omega \approx 0.1$. They found $q_c = 213$. Further details and numerical simulations concerning these predictions have been reported in Bunde *et al.* (1992), Bunde and Roman (1992), Roman (1992b), and Aharony and Harris (1992).

C. Observation of fractons in real materials: Neutron-scattering experiments

1. Fractality of silica aerogels and other disordered systems

Kistler (1932) found a way to dry gels without collapsing them, and produced extremely light materials with porosities as high as 98%, which are called *aerogels.* They have a very low thermal conductivity, solid-like elasticity, and very large internal surfaces. As a consequence, aerogels exhibit unusual physical properties, making them suitable not only for a number of practical applications, such as detectors of Čerenkov radiation, supports for catalysts, or thermal insulators (see, for example, Fricke, 1986, 1988; Brinker and Scherer, 1990), but also for basic research studies. For example, a number of experiments have shown that these porous structures can have profound effects on critical phenomena (Chan *et al.*, 1988; Wong *et al.*, 1990; Wong and Chan, 1990; Frisken, Ferri, and Cannell, 1991; Mulders *et al.*, 1991. See also the conference proceedings edited by Fricke, 1992).

The initial step in the preparation of silica aerogels is the hydrolysis of an alkoxysilane $Si(OR)_4$, where R is CH_3 or C_2H_5 (Kistler, 1932; Prassas *et al.*, 1984). The hydrolysis produces silicon hydroxide $Si(OH)_4$ groups that polycondense into siloxane bonds -Si-O-Si-, and small particles start to grow in the solution. These particles bind to each other by cluster-cluster aggregation, forming more siloxane bonds and eventually producing a disordered network filling the reaction volume, at which point the solution gels. The reactions are normally not complete at this gel point, and the cluster networks continue to grow in the alcogel phase. After suitable aging, if the solvent is extracted above the critical point, the open porous structure of the network is preserved and decimeter-size monolithic blocks with a range of densities from 50 to 500 kg/m^3 can be obtained.

Small-angle scattering techniques using neutrons and x rays are very well suited to systematically investigate the structure of silica aerogels. It has been found (Schaefer and Keefer, 1984, 1986; Courtens and Vacher, 1987; Vacher, Woignier, Pelous, and Courtens, 1988; Vacher, Woignier, Phalippou, Pelous, and Courtens, 1988; Woignier *et al.*, 1990; Posselt, Pedersen, and Mortensen, 1992) that aerogels take fractal structures, as in the cases of colloidal gels (Dietler *et al.*, 1986, 1987). Direct electron microscope observations on silica aerogels were done by Brinker and Scherer (1990), Brinker *et al.* (1982), Rousset *et al.* (1990), Vacher *et al.* (1991), and Buckley and Greenblatt (1992). Bourret (1988) and Duval *et al.* (1992) reported high-resolution electron microscopy (HREM) observations that are compatible with a fractal geometry. Beck *et al.* (1989) and Ferri, Frisken, and Cannell (1991) used light-scattering techniques for characterizing geometrical features. Phalippou *et al.* (1991) applied thermoporometry for an *in situ* study of silica aerogels.

The scattering differential cross section measures the Fourier components of the spatial fluctuations in the scattering length density. For aerogels, the differential cross section is composed of the product of three factors, namely,

$$\frac{d\sigma}{d\Omega} = A f^2(q) S(\mathbf{q}) \Phi(q) + B \ .$$

Here A is a coefficient proportional to particle concentration, $f^2(q)$ is the *elemental-particle form factor,* the structure factor $S(\mathbf{q})$ describes the correlation between *particles* in a cluster, and $\Phi(q)$ takes account of the *cluster-cluster* correlations. B gives the incoherent background. The Fourier transform of the particle density-density correlation function $G(r)$ gives

$$S(\mathbf{q}) = 1 + \frac{N}{V} \int_V |G(\mathbf{r}) - 1| e^{i\mathbf{q}\cdot\mathbf{r}} d\mathbf{r} \ . \tag{5.22}$$

Fractal (self-similar) structures, extending up to a correlation length ξ, can be modeled by the correlation function $G(\mathbf{r})$ (Teixeira, 1986; Courtens and Vacher, 1989),

$$G(\mathbf{r}) - 1 \propto r^{D_f - 3} \exp(-r/\xi) \ . \tag{5.23}$$

This is the most convenient, but not unique, choice. Equation (5.23) is a consequence of the mass $M(r)$ within a sphere centered on a particle at $r=0$, scaling as $M(r) \propto r^{D_f}$. Hence the density in the sphere scales as $\rho(r) \propto r^{D_f - 3}$. Two limiting regimes are of interest. At small q, $q\xi \ll 1$, $S(q)$ is almost independent of q. When $q\xi \gg 1$, one obtains by substituting Eq. (5.23) into Eq. (5.22) the following simple result for the scattering function,

$$S(\mathbf{q}) \propto q^{-D_f} \ . \tag{5.24}$$

In the ideal case, the value of D_f can be deduced from the slope of the observed corrected intensity versus momentum transfer in a double-logarithmic plot. This is illustrated in Fig. 19, which shows the results of elastic-scattering experiments on silica aerogels (Vacher, Woignier, Pelous, and Courtens, 1988).

The various curves are labeled by the macroscopic density ρ of the corresponding sample, N095, meaning "neutrally reacted" with $\rho=95$ kg/m^3. The solid lines represent the best fits. They are extrapolated into the particle regime ($q>0.15$ Å^{-1}) to emphasize that the fits do not apply in that region, particularly for the denser samples. Remarkably, D_f is independent of sample density to within experimental accuracy: $D_f=2.40\pm0.03$ for samples N095 to N360. Furthermore, ξ scales with ρ as $\xi\propto\rho^{-1.67\pm0.05}$. The departure of $S(\mathbf{q})$ from the q^{-D_f} dependence at large q indicates the presence of particles with gyration radii of a few Å.

The lower three curves in Fig. 19 are the results of $S(\mathbf{q})$ for samples prepared under basic catalysis. They are very different from the upper three curves. Comparing N200 to B220, one notes that the extension of the power-law region is very different for these two curves. A most striking effect is found in the value of D_f. All curves from base-catalyzed samples with an extended fractal range have $D_f=1.8\pm0.1$.

To summarize, silica aerogels exhibit three different length-scale regions: At short distance, elemental particles of radial size R are found. The particles are aggregated into clusters with size ξ at intermediate distance, and a gel is formed by connection of the clusters at large distance. At intermediate length scales, the clusters possess fractal structure, and at large length scales the gel is a homogeneous porous glass. The fractal structure of silica aerogels and their dynamics have been reviewed by Courtens, Vacher, and Stoll (1989), Vacher, Courtens, and Pelous (1990), Kjems (1991, 1993), and Courtens and Vacher (1992).[12]

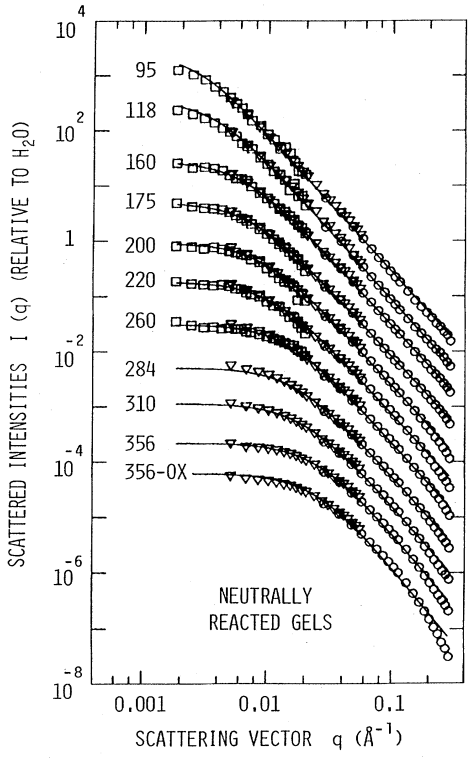

FIG. 19. Scattered intensities for 11 samples. From top to bottom: ten untreated, neutrally reacted samples of increasing density, and one oxidized sample. The curves are labeled with ρ in kg/m^3. After Vacher, Woignier, Pelous, and Courtens (1988).

2. Observed density of states

A direct way to obtain the fracton dimension $\tilde{d}$ for real materials is to measure the density of states (DOS). A very direct method is incoherent inelastic neutron-scattering experiments, which measure the amplitude-weighted DOS. The scattered intensity is given by

$$I(q,\omega)\propto q^2\frac{k'}{k}\frac{n(\omega)}{\omega}\sum_i e^{-2W_i}D_i(\omega)\ ,$$

where $n(\omega)$ is the Bose-Einstein distribution function. The wave vectors $\mathbf{k}$ and $\mathbf{k}'$ correspond to the incident and scattered neutrons, respectively, and $\mathbf{q}=\mathbf{k}'-\mathbf{k}$. $D_i(\omega)$ and W_i are the DOS and the Debye-Waller factor characteristic of the ith site, respectively. The summation extends over the different sites for the atoms, each of which contributes (proportionally to the amplitude of vibration at frequency ω) to the incoherent-scattering cross section. Incoherent neutron scattering from protons chemically bonded to the particle surfaces can be used to determine the DOS in porous media (Richter and Passell, 1980). A careful analysis has been applied to extract the intrinsic DOS by extrapolation to zero-momentum transfer.

Measurements of the incoherent inelastic scattering have been performed in aerogels (Courtens and Vacher, 1988; Coddens *et al.*, 1989; Conrad, Fricke, and Reichenauer, 1989; Conrad, Reichenauer, and Fricke, 1989; Page, Buyers, *et al.*, 1989; Page, Schaefer, *et al.*, 1989; Pelous *et al.*, 1989; Reichenauer, Fricke, and Buchenau, 1989; Vacher and Courtens, 1989a, 1989b; Vacher, Woignier, Pelous, *et al.*, 1989; Vacher, Woignier, Phalippou, *et al.*, 1989; Conrad *et al.*, 1990; Courtens, Vacher, and Pelous, 1990; Schafer, Brinker, *et al.*, 1990; Schaefer, Richter, *et al.*, 1990; Vacher, Courtens, Coddens, *et al.*, 1990; Courtens and Vacher, 1992). Vacher and Courtens (1989a, 1989b), Buchenau, Morkenbusch, *et al.* (1992), and Kjems (1993) have reviewed these results.

Investigations on the phonon-fracton crossover in silica aerogels have been made using inelastic neutron-scattering experiments. These have been done on back-

[12]There are several reports on disordered materials which are said to exhibit fractal structures and properties: polymers (Fischer *et al.*, 1990; Zemlyanov *et al.*, 1992), vitreous silica (Dianoux *et al.*, 1986; Dianoux, 1989), fumed silica (Page, Buyers, *et al.*, 1989; Page, Schaefer, *et al.*, 1989), smoke-particle aggregates of silica particles (Richter *et al.*, 1987), and superionic borate glasses (Fontana *et al.*, 1987, 1990).

scattering spectrometers (Conrad, Fricke, and Reichenauer, 1989; Conrad, Reichenauer, and Fricke, 1989; Pelous *et al.*, 1989; Conrad *et al.*, 1990; Vacher, Courtens, and Pelous, 1990) and using the spin-echo technique (Courtens, Vacher, and Pelous, 1990; Schaefer, Brinker, *et al.*, 1990; Schaefer, Richter, *et al.*, 1990). The backscattering technique has the advantage that the low-frequency Debye range is seen as a constant-intensity level extending from the elastic line to the crossover frequency.[13] Thus any excess modes at the phonon-fracton crossover would show up as a peak in the scattering intensity at that frequency, if present. However, such a peak has not been observed in the two backscattering experiments (Conrad *et al.*, 1990; Vacher, Courtens, and Pelous, 1990). Rather, a gradual decrease is observed as one passes through the crossover regime.

The neutron-scattering spin-echo technique has several advantages over these other techniques. The larger spectral range makes it a suitable tool for the determination of the fracton dimension.

The crossover frequencies determined by both backscattering and spin-echo measurements are generally in good agreement with those determined by Brillouin scattering (Courtens *et al.*, 1987b; Courtens, Pelous, Vacher, and Woignier, 1987). As far as investigations at higher frequencies are concerned, there are several early results (Reichenauer, Fricke, and Buchenau, 1989; Vacher, Woignier, Pelous, *et al.*, 1989; Vacher, Woignier, Phalippou, *et al.*, 1989). These results exhibited a change of slope in the log-log plot of the DOS at 200 GHz, giving a stronger increase with frequency at higher frequencies. Investigators interpreted their data as a crossover from fractons to vibrational modes *within* the particles. Courtens and Vacher (1989) compared the data at high frequencies to a formula which has been derived for the DOS of small particles (Baltes and Hilf, 1973). In the regime of particle contribution, the effective slope of the DOS is around 1.5. This seems to originate from the contribution of both surface (proportional to ω) and bulk (proportional to ω^2) particle modes. The energy resolution was insufficient to observe the crossover to the long-wavelength phonon regime.

Measurements (Coddens *et al.*, 1989; Vacher, Woignier, Phalippou, *et al.*, 1989) at higher resolution on a sample prepared in a different manner have confirmed the extended fracton region. The DOS in silica aerogels has been studied in a wider frequency range by combining data from neutron time-of-flight and spin-echo experiments (Vacher, Courtens, and Pelous, 1990). These results, exhibited in Fig. 20, indicate that different types of modes contribute to the scattering in the fracton range,

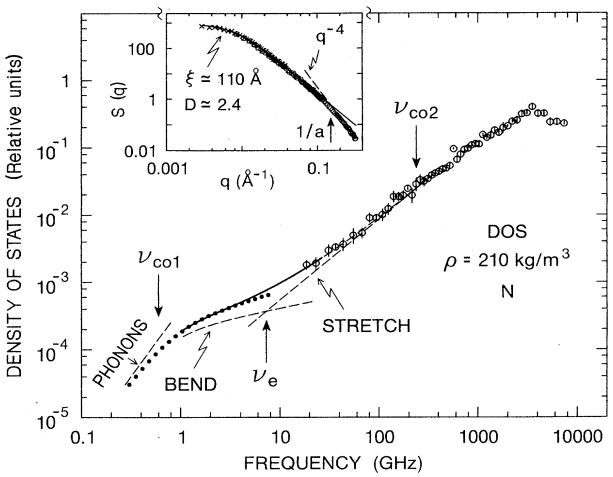

FIG. 20. Density of states of neutrally prepared silica aerogel. The open circles are time-of-flight measurements. The dotted curve indicates the DOS that fits the neutron spin-echo data. The dashed lines indicate the asymptotic phonon as well as the independent bend and stretch contributions. Inset: small-angle neutron-scattering data from the same fit described in Fig. 1 of Vacher, Woignier, Pelous, and Courtens (1988). A straight line shows the Porod region at high q. After Vacher, Courtens, Coddens, *et al.* (1990).

suggesting that the modes have predominantly *bending character* at low frequencies and *stretching character* at higher frequencies. In the fracton domain, a power law is observed over more than one order of magnitude. It has a slope $\tilde{d}_s - 1 \sim 1.2$.

We should mention neutron-scattering experiments on other disordered materials, which were analyzed in terms of the fracton theory. Freltoft, Kjems, and Richter (1987) measured the low-frequency density of states for fractal silica aggregates by inelastic neutron scattering. They obtained their fracton dimensionalities. Page, Buyers, *et al.* (1989) performed neutron inelastic-scattering measurements on fumed silica and compared the results with analogous results for amorphous quartz. They saw no evidence for a hump[14] in the DOS near the phonon-fracton crossover. It was also found that neither the temperature and wave-vector dependence of the intensity nor the absolute intensity was in accord with simple phonon models. Fontana *et al.* (1990) reported a study of low-frequency vibrational dynamics and electron-vibration coupling in AgI-doped silver borate

[13]In general, the Debye range of dense solids cannot be obtained by the backscattering technique because of the extremely small value of $\mathcal{D}(\omega)/\omega^2 = (1/2\pi^2)(1/v_L^3 + 2/v_T^3)$. In silica aerogels, however, the sound velocities are lower by a factor of about 40 (Conrad *et al.*, 1990).

[14]Earlier inelastic neutron-scattering experimental results that exhibit steepness or a hump in the DOS (Buchenau, Nuecker, and Dianoux, 1984; Buchenau *et al.*, 1986; Rosenberg, 1985) had been analyzed according to the fracton viewpoint. Buchenau, Nuecker, and Dianoux (1984), Buchenau *et al.* (1986), and Dianoux *et al.* (1986) have suggested, however, that the observed hump in the vitreous silica can be attributed to some intrinsic modes peculiar to amorphous materials.

glasses. By using both time-of-flight neutron-scattering and Raman-scattering spectroscopies, they were able to determine the vibrational DOS and the frequency dependence of the electron-vibration coupling. The fracton dimension of this system was determined to be 1.4. Zemlyanov *et al.* (1992) employed inelastic neutron-scattering measurements to study low-frequency vibrational excitations in polymethyl metacrylate (PMMA). The DOS obtained in the 2.5–10 meV range follows a power law in energy, with a spectrum corresponding to a fracton dimension $\tilde{d}=1.8\pm0.05$. Dianoux, Page, and Rosenberg (1987) and Arai and Jørgensen (1988) performed inelastic neutron-scattering experiments on epoxy resins. Dianoux, Page, and Rosenberg (1987) found that the DOS above $E=1.2$ meV was proportional to $E^{\tilde{d}-1}$, with $\tilde{d}=1.5$, whereas the DOS below 1.2 meV was proportional to E^2. They also found a rapid rise in the DOS near the phonon-fracton crossover energy. The results by Arai and Jørgensen (1988) exhibit a fracton dimension $\tilde{d}=1.9\pm0.1$, with a crossover energy of 1.8 meV, but they found no rapid rise in the DOS around $E=1.8$ meV.

There are experiments that investigate the dynamical properties of fractal materials, but that do not involve scattering techniques. Helman, Coniglio, and Tsallis (1984) have shown that a proper description of the temperature dependence of the spin-lattice relaxation rate of low-spin hemoproteins and ferrodoxin measured by Stapleton *et al.* (1980) and Allen *et al.* (1982) requires that both the fractal structure of the protein backbone and the cross connections between segments of the folded chain be taken into account. This work led to several investigations regarding fractons in protein dynamics (Stapleton *et al.*, 1985; Herrmann, 1986; MacDonald and Jan, 1986; Yup Kim, 1988). It is obvious that the exponent $\tilde{d}$ is obtained by spin-lattice relaxation experiments; but the analysis of data is not straightforward, because one cannot use the ensemble-averaged fracton wave functions to calculate matrix elements. Theoretical works (Alexander, Entin-Wohlman, and Orbach, 1985a, 1986; Entin-Wohlman, Alexander, and Orbach, 1985; Shrivastava, 1986, 1989b) have been done assuming the ensemble-averaged superlocalized fracton wave functions given by Eq. (5.18). The arguments taking into account the proper averaged procedure for the matrix elements as done by Alexander, Courtens, and Vacher (1993) for inelastic light scattering are required. Kopelman, Parus, and Prasad (1986) and Fischer, von Borczyshowski, and Schwentner (1990) have determined the fracton dimension $\tilde{d}$ by considering exciton recombination in disordered systems. Kopelman, Parus, and Prasad (1986) measured the exciton recombination characteristics of naphthalene-doped microporous materials. This technique yields the fracton dimension of the embedded naphthalene structure, or, equivalently, the effective random-walk dimension of the porous network. The values of $\tilde{d}$ obtained are between 1 and 2. Fischer, von Borczyshowski, and Schwentner (1990) have studied the trap-depth distribution of dibenzofuran singlet excitons and the temperature-dependent energy migration by time-resolved spectroscopy via synchrotron radiation and two photon laser excitation. They obtained $\tilde{d}=1.14$ from their experimental results. Krumhansl (1986) stressed that for polymers consisting of long chains, the translational symmetry is effectively valid; namely, the conventional phonon picture is valid for chains. It should be kept in mind, however, that all configurations of linear polymers have $\tilde{d}=1$ (Alexander, 1986).

Sintered metal powders possess a random structure consisting of small metal particles of the size $a\sim500$ Å. The study of the vibrational modes of these materials might be important for understanding the anomalous Kapitza resistance at millikelvin temperatures (see the review by Nakayama, 1989). Malieppard *et al.* (1985) and Page and McCulloch (1986) measured the ultrasound propagation in sintered metal powders. They found that a band edge exists, at $\lambda\sim10a$, below which sound does not propagate. They suggested that this edge is associated with a transition from phonon to fracton vibrational modes of the sinter. Wu *et al.* (1987) have investigated fracton modes using thin metallic planes, which are randomly degraded square lattices of bonds. Their system maps onto the percolation model with scalar displacements. Hayashi *et al.* (1990) have studied low-frequency vibrational modes in sintered copper and silver powders using Au Mössbauer spectroscopy. The energies of the vibrational modes coincide with the values estimated from ultrasonic data (Malieppard *et al.*, 1985; Page and McCulloch, 1986) using a fracton model, providing support for the localized nature of the modes.

Finally, we should mention experiments on fractal superconducting networks. Alexander (1983) has pointed out that the linearized Ginzburg-Landau equation close to the superconducting transition temperature T_c can be mapped onto the equation for random resistor network (or elastic network with scalar displacements). Modern lithography techniques have enabled the fabrication of superconducting percolating networks or Sierpinski gaskets. These are obvious candidates for a quantitative experimental test of the fracton concept. These were done by Gordon and Goldman (1987, 1988a, 1988b), Gordon, Goldman, and Whitehead (1987), Gordon *et al.* (1986), Yu, Goldman, and Bojko (1990), Yu, Goldman, Bojko, *et al.* (1990), Senning *et al.* (1991), and Meyer *et al.* (1991; Meyer, Martinoli, *et al.*, 1992; Meyer, Nussbaum, *et al.*, 1992).

VI. SCALING BEHAVIOR OF THE DYNAMICAL STRUCTURE FACTOR

Scattering experiments yield $S(\mathbf{q},\omega)$, providing rich information on the dynamic properties of fractal structures. A variety of scattering experiments have been performed so far for physical realizations of fractal materials, such as sol-gel glasses, silica-aerogels, and borate glasses. In this section, we review theoretical and experi-

mental developments for this quantity. Scaling arguments on the dynamical structure factor $S(\mathbf{q},\omega)$ will be presented in Sec. VI.A.2, in order to interpret experimental data or simulated results on $S(\mathbf{q},\omega)$.

Before discussing the results for $S(\mathbf{q},\omega)$, we should clarify the meaning of energy width of fractons. Obviously, one could find exact eigenstates of the random structure which would have no energy width: they would be precisely defined in energy. It is only when one projects them onto plane-wave states that a lifetime is generated, equally in frequency or wave-vector space because of the linear phonon-dispersion relation. When we calculate an energy width for the fractons, it should be understood to be that width that a plane wave would experience.

A. Theoretical treatments of the dynamical structure factor $S(\mathbf{q},\omega)$

1. Expression for the intensity of inelastic scattering

In general, the intensity $I(\mathbf{q},\omega)$ of inelastic neutron or light scattering with a frequency shift $\omega(=\omega-\omega_0)$ is proportional to the Fourier transform of the density-density correlation function, defined by $G(\mathbf{r}-\mathbf{r}',t)=\langle\rho(\mathbf{r},t)\rho(\mathbf{r}',0)\rangle$, where $\rho(\mathbf{r},t)$ is the density and the angular brackets denote an equilibrium ensemble average. A general form is obtained by introducing the density fluctuation $\delta\rho(\mathbf{r},t)$ defined by

$$\delta\rho(\mathbf{r},t)=\rho(\mathbf{r},t)-\rho(\mathbf{r}) , \tag{6.1}$$

where $\rho(\mathbf{r})$ is the static density given by

$$\rho(\mathbf{r})=\sum_i \delta(\mathbf{R}_i-\mathbf{r}) ,$$

and $\mathbf{R}_i$ is the equilibrium position of the ith atom. One usually neglects the term contributing only to elastic scattering ($\omega=0$). $\mathcal{S}(\mathbf{q},\omega)$ is then expressed in terms of the Fourier transform of the density fluctuation $\delta\rho(\mathbf{r},t)$,

$$\mathcal{S}(\mathbf{q},\omega)=\frac{1}{2\pi}\int dt e^{-i\omega t}\langle\delta\rho_{-\mathbf{q}}(0)\delta\rho_{\mathbf{q}}(t)\rangle . \tag{6.2}$$

Because the density fluctuation $\delta\rho(\mathbf{r},t)$ induced by lattice vibrations with displacements $\mathbf{u}_i(t)$ is written $\delta\rho(\mathbf{r},t)=\sum_i[\delta(\mathbf{R}_i+\mathbf{u}_i(t)-\mathbf{r})-\delta(\mathbf{R}_i-\mathbf{r})]$, the Fourier transform $\delta\rho_{\mathbf{q}}(t)$ becomes

$$\delta\rho_{\mathbf{q}}(t)=\sum_i\{e^{-i\mathbf{q}\cdot(\mathbf{R}_i+\mathbf{u}_i(t))}-e^{-i\mathbf{q}\cdot\mathbf{R}_i}\} .$$

Decomposing $\mathbf{u}_i(t)$ into normal modes $\mathbf{u}_i=\sum_\lambda \mathbf{u}_i^\lambda e^{-i\omega_\lambda t}$, one obtains

$$\delta\rho_{\mathbf{q}}(t)=\sum_\lambda \delta\rho_\lambda(\mathbf{q},t)+O(u^2) , \tag{6.3}$$

where

$$\delta\rho_\lambda(\mathbf{q},t)=e^{-i\omega_\lambda t}\delta\rho_\lambda(\mathbf{q}) ,$$

and $\delta\rho_\lambda(\mathbf{q})$ is defined by

$$\delta\rho_\lambda(\mathbf{q})=-i\sum_i(\mathbf{q}\cdot\mathbf{u}_i^\lambda)e^{-i\mathbf{q}\cdot\mathbf{R}_i} . \tag{6.4}$$

Substitution of Eq. (6.3) into Eq. (6.2) yields

$$\mathcal{S}(\mathbf{q},\omega)=\sum_\lambda \delta(\omega-\omega_\lambda)\langle\delta\rho_\lambda(\mathbf{q})\delta\rho_\lambda(-\mathbf{q})\rangle . \tag{6.5}$$

For convenience, the *reduced* dynamical structure factor $S(\mathbf{q},\omega)$ will be used hereafter. The usual mode quantization and thermal factor $[n(\omega)+1]/\omega$, where $n(\omega)$ is the Bose-Einstein distribution function, are factored out from $\mathcal{S}(\mathbf{q},\omega)$ by the relation

$$S(\mathbf{q},\omega)=\frac{\omega}{[n(\omega)+1]}\mathcal{S}(\mathbf{q},\omega) .$$

Changing the summation in Eq. (6.5) into a frequency integral, one has

$$S(\mathbf{q},\omega)=\mathcal{D}(\omega)\langle\delta\rho_\lambda(\mathbf{q})\delta\rho_\lambda(-\mathbf{q})\rangle_\omega , \tag{6.6}$$

where the angular brackets denote the average of $\delta\rho_\lambda(\mathbf{q})$ over all modes λ with frequencies close to ω. Finally, one has the expression for the intensity of inelastic scattering,

$$I(\mathbf{q},\omega)\propto\frac{n(\omega)+1}{\omega}\mathcal{D}(\omega)\langle\delta\rho_\lambda(\mathbf{q})\delta\rho_\lambda(-\mathbf{q})\rangle_\omega .$$

In principle, $S(\mathbf{q},\omega)$ can be calculated analytically from Eq. (6.5) or Eq. (6.6) if one knows $\delta\rho_\lambda(\mathbf{r})$ [or the fracton wave function $\phi_\lambda(\mathbf{r})$] for a specific realization. However, this is not straightforward, because of the extremely complicated character of fractons (see, for example, Fig. 15). Although some general remarks can be made about $S(\mathbf{q},\omega)$ using scaling arguments (Aharony *et al.*, 1988) and an analysis can be carried out within the effective-medium approximation (EMA; Polatsek and Entin-Wohlman, 1988; Entin-Wohlman, Orbach, and Polatsek, 1989; Polatsek *et al.*, 1989), its explicit form is not known except for deterministic fractals. Sivan *et al.* (1988) and Entin-Wohlman *et al.* (1989) have analytically calculated $S(\mathbf{q},\omega)$ for the $d=2$ Sierpinski gasket in terms of Green's function, where $S(\mathbf{q},\omega)$ was defined through the displacement-displacement correlation function. They have shown that fracton excitations on the Sierpinski gasket obey a single-length-scale postulate (SLSP), in addition to $S(\mathbf{q},\omega)$ being peaked at $q_{\max}\approx\omega^{2/2+\theta}$, indicating the appropriate dispersion.

2. Scaling arguments on $S(\mathbf{q},\omega)$

Alexander (1989) and Alexander, Courtens, and Vacher (1993) have produced arguments supporting the asymptotic behavior of the dynamical structure factor $S(\mathbf{q},\omega)$ based on the SLSP (single-length-scale postulate; see Sec. IV.B). The following argument is a summary of the theory proposed by Alexander *et al.* (1993).

If the SLSP is valid, the correlation function $S(\mathbf{q},\omega)$ should have the following scaling form, depending only on the single length scale $\Lambda(\omega)$,

$$S(q,\omega)=q^y H(q\Lambda(\omega)) , \tag{6.7}$$

where the dynamical structure factor is a function of $q=|\mathbf{q}|$ because of the spherical symmetry for the averaged structure of random networks. The asymptotic behavior of the scaling function $H(x)$ for $x \ll 1$ and for $x \gg 1$ is of power-law form,

$$H(x) \propto \begin{cases} x^{a}, & x \ll 1 ; \\ x^{-a'}, & x \gg 1 . \end{cases}$$

Here a and a' are new scaling indices. Accordingly, one has

$$S(q,\omega) \propto \begin{cases} q^{y+a}\omega^{-a\tilde{d}/D_f}, & q\Lambda(\omega) \ll 1 ; \\ q^{y-a'}\omega^{a'\tilde{d}/D_f}, & q\Lambda(\omega) \gg 1 . \end{cases} \tag{6.8a}$$

(6.8b)

In the case of $q\Lambda \ll 1$, Eq. (6.4) can be expanded as

$$\delta\rho_\lambda(\mathbf{q}) \simeq -e^{-i\mathbf{q}\cdot\mathbf{R}_\lambda} \sum_i (\mathbf{q}\cdot\mathbf{R}_i^\lambda)(\mathbf{q}\cdot\mathbf{u}_i^\lambda) , \tag{6.9}$$

where $\mathbf{R}_i^\lambda = \mathbf{R}_i - \mathbf{R}_\lambda$ and $\mathbf{R}_\lambda$ is the center of the λ-mode fracton. The summand in Eq. (6.9) can be written as $\mathbf{q}\cdot\{\mathbf{R}_i^\lambda \otimes \mathbf{u}_i^\lambda\}\cdot\mathbf{q}$ in terms of the dyadic product. Choosing the center of the fracton as the origin, i.e., $\mathbf{R}_\lambda = 0$, and $\sum_i \mathbf{R}_i^\lambda = 0$ from the condition $\sum_i u_i^\lambda = 0$ (see footnote 10 in Sec. V.B.1)

$$\delta\rho_\lambda(\mathbf{q}) \simeq -\sum_i^{\nu_\lambda} \mathbf{q}\cdot\{\mathbf{R}_i^\lambda \otimes [\mathbf{u}_i^\lambda - \mathbf{u}_\lambda]\}\cdot\mathbf{q} ,$$

where $\mathbf{u}_\lambda$ is the amplitude at the center of the λ-mode fracton, and the summation is restricted to a vibrating region ν_λ which is chosen as the smallest region for which the boundary condition plays no significant role for the vibration λ. If an average strain tensor, $\hat{e}_\lambda$, is defined as

$$\mathbf{u}_i^\lambda - \mathbf{u}_\lambda = \hat{e}_\lambda \cdot \mathbf{R}_i^\lambda ,$$

one obtains

$$\delta\rho_\lambda(\mathbf{q}) \simeq -\mathbf{q}\cdot\left\{\sum_i^{\nu_\lambda} (\mathbf{R}_i^\lambda \otimes \mathbf{R}_i^\lambda)\hat{e}_\lambda\right\}\cdot\mathbf{q} .$$

The $\mathbf{R}_i^\lambda$ in ν_λ are all at most of order Λ, so that the magnitude of $\delta\rho_\lambda(\mathbf{q})$ can be estimated as

$$\delta\rho_\lambda \propto q^2\Lambda^{D_f+2}\hat{e}_\lambda .$$

Using the definition of $S(\mathbf{q},\omega)$ from Eq. (6.6), one has

$$S(q,\omega) \propto \mathcal{D}(\omega) q^4 [\Lambda(\omega)]^{2D_f+4} \langle (\hat{e}_\lambda)^2 \rangle_w . \tag{6.10}$$

Alexander, Courtens, and Vacher (1993) assume that $\langle (e_\lambda)^2 \rangle_\omega$ has a scaling form, which to leading order is

$$[\langle (e_\lambda)^2 \rangle_\omega]^{1/2} \propto \frac{u(\omega)}{[\Lambda(\omega)]^\sigma} , \tag{6.11}$$

where the root-mean-squared amplitude $u(\omega)$ of the fracton modes is given by

$$u(\omega) = \left[\left\langle \frac{1}{N_\lambda} \sum_i^{\nu_\lambda} |u_i^\lambda|^2 \right\rangle_w\right]^{1/2} ,$$

and N_λ is the number of sites contained in the region of vibration, ν_λ (i.e., $\langle N_\lambda \rangle_\omega \propto \Lambda^{D_f}$). Thus the new exponent σ characterizes an effective length relevant to an *average strain,* analogous to the relationship between the chemical and Euclidean lengths. The magnitude of $u(\omega)$ is proportional to $[\Lambda(\omega)]^{-D_f/2}$ because of the normalization condition $\sum_i |\mathbf{u}_i^\lambda|^2 = 1$ (footnote 15). From Eqs. (6.10) and (6.11) and from the use of the dispersion relation $\Lambda \propto \omega^{-\tilde{d}/D_f}$, Alexander, Courtens, and Vacher (1993) obtain

$$S(q,\omega) \propto q^4 \omega^{(2\sigma-4)(\tilde{d}/D_f)-1} , \quad q\Lambda \ll 1 .$$

Thus the exponents y and a in Eq. (6.8a) are determined through σ as

$$y = 2\sigma - \frac{D_f}{\tilde{d}} \tag{6.12}$$

and

$$a = 4 + \frac{D_f}{\tilde{d}} - 2\sigma . \tag{6.13}$$

In the case $q\Lambda \gg 1$, the phase factor $e^{i\mathbf{q}\cdot\mathbf{R}_i}$ in Eq. (6.4) is uniform (coherent) only over small regions of size $l_q \propto q^{-1}$ ($\ll \Lambda$) (see Fig. 17). Provided that the vibrating region ν_λ is divided into "blobs" of size $l_q \ll \Lambda$, the number of blobs in the region ν_λ is proportional to $(q\Lambda)^{D_f}$ and each blob has $\sim(qa)^{-D_f}$ particles. Then, as for the derivation of Eq. (6.9), one can expand Eq. (6.4) for small $\mathbf{q}$ as

$$\delta\rho_\lambda(\mathbf{q}) \simeq \sum_\beta e^{-\mathbf{q}\cdot\mathbf{R}_\beta}[i(qa)^{-D_f}(\mathbf{q}\cdot\mathbf{U}_\lambda^\beta) - \sum_i^{\nu_\lambda^\beta} (\mathbf{q}\cdot\mathbf{r}_i)(\mathbf{q}\cdot\mathbf{u}_i^\lambda)] , \tag{6.14}$$

where $\mathbf{R}_\beta$ is the center of mass in the "blob" β and $\mathbf{r}_i = \mathbf{R}_i - \mathbf{R}_\beta$. The factor $\mathbf{U}_\lambda^\beta \simeq (qa)^{D_f} \sum_i^{\nu_\lambda^\beta} \mathbf{u}_i^\lambda$ is the averaged motion of the blob β in the eigenmode λ. The second summation in Eq. (6.14) is taken over the region of the blob β. Inserting Eq. (6.14) into Eq. (6.6), one has phase factors $\exp[-i\mathbf{q}\cdot(\mathbf{R}_\beta - \mathbf{R}_{\beta'})]$. Because there is no coherent contribution of the scattering from different blobs in the limit ($q\Lambda \gg 1$), only terms with $\beta = \beta'$ remain. Alexander, Courtens, and Vacher (1993) suggest that the first term dominates the second term in Eq. (6.14) for $q\Lambda \gg 1$.

---

[15] For $\mathcal{S}(\mathbf{q},\omega)$ defined by Eq. (6.5), the normalization condition becomes $\sum_i |\mathbf{u}_i^\lambda|^2 = [n(\omega)+1]/\omega$.

Thus one has the result

$$S(\mathbf{q},\omega)\propto\mathcal{D}(\omega)[\Lambda(\omega)]^{D_f}q^{2-D_f}\langle(U_\lambda^\beta)^2\rangle_\omega .$$

When the number of particles in each blob becomes large, i.e., $(qa)^{-D_f}\gg 1$, the magnitude of $\langle(U_\lambda^\beta)^2\rangle_\omega$ is assumed to be

$$\langle(U_\lambda^\beta)^2\rangle_\omega\simeq(qa)^x\langle(u_\lambda)^2\rangle_\omega . \tag{6.15}$$

Using the relation $u(\omega)\propto[\Lambda(\omega)]^{-D_f/2}$, Alexander, Courtens, and Vacher (1993) have obtained $S(q,\omega)$, expressed by

$$S(\mathbf{q},\omega)\propto\omega^{\bar{d}-1}q^{2-D_f+x} .$$

Comparing this expression with Eq. (6.8b), one has

$$2-D_f+x=y-a' \tag{6.16a}$$

and

$$a'=\frac{D_f}{\bar{d}}(\bar{d}-1) . \tag{6.16b}$$

Equations (6.12) and (6.16a) for y yield

$$x=2(\sigma-1) . \tag{6.17}$$

To summarize, the scaling argument based on the SLSP predicts, by introducing the averaged strain exponent σ, the dynamical structure factor behaving as

$$S(q,\omega)\propto\begin{cases}q^4\omega^{(2\sigma-4)(\bar{d}/D_f)-1}, & q\Lambda(\omega)\ll 1 ,\\ q^{2\sigma-D_f}\omega^{\bar{d}-1}, & q\Lambda(\omega)\gg 1 .\end{cases} \tag{6.18}$$

B. Numerical simulations of $S(\mathbf{q},\omega)$

Computer experiments are crucial for gaining insight into the properties of the dynamical structure factor $S(\mathbf{q},\omega)$, as well as for calculating the DOS or the dispersion relation for fractal structures. In this subsection, numerical results for the dynamical structure factor of vibrating percolating networks are presented and compared with the scaling arguments of Alexander, Courtens, and Vacher (1993).

Montagna *et al.* (1990), Pilla *et al.* (1992), and Mazzacurati *et al.* (1992) have calculated the dynamical structure factor $S(\mathbf{q},\omega)$ by numerically diagonalizing the dynamical matrix. They have obtained results for site-percolating (SP) networks formed on 65×65 square lattices and $29\times29\times29$ cubic lattices. Stoll, Kolb, and Courtens (1992) have calculated $S(\mathbf{q},\omega)$ for bond-percolating (BP) networks by a direct diagonalization technique for $d=2$ (68×68) lattices and $d=3$ ($21\times21\times21$) lattices.

Nakayama and Yakubo (1992a, 1992b) have performed numerical simulations for $S(\mathbf{q},\omega)$ for very large-scale SP networks (500×500). They considered $d=2$ SP networks at the percolation threshold ($p_c=0.593$) with a periodic boundary condition. The dynamical structure factors $S(q,\omega)$ for percolation systems were obtained by the same numerical technique employed in a series of works (Yakubo and Nakayama, 1987a, 1987b, 1989a, 1989b, 1989c; Yakubo, Courtens, and Nakayama, 1990; Yakubo, Takasugi, and Nakayama, 1990). By using this algorithm, they excited several modes simultaneously with frequencies close to a fixed frequency ω, thereby decreasing slightly the monochromaticity of the excited modes. Their algorithm then automatically performed the frequency average $\langle\cdots\rangle_\omega$ in Eq. (6.6) for $S(\mathbf{q},\omega)$. Using these mode-mixed displacement patterns $\{v_i^\omega\}$, which are normalized by $\sum_i(v_i^\omega)^2=1$, we see that $S(\mathbf{q},\omega)$ is given by

$$S(\mathbf{q},\omega)=\mathcal{D}(\omega)\left\langle\sum_{ij}(\mathbf{q}\cdot\mathbf{v}_i^\omega)(\mathbf{q}\cdot\mathbf{v}_j^\omega)e^{-i\mathbf{q}\cdot(\mathbf{R}_i-\mathbf{R}_j)}\right\rangle , \tag{6.19}$$

where the angular brackets denote the sample average. Scalar displacements have been employed, whence $\mathbf{q}\cdot\mathbf{v}_i^\omega=qv_i^\omega$. The Fourier transform of the correlation function $\langle v_i^\omega v_j^\omega\rangle$ has been calculated by assuming a spherically symmetric correlation function $G^\omega(\mathbf{r}_i-\mathbf{r}_j)\equiv\langle v_i^\omega v_j^\omega\rangle$. This leads to

$$\sum_{ij}\langle v_i^\omega v_j^\omega\rangle\exp[-i\mathbf{q}\cdot(\mathbf{R}_i-\mathbf{R}_j)]\propto\sum_R RG^\omega(R)J_0(qR) ,$$

where $R=|\mathbf{r}_i-\mathbf{r}_j|$ and $J_0(x)$ is the 0th Bessel function. The ensemble average has been taken over five percolating networks formed on 500×500 square lattices. The maximum site number of our systems is $N=110\,793$; the minimum, $N=93\,382$.

The results for $S(q,\omega)$ are shown in Figs. 21 and 22. Figure 21 shows the calculated results of the q dependence of $S(q,\omega)$ for 50 different frequencies ($0.005\le\omega\le0.5$). The abscissa indicates the reduced

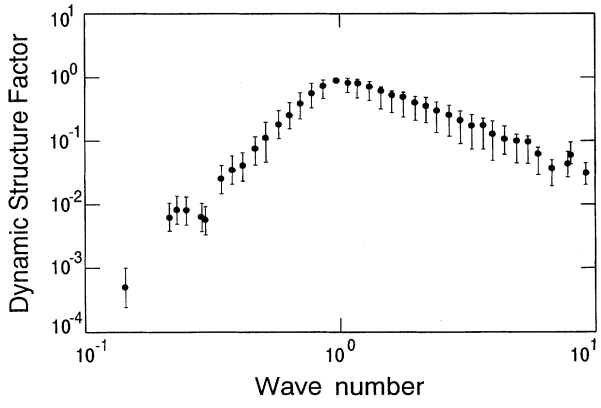

FIG. 21. Wave-number (q) dependence of $S(q,\omega)$ for 50 different frequencies ($0.005\le\omega\le0.5$). The abscissa indicates the reduced wave number q/q_0. Solid circles are plotted by averaging data over a narrow wave-number range close to the reduced wave number q/q_0. The ensemble average has been taken over five percolating networks formed on 500×500 square lattices. Error bars indicate the statistical errors of the data. After Nakayama and Yakubo (1992b).

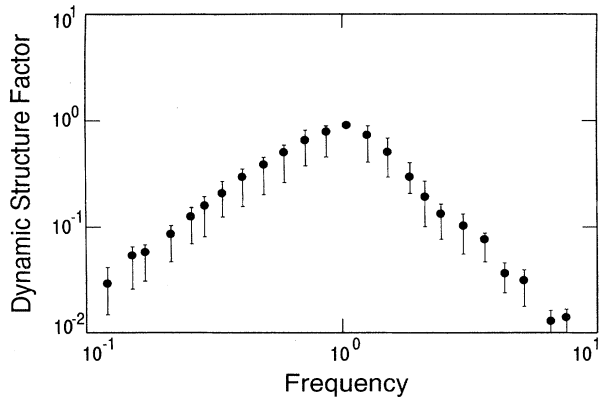

FIG. 22. Frequency (ω) dependence of $S(q,\omega)$ for 125 different wave numbers ($2\pi/250 \leq q \leq \pi$). The abscissa indicates the reduced frequency ω/ω_0. Solid circles are plotted by averaging data over a narrow frequency range close to the reduced frequency ω/ω_0. The ensemble average has been taken over five percolating networks formed on 500×500 square lattices. Error bars indicate the statistical errors of the data. After Nakayama and Yakubo (1992b).

wave number $q/q_0(\omega)$, where $q_0(\omega)$ is the wave number at which $S(q,\omega)$ has the maximum value $S_{\max}(\omega)$ for each fixed frequency. The values of $S(q,\omega)$ are rescaled by $S_{\max}(\omega)$. Solid circles are plotted by averaging over data within a narrow range close to the reduced wave number q/q_0 (one solid circle is obtained by averaging about 100 data points). The results exhibit a $S(q,\omega)$ for different ω which can be scaled by a single characteristic wave number q_0. In particular, the wave-number dependence obeys the power law: $S(q,\omega) \propto q^{4.0\pm0.1}$ below q_0, and $S(q,\omega) \propto q^{-1.6\pm0.1}$ above q_0. Figure 22 shows the results of the ω dependence of $S(q,\omega)$ for 125 different wave numbers ($2\pi/250 \leq q \leq \pi$). The abscissa represents the reduced frequency $\omega/\omega_0(q)$, where $\omega_0(q)$ is the frequency at which $S(q,\omega)$ has the maximum value $S_{\max}(\mathbf{q})$ for each fixed wave number. The values of $S(q,\omega)$ are also rescaled by $S_{\max}(\mathbf{q})$. Solid circles indicate the average values over the data within a narrow frequency range close to the reduced frequency ω/ω_0. Their result demonstrates universal behavior scaled by the single frequency ω_0. This result also shows that the asymptotic behavior of $S(q,\omega)$ can be expressed as $S(q,\omega) \propto \omega^{1.7\pm0.1}$ in the frequency regime $\omega \ll \omega_0$, and as $S(q,\omega) \propto \omega^{-2.25\pm0.1}$ for $\omega \gg \omega_0$.

Nakayama and Yakubo (1992b) obtained the values of the exponents a, a', and y from four asymptotic forms (q dependence for both $q \ll q_0$ and $q \gg q_0$, and the ω dependence for both $\omega \ll \omega_0$ and $\omega \gg \omega_0$) of $S(q,\omega)$. They found $a = 3.2\pm0.1$, $a' = 2.4\pm0.1$, and $y = 0.8\pm0.1$, which explain consistently four asymptotic relations of Eq. (6.18).

Inserting the simulated result $y = 0.8\pm0.1$ [or $a = 3.2\pm0.1$] into Eq. (6.12) [or into Eq. (6.13)], one finds that σ takes the value of 1.1. This value of σ is larger than unity and in agreement with the prediction ($\sigma > 1$) by Alexander, Courtens, and Vacher (1993).

Stoll, Kolb, and Courtens (1992) have computed $S(q,\omega)$ for BP networks. They treated 68×68 square lattices and $21\times21\times21$ cubic lattices and employed the standard diagonalization technique. As mentioned in Sec. II, the scale range for fractal geometry of a BP network is much wider than that of a SP network. Therefore BP networks are more suitable for determining the nature of fracton eigenfunctions belonging to high eigenfrequencies. Their results were obtained by averaging 40 and 20 realizations of $d=2$ and $d=3$ BP networks, respectively. Their values for the exponent a defined in Eq. (6.8) are $a=3.32$ for $d=2$, and $a=3.65$ for $d=3$. The value $a=3.32$ ($d=2$) is in accord with the result of Nakayama and Yakubo (1992b). They obtained the exponent σ defined by Eq. (6.11): $\sigma=1.05$ and 1.11 for $d=2$ and $d=3$, respectively, close to the value obtained by Nakayama and Yakubo (1992b).

In this subsection, we have described experiments, scaling arguments, and numerical simulations for the dynamical structure factor $S(q,\omega)$. The scaling argument postulates that, for the strongly disordered fractals, one is always in the Ioffe-Regel strong scattering limit, so that three distinct length scales (a wavelength, a scattering length, and a localization length) collapse to one (SLSP). For percolating networks, this length scale should have the frequency dependence $\Lambda(\omega) \propto \omega^{-\tilde{d}/D_f}$. Namely, all waves with the wavelength $\lambda < \xi$ satisfy the Ioffe-Regel condition $\lambda \sim l_s$ (Ioffe and Regel, 1960), indicating that fractons are strongly localized with the localization length $\Lambda(\omega)$ (see also Aharony *et al.*, 1987a). For weakly localized phonons, the characteristic lengths have different frequency dependencies (John, Sompolinsky, and Stephen, 1983). The numerical simulations by Stoll, Kolb, and Courtens (1992) and Nakayama and Yakubo (1992a, 1992b) confirm this postulate and show that the asymptotic behaviors of $S(q,\omega)$ can be characterized by the exponent σ introduced by Alexander, Courtens, and Vacher (1993). In summary: (i) The SLSP holds for fractons in percolating networks; (ii) the asymptotic form of the dynamical structure factor $S(q,\omega)$ follows a power law in both q and ω; and (iii) the exponents σ characterizing the average strain take the values 1.05 and 1.11 for $d=2$ and $d=3$, respectively.

C. Inelastic light scattering for fractal materials

1. Raman-scattering experiments

Boukenter *et al.* (1986, 1987) made the first attempt to measure the Raman-scattering intensity for silica aerogels. They analyzed the results, assuming the ensemble-averaged form for the fracton wave functions, Eq. (5.18), introduced by Alexander, Entin-Wohlman, and Orbach (1985a, 1985b, 1985c, 1986a). Keys and Ohtsuki (1987) questioned the validity of the analysis, but also used the averaged wave function. Boukenter *et al.* (1986, 1987)

used two kinds of silica aerogel samples in their Raman-scattering experiments. Sample A was prepared by acid-catalyzed hydrolysis and condensation of silicon tetraethoxide in ethanol, and sample B by base-catalyzed hydrolysis and condensation of silicon methoxide in alcohol. The condensation leads to gels dried by a hypercritical procedure. They extracted values for the fracton dimension from their analysis of $\tilde{d}=1.21$ for type A and $\tilde{d}=1.31$ for type B. Since these pioneering studies, a number of studies on the dynamical properties of fractal materials have been performed using inelastic light scattering. The dynamical properties of silica aerogels have been vigorously investigated by Courtens, Vacher, and their collaborators (Courtens, Pelous, Vacher, and Woignier, 1987; Woignier *et al.*, 1987; Courtens *et al.*, 1987a, 1987b, 1988; Courtens and Vacher, 1987, 1988, 1989, 1992; Tsujimi *et al.*, 1988; Vacher, Woignier, Pelous, and Courtens, 1988; Vacher, Woignier, Phalippou, Pelous, and Courtens, 1988; Vacher and Courtens, 1989a, 1989b; Vacher, Courtens, Pelous, *et al.*, 1989; Vacher, Woignier, Pelous, *et al.*, 1989; Vacher, Woignier, Phalippou, *et al.*, 1989; Xhonneux *et al.*, 1989; Courtens, Lartigue, *et al.*, 1990; Courtens, Vacher, and Pelous, 1989; Vacher, Courtens, Coddens, *et al.*, 1990; Vacher, Courtens, and Pelous, 1990). Mariotto *et al.* (1988a, 1988b) have reported low-frequency Raman spectra of gel-derived silica glasses annealed at different temperatures. The very low-frequency spectrum is interpreted in terms of localized "extra modes" coexisting with phonons. Besides these experiments on silica aerogels, inelastic light-scattering measurements have been reported for polymers such as PMMA (Malinovskii *et al.*, 1988); epoxy or diglycidyl ether of bisphenol A (DGEBA; see Boukenter, Duval, and Rosenberg, 1988); glasses such as silver borate glasses (Rocca and Fontana, 1989; Fontana *et al.*, 1990) or lithium borate glasses (Borjesson, 1989); and amorphous arsenic (Lottici, 1988).

Information on the DOS can also be obtained by means of Raman scattering. Saikan *et al.* (1990) have made Raman-scattering studies for the DOS of epoxy resins. Fontana, Rocca, and Fontana (1987) have determined the crossover frequency ω_c between the phonon and fracton regime from the low-frequency inelastic light scattering for superionic borate glasses of the type $(AgI)_x(Ag_2O\cdot nB_2O_3)_{1-x}$. Duval *et al.* (1987) have performed very low-energy Raman scattering on Na-colloids in NaCl. They analyzed the data from the viewpoint of fractal structures. Low-frequency Raman-scattering spectra in yttria-stabilized zirconia (YSZ) were measured by Yugami, Matsuo, and Ishigame (1992). They found that the frequency dependence of the Raman intensity can be separated into two regions, namely, the region below the characteristic frequency ω_{co} obeying the ω^4 law and the region above not following Debye theory. They analyzed the data in terms of fracton excitations above ω_{co}. In these cases, the observed intensity involves the product of DOS and the square of the polarization amplitude produced by the strain of the fracton excitation.

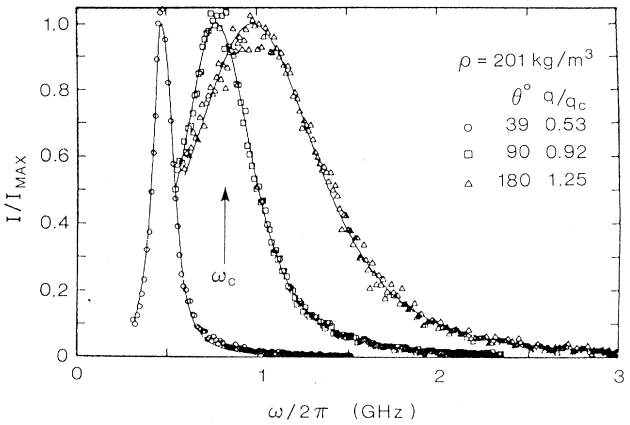

FIG. 23. Brillouin-scattering spectra (points) and fits (lines) as explained in the text: ○, $\theta=39°$, $q/q_c=0.53$; □, $\theta=90°$, $q/q_c=0.92$; △, $\theta=180°$, $q/q_c=1.25$. The intensities have been normalized to their peak values. The arrow indicates the position of the average crossover $\omega_c/2\pi$ for $\rho=201$ kg/m^3. After Courtens *et al.* (1988).

This means that the observed power law involves more than a single exponent.

All these experimental results have been analyzed by using the ensemble-averaged fracton wave function of Eq. (5.18) (Montagna, Pilla, and Viliani, 1989; Shrivastava, 1989a).[16] As first pointed out by Nakayama, Yakubo, and Orbach (1989), and as mentioned in the previous section, the use of an ensemble-averaged form for the fracton wave functions to obtain the matrix elements of the strain tensor is not correct in general. Theoretical arguments avoiding this error were made by Alexander (1989), Mazzacurati *et al.* (1992), Pilla *et al.* (1992), and Alexander, Courtens, and Vacher (1993).

2. Analysis of inelastic light-scattering results for silica aerogels

We have shown in Sec. V.A.3 that there exist two characteristic frequencies ω_ξ and ω_{l_c} for networks incorporating vector forces between particles. Under realistic conditions of the network ($\xi > l_c$), bending fractons characterized by $\tilde{d}_b$ are important below $\omega < \omega_{l_c}$, whereas stretching fractons are important for $\omega > \omega_{l_c}$ (see Fig. 8). Courtens *et al.* (1987a, 1988; see also Courtens, Pelous, Vacher, and Woignier, 1987) have measured the Brillouin-scattering spectrum for silica aerogels. Figure 23 presents the results for a silica aerogel with density

[16]Benoit, Poussigue, and Assaf (1992) have calculated the Raman intensity of the Sierpinski gasket without using the averaged fracton wave function. The results show that, in the fracton regime, the Raman intensity behaves with a power law.

$\rho=201$ kg/m^3 in polarized scattering [VV (vertical-vertical) polarization], in which the relevant frequency region is low ($\omega<\omega_{l_c}$). They have analyzed the data, assuming the following form for the scattering intensity $I(q,w)$,

$$I(q,\omega)=\frac{Av^2q^2}{\omega^2}\frac{\Gamma}{(\omega^2+\Gamma^2-v^2q^2)^2+4\Gamma^2v^2q^2}\ , \tag{6.20}$$

where A is a numerical constant, and v and Γ are the group velocity of phonons and the decay rate of phonons, respectively.

The dispersion relation is expressed as $\omega=v_0k$ in the phonon regime and as $\omega\sim k^{-D_f/\tilde{d}_b}$ in the fracton regime, whereas the decay rates are taken as $\Gamma\propto\omega^4/\omega_c^3$ in the phonon regime (Rayleigh-scattering regime) and $\Gamma\propto\omega$ in the fracton regime (Ioffe-Regel regime). Courtens *et al.* (1988) have used the following relations for $v(\omega)$ and $\Gamma(\omega)$ in order to connect smoothly the phonon and fracton regimes in Eq. (6.20),

$$v(\omega)=v_0[1+(\omega/\omega_c)^m]^{x/m} \tag{6.21}$$

and

$$\Gamma(\omega)=\frac{\omega^4}{\omega_c^3[1+(\omega/\omega_c)^m]^{3/m}}\ . \tag{6.22}$$

Substituting Eqs. (6.21) and (6.22) into Eq. (6.11), and using the experimental data, they obtained the following values for the parameters: $m=2$, $\omega_c/2\pi=9.926\rho^{3.47\pm0.04}$ Hz, and $v_0=4.79\rho^{1.63\pm0.04}$ cm/sec. From these values, they have obtained the *acoustic* correlation length defined by $\xi_{ac}=v_0/\omega_c=8.3\times10^6\rho^{-1.84}$ Å. The value of ξ_{ac} is larger than that of the static correlation length ξ estimated from neutron-scattering experiments (Courtens and Vacher, 1987). They find $\xi_{ac}\approx5\xi$. From the value of ξ_{ac}, the fractal dimension was extracted using the formula $\xi\propto\rho^{1/(D_f-d)}$: $D_f=2.46$. It should be stressed that this value of D_f is very close to the value obtained from neutron-scattering experiments, $D_f=2.4$ (Vacher, Woignier, Pelous, and Courtens, 1988).

Courtens and Vacher (1988) also obtained the dispersion relation $\omega_c\propto\xi_{ac}^{-1.88}$ from the data for various densities of silica aerogels, as shown in Fig. 24. Substituting this dispersion relation into Eq. (4.16), and using $D_f=2.46$, they obtained $\tilde{d}_b=1.3$. Vacher, Courtens, Coddens, *et al.* (1990) performed inelastic neutron-scattering experiments for silica aerogels with a density 210 kg/m^3 and $D_f=2.4$. They estimated the crossover frequency $\omega_{l_c}/2\pi\approx10$ GHz, above and below which the fracton dimensions were estimated to be $\tilde{d}_b=1.3$ and $\tilde{d}_s=2.2$. The value for $\tilde{d}_b$ is very close to that obtained by Courtens *et al.* (1988) from light scattering.

Tsujimi *et al.* (1988) have reported the results of depolarized Raman spectroscopy on fractal silica aerogels at frequencies from 0.3 to 50 cm^{-1}. They found in the fracton region a power-law dependence of the Raman susceptibility on frequency. A typical spectrum is shown in Fig. 25, showing the scattering spectra for a silica aerogel with $\rho=357$ kg/m^3 in depolarized 90° scattering [VH (vertical-horizontal) polarization]. In the VH polarization the contribution from the bending fracton is most important, and that of longitudinal phonons is irrelevant.

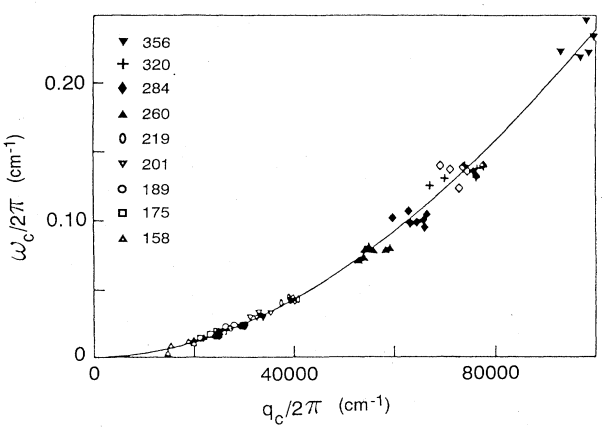

FIG. 24. Plot of the values of ω_c vs q_c derived from various Brillouin-scattering measurements performed on a series of mutually self-similar aerogels. Different symbols correspond to different sample densities, as indicated in units of kg/m^3. The points for each individual sample were obtained at various scattering angles. After Courtens and Vacher (1988).

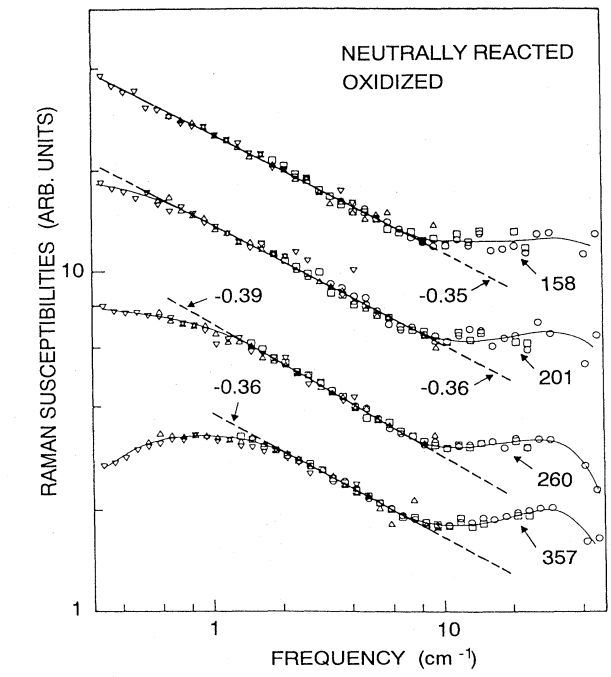

FIG. 25. Raman susceptibilities $I(\omega)/n(\omega)$ for four samples designated by their densities in kg/m^3. The corresponding acoustic correlation lengths ξ_{ac} are 750, 480, 300, and 170 Å, in order of increasing density. The straight lines are fits with the indicated slopes, whereas the tin curves are meant as guides to the eye. The different symbols correspond to the four different mirror spacings L. After Tsujimi *et al.* (1988).

They have shown, by comparing polarized (VV) and depolarized (VH) scattering intensities, that the effect of the far wing of the elastic line is negligible for the spectra beyond 6% of an order away from the central line. To cover the spectral region of interest with sufficient overlap, they have selected four mirror spacings ($L=0.015$, 0.029, 0.075, and 0.165 cm). The spectra were divided by the Bose-Einstein factor to obtain the Raman susceptibilities, and both Stokes and anti-Stokes channels were averaged over logarithmically spaced increments. They matched the results obtained with different spacings by using constant multiplicative factors, leading to the presentation in Fig. 25.

On the four curves of Fig. 25, one recognizes a linear region in the logarithmic plot of the susceptibilities, as indicated by the straight lines. For the lightest sample, this behavior extends over at least 1.5 orders of magnitude in ω. The large extension to lower frequencies can be related to the low value of $\omega_c \sim 0.02$ cm^{-1} derived from the Brillouin data on this sample (Courtens *et al.*, 1988). For the heaviest sample, the same data give $\omega_c \sim 0.3$ cm^{-1}, and this corresponds qualitatively to the onset seen in that region in Fig. 25. The rounding-out of the curves measured on the three heaviest samples at low frequencies scales with their respective phonon-fracton crossover frequencies as determined from the Brillouin experiment (Courtens *et al.*, 1988). This establishes the origin of that feature, and also that the straight-line behavior corresponds to the fracton regime. The Raman susceptibility is given by

$$I(q,\omega)/n(\omega/k_B T) \propto \omega^{-x} ,$$

with $x=0.35\sim0.39$. Alexander, Courtens, and Vacher (1993) have given an equation for the exponent x incorporating the long-range dipole-induced-dipole (DID) mechanism and introducing an averaged strain exponent σ. The exponent x is expressed as

$$x=2[(\tilde{d}_b/D_f)(D_f-d-\sigma)+1] .$$

Using the observed values $x=0.36$, $\tilde{d}_b=1.3$, and $D_f=2.4$, we can estimate the exponent σ for strain to be $\sigma\approx1$.

Montagna *et al.* (1990), Pilla *et al.* (1992), and Mazzacurati *et al.* (1992) have calculated numerically the polarized Raman-scattering activity coefficient $C(\omega)$ for the DID effective polarizability model for SP on 65×65 lattices for $d=2$ and on $29\times29\times29$ lattices for $d=3$ (footnote 17). The Raman coefficient $C(\omega)$ is defined by

$$C(\omega)=\frac{\omega}{[n(\omega)+1]}\frac{1}{\mathcal{D}(\omega)}I(\omega) ,$$

where the Raman intensity $I(\omega)$ is

$$I(\omega)=\frac{1}{2N\pi}\int dt e^{i\omega t}\sum_{ij}\langle\mu_i(t)\mu_j(0)\rangle ,$$

and $\mu_i(t)$ is the induced dipole of the ith atom. When the induced dipole is proportional to the local strain, the Raman intensity $I(\omega)$ becomes equivalent to the dynamical structure factor $S(q,\omega)$ as $q\to0$. The results for $C(\omega)$ of Montagna *et al.* (1990) and Mazzacurati *et al.* (1992) suggest that the DID Raman coefficients depend linearly on ω for both $d=2$ and $d=3$ percolation networks at p_c, which is not in accord with the simulation results by Stoll, Kolb, and Courtens (1992). The source of disagreement may lie with the use of SP lattices by Montagna *et al.* (1990) and Mazzacurati *et al.* (1992). As shown by Stoll *et al.* (1992) (see Fig. 2), the SP lattice does not reach the scaling regime until roughly ten lattice sites have been covered. Only a few lattice sites are required for BP. This means that the geometry of a spatial region of characteristic dimension less than approximately ten lattice sites for SP would not exhibit fractal structure. Hence any vibrational excitations localized over spatial ranges less than this amount would not exhibit the scaling properties expected for fractons. Therefore the lack of scaling noted by Montagna *et al.* (1990) and Mazzacurati *et al.* (1992) may be attributable to the small lattice size used by them for their simulations.

Stoll, Kolb, and Courtens (1992) have calculated the Raman coupling coefficient $C(\omega)$ for the DID scattering process. The results are shown in Fig. 26. The symbol F means the full-DID calculation in which the polarization of an atom is induced by polarizations of *all* remaining atoms, while NN means the polarization is affected by only the nearest-neighbor polarizations. Their results indicate that the coefficients $C_F(\omega)$ follow the relations $C_F(\omega)\propto\omega^{0.38}$ and $\propto\omega^{0.29}$ for $d=2$ and $d=3$ BP networks, respectively. These results are in accord with the

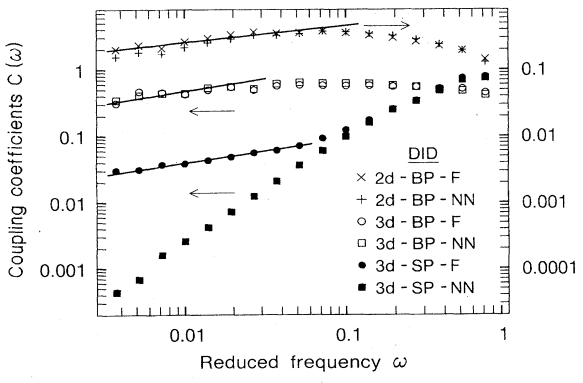

FIG. 26. Relative DID coupling coefficients for the six cases indicated. The straight lines were drawn according to a theory of Alexander, Courtens, and Vacher (1993). After Stoll, Kolb, and Courtens (1992).

[17]The net electric field incident on a given atom is composed of the incident field plus the sum of all previously scattered fields. When the incident field, modified by the effect of the index of refraction is much stronger than the scattered field, one can neglect the latter. This corresponds to Raman scattering by the direct process or neutron scattering. When the scattered field is strong, the dipole-induced-dipole mechanism becomes relevant.

scaling predictions of Alexander, Courtens, and Vacher (1993).

VII. MAGNONS AND FRACTONS IN PERCOLATING MAGNETS

Diluted Heisenberg magnets represent realizations of fractal structure. We discuss the nature of spin-wave and magnetic fracton excitations in this section and use isotropic percolating Heisenberg magnets. We focus, in particular, on the dynamical property of percolating *antiferromagnets,* because they can be readily prepared and studied.

A. Fractons on percolating ferromagnets

The Hamiltonian for a diluted Heisenberg magnet on a percolating network is given by

$$H=\sum_{i,j} J_{ij}\mathbf{S}_i\cdot\mathbf{S}_j \ . \tag{7.1}$$

Here the symbol $\mathbf{S}_i$ denotes the spin vector at the site i, and J_{ij} the exchange coupling between nearest-neighbor spins, respectively. The coupling constant J_{ij} is taken as $J_{ij}=J$, if both sites i and j are occupied, and $J_{ij}=0$ otherwise.

We first discuss the case $J<0$ in this subsection, namely, the ferromagnetic system. The linearized equations of motion for spin deviations S_i^+ from perfect ferromagnetic order are expressed in units of $2S/\hbar=1$ (S is the magnitude of single spin) by

$$i\frac{\partial S_i^+}{\partial t}=\sum_j J_{ij}(S_j^+-S_i^+) \ , \tag{7.2}$$

where $S_i^+\equiv S_i^x+iS_i^y$. The same equation holds for S_i^- ($\equiv S_i^x-iS_i^y$).

For $p<p_c$, there is no long-range magnetic order of spin configurations, because no infinitely connected cluster exists for $p<p_c$. Shender (1976b) has shown that the Curie temperature T_c is proportional to $(p-p_c)^{\mu-\nu}$. At $p=1$, one has conventional spin waves with dispersion relation

$$\omega=Jk^2 \ .$$

It has been shown, using a variational approach (Murray, 1966), that spin waves persist above the percolation threshold. For the case of $p>p_c$ and $\lambda\gg\xi$, where λ is the spin-wave wavelength, Edwards and Jones (1971) and Tahir-Kheli (1972a) have demonstrated that weakly damped spin waves exist on diluted percolating ferromagnets, for which the dispersion relation is given by

$$\omega=D(p)k^2 \ , \tag{7.3}$$

where $D(p)$ is an effective spin-stiffness coefficient. The concentration dependence of $D(p)$ for ferromagnetic spin waves in the hydrodynamic limit has been determined by Kirkpatrick (1973b). He has related the stifffness coefficient $D(p)$ with the conductivity $\sigma(p)$ of the network, using the corresponding relationship between the equation of spin motion (7.2) and Kirchhoff's equation of the resistor network. He found

$$\sigma(p)=\frac{e^2}{k_BT}g_0P_\infty(p)D(p) \ , \tag{7.4}$$

where g_0 is the conductance of a single bond. From this, $D(p)$ becomes[18] [see also Eq. (3.4)]

$$D(p)\propto\frac{\sigma(p)}{P_\infty(p)}\propto(p-p_c)^{\mu-\beta} \ . \tag{7.5}$$

To make the connection with fracton excitations, we introduce dynamic scaling for the dispersion relation

$$\omega=k^{z_f}F(k\xi) \ , \tag{7.6}$$

where z_f is a dynamic exponent (Halperin and Hohenberg, 1967, 1969; Kumar, 1984; Christou and Stinchcombe, 1986a). The scaling function $F(x)$ satisfies $F(x)\propto x^{2-z_f}$ for $x\gg1$, because dispersion relation (7.3) must hold in the hydrodynamic limit; and $F(x)=$const for $x\ll1$, because the dispersion relation cannot depend on ξ in this limit. Thus, for long-wavelength magnetic excitations ($k\xi\ll1$), one has $\omega\propto\xi^{2-z_f}k^2$. From Eq. (7.3), $D(p)\propto\xi^{(\beta-\mu)/\nu}$; and one finds

$$z_f=2+(\mu-\beta)/\nu \ . \tag{7.7}$$

But $z_f=2D_f/\tilde{d}_f$ (Alexander and Orbach, 1982; Rammal and Toulouse, 1983), where $\tilde{d}_f$ is the fracton dimension of ferromagnetic fractons, so that

$$\tilde{d}_f=\frac{2\nu D_f}{\mu-\beta+2\nu} \ . \tag{7.8}$$

This equation for $\tilde{d}_f$ is the same as that for the fracton dimension $\tilde{d}$ of the vibrational problem. This is a natural consequence of the equivalence between the equation of motion (7.2) for spin waves and Eq. (5.1) for vibrations with scalar interactions. The only difference is the power of the eigenfrequency ω in the corresponding secular equations. The above scaling argument suggests that ferromagnetic fractons belong to the same universality class as that for vibrational fractons with scalar interactions. Magnetic excitations on percolating ferromagnets were discussed in some detail by Shender (1976a, 1976b) prior to the formulation of the scaling theory of vibrational

[18]It might be expected from Eq. (7.5) that the ordered ground state for $p>p_c$ would be stable against long-wavelength spin fluctuations. However, the derivation of Eq. (7.5) is based on the linearized equations of motion valid when the magnetization is near full polarization, that is, $\langle\mathbf{S}_i\rangle$ is large and one is at low temperatures.

fractons (Alexander and Orbach, 1982; Rammal and Toulouse, 1983).

The DOS of ferromagnetic fractons is given by

$$\mathcal{D}_f(\omega) \propto \omega^{\tilde{d}_f/2-1} ; \tag{7.9}$$

and the dispersion relation becomes

$$\Lambda(\omega) \propto \omega^{-\tilde{d}_f/2D_f} , \tag{7.10}$$

where Λ has the meaning of a localization length, a wavelength, and a scattering length, as in the case of vibrational fractons. From Eq. (7.10), one sees that the crossover frequency ω_c from magnons to fractons is given by

$$\omega_c \propto (p-p_c)^{2\nu D_f/\tilde{d}_f} , \tag{7.11}$$

which is different from the case of vibrations [see Eq. (4.17)] by a factor of 2 arising from the difference in order of the time derivative in the equation of motion.

Numerical calculations for the ferromagnetic systems have been performed by Lewis and Stinchcombe (1984), Evangelou (1986a), Evangelou, Papanicolaou, and Economou (1991), Argyrakis, Evangelou, and Magoutis (1992). Lewis and Stinchcombe (1984) calculated the DOS of magnetic excitations for $d=2$ diluted Heisenberg ferromagnets. They treated percolating networks at p_c on 64×64 square lattices with periodic boundary conditions. The computation was carried out for 15 different random clusters. They found that the DOS is proportional to $\omega^{\tilde{d}_f/2-1}$ with $\tilde{d}_f=1.34\pm0.06$. Evangelou (1986a) also calculated the DOS of spin waves in $d=2$ site-percolating Heisenberg ferromagnets formed on square lattices by the Gaussian elimination technique (Evangelou, 1986b). The results obtained for systems with $\sim10^4$ sites follow the power law $\mathcal{D}_f(\omega)\propto\omega^{-0.32\pm0.02}$, indicating $\tilde{d}_f=1.36\pm0.04$. Evangelou also obtained the dispersion relation from the concentration dependence of the crossover frequency ω_c from magnons to fractons, checking the relation Eq. (7.11). The DOS of $d=3$ ferromagnetic fractons has been calculated by Evangelou, Papanicolaou, and Economou (1991) using the maximum-entropy method (Jaynes, 1957a, 1957b; Mead and Papanicolaou, 1984). They estimated a value for the fracton dimension of $\tilde{d}_f=1.52\pm0.05$. Argyrakis, Evangelou, and Magoutis (1992) have calculated the DOS of spin waves in the SP network using the Lanczos method. Their results demonstrate that the DOS is proportional to the power law $\omega^{\tilde{d}_f/2-1}$ with $\tilde{d}_f=1.32$ and $\tilde{d}_f=1.30$ for $d=2$ and $d=3$ networks, respectively, and that it is smooth at the magnon-fracton crossover.

Effective-medium approximations (EMA; see Yu, 1984 and Wang and Gong, 1989) suggest that $\tilde{d}_f=1$ for percolating ferromagnets in any Euclidean dimensions d. The DOS of percolating ferromagnets above p_c have been calculated, and results show a sharp crossover from the magnon spectrum $[\mathcal{D}(\omega)\propto\omega^{d/2-1}]$ for $\omega\ll\omega_c$ to the fracton spectrum $[\mathcal{D}(\omega)\propto\omega^{-1/2}]$ for $\omega\gg\omega_c$. The crossover frequency ω_c depends on the concentration p through $\omega_c\propto(p-p_c)^2$. Provided that the Alexander-Orbach conjecture, $\tilde{d}_f=4/3$, holds, the DOS of ferromagnetic fractons should obey $\mathcal{D}(\omega)\propto\omega^{-1/3}$ and the crossover frequency ω_c should be proportional to $(p-p_c)^{3.24}$ for $d=3$. The difference between the exponents 1/2 and 1/3 is due to the fact that the spatial correlations of percolating networks are neglected in the EMA. The DOS at the crossover frequency obtained by the EMA exhibits very sharp structure. There is no sign of structure in the crossover region from numerical simulation studies (Evangelou, 1986a).

The values of z_f and $\tilde{d}_f$ have also been calculated analytically by Stinchcombe and Harris (1983) and by Pimentel and Stinchcombe (1989). Stinchcombe and Harris (1983) treated ferromagnetic spin-wave dynamics near the percolation threshold by the renormalization-group technique and the continuum approach, valid for small wave vectors and long correlation lengths ξ. Both approaches yielded the same dynamic exponent $z_f=2$. This implies $\tilde{d}_f=D_f$ for ferromagnetic fractons. Pimentel and Stinchcombe (1989) studied spin-wave fracton dynamics using Nagatani's model (Nagatani, 1985) as a $d=2$ deterministic fractal model for the BP network. They obtained the values of $z_f=\ln22/\ln3\simeq2.81$ and $\tilde{d}_f=2\ln8/\ln22\simeq1.34$. These results are in good agreement with the numerical results and the Alexander-Orbach conjecture. The dynamical structure factor of damped magnons ($k\xi\ll1$) in percolating ferromagnets has been obtained through a diagrammatic perturbation technique (Christou and Stinchcombe, 1986a, 1986b).

The DOS of ferromagnetic fractons have been obtained experimentally by measurements of the temperature dependence of the magnetization $M(T)$ of diluted Heisenberg ferromagnets (Salamon and Yeshurun, 1987; Yeshurun and Salamon, 1987). Because each spin excitation reduces the magnetization of the ferromagnet by one Bohr magneton, the well-known Bloch's law for homogeneous systems, $M(T)/M(0)=1-BT^{3/2}$, follows from a Bose-Einstein integration of the spin-wave DOS per unit volume ($\mathcal{D}\sim\omega^{1/2}$) (Bloch, 1932; Keffer, 1966). Magnetic fractons in percolating Heisenberg ferromagnets cause a deviation in the temperature dependence of the magnetization from the Bloch $T^{3/2}$ law because of their anomalous DOS (Stinchcombe and Pimentel, 1988). Salamon and Yeshurun (1987; Yeshurun and Salamon, 1987) have measured the temperature dependence of the magnetization of amorphous $(Co_pNi_{1-p})_{75}P_{16}B_6Al_3$ alloys with $0.34\le p\le0.5$. They found departures from Bloch's $T^{3/2}$ law and obtained the DOS of magnetic fractons. Their results agree well with the numerically obtained DOS.

B. Fractons on percolating antiferromagnets

1. Scaling arguments

In the case of diluted Heisenberg antiferromagnets, the Hamiltonian (7.1) is taken, but $J>0$. The linearized

equations of spin motion are given by

$$i\frac{\partial S_i^+}{\partial t}=\sigma_i\sum_j J_{ij}(S_j^+ + S_i^+)\ , \tag{7.12}$$

and the same equations hold for S_i^-. In Eq. (7.12), σ_i is taken to be $+1$ for the site i belonging to the up-spin sublattice and -1 to the down-spin sublattice. These equations have quite different symmetry from the equations of motion for ferromagnetic spin waves, Eq. (7.2), or vibrations with scalar displacements, Eq. (5.1).

To explore the consequences of this difference, consider the corresponding secular equation $\omega\chi_i=\sum_j Q_{ij}\chi_j$, where χ_i is the normal mode belonging to the eigenfrequency ω, i.e., $S_i^+(t)=\sum_\lambda A_\lambda\chi_i(\lambda)e^{-i\omega_\lambda t}$. The matrix elements Q_{ij} are given by $Q_{ij}=\sigma_i[J_{ij}-\delta_{ij}\sum_k J_{ki}]$. The matrix $\mathbf{Q}$ is not symmetric ($Q_{ij}=-Q_{ji}$ for $i\neq j$) and $\sum_j Q_{ij}\neq 0$ because of the factor σ_i, whereas the dynamical matrix $\mathbf{D}$ for lattice vibrations or ferromagnetic spin waves is symmetric and satisfies the condition $\sum_j D_{ij}=0$. These differences are the reason that the equations of motion for antiferromagnets cannot be mapped onto the master equation.

Shender (1978) has shown that the Néel temperature T_c of a percolating antiferromagnet is proportional to $(p-p_c)^{\mu-\nu}$, so that one can expect spin-wave excitations on percolating antiferromagnets for $p>p_c$, as was found for ferromagnets. This has been confirmed by a Green's-function approach (Jones and Edwards, 1971) and the coherent-potential approximation (Buyers, Pepper, and Elliott, 1972; Tahir-Kheli, 1972a, 1972b; Elliott and Pepper, 1973; Holcomb, 1974, 1976). These theories predict a linear dispersion relation for low-frequency spin waves,

$$\omega=C(p)k\ . \tag{7.13}$$

Using the phenomenological expression for the hydrodynamic long-wavelength spin waves, Harris and Kirkpatrick (1977) have shown that the stiffness constant $C(p)$ in Eq. (7.13) is given by

$$C=\gamma\sqrt{2A/\chi_\perp}\ . \tag{7.14}$$

Here γ is the gyromagnetic ratio; $\chi_\perp$, the transverse susceptibility; and A is defined as a measure of the energy needed to create a spatial variation in the staggered magnetization. The quantity A is proportional to the conductivity of a related resistor network (Brenig *et al.*, 1971; Kirkpatrick, 1973a; Harris and Kirkpatrick, 1977). Thus one can set $A\propto(p-p_c)^\mu$. Breed *et al.* (1970, 1973) have shown experimentally that the transverse susceptibility $\chi_\perp$ diverges as $p\to p_c$. The p dependence of $\chi_\perp$ was first elucidated by Harris and Kirkpatrick (1977), who found numerically that $\chi_\perp\propto(p-p_c)^{-\tau}$ with $\tau=0.5$ for $d=3$. The stiffness constant $C(p)$ in Eq. (7.14) therefore varies with concentration p as

$$C(p)\propto(p-p_c)^{(\mu+\tau)/2}\ . \tag{7.15}$$

The dynamical scaling argument for spin waves on percolating antiferromagnets can be extended with the aid of the hydrodynamic descriptions, Eqs. (7.14) and (7.16). The dispersion relation is given, as in the ferromagnetic case [Eq. (7.6)], by

$$\omega=k^{z_a}G(k\xi)\ , \tag{7.16}$$

where z_a is a dynamical exponent for antiferromagnets. Since the linear dispersion relation, Eq. (7.13), holds in the hydrodynamic limit ($k\xi\ll 1$), the scaling function $G(x)$ should satisfy $G(x)\propto x^{1-z_a}$ for $x\ll 1$. At the opposite extreme, $G(x)$ should be constant for $x\gg 1$. From these behaviors of the scaling function in two asymptotic regimes, one finds $\omega\propto k^{z_a}$ with

$$z_a=1+\frac{\mu+\tau}{2\nu}\ . \tag{7.17}$$

The dynamical exponent z_a is related to the fracton dimension $\tilde{d}_a$ as $z_a=D_f/\tilde{d}_a$, and one obtains

$$\tilde{d}_a=\frac{2\nu D_f}{\mu+\tau+2\nu}\ . \tag{7.18}$$

It should be noted that this relation becomes the same with the expression for $\tilde{d}_f$ [Eq. (7.8)] or $\tilde{d}$ [Eq. (4.15)] if one replaces τ by $-\beta$. Because τ and β are positive, and so $\tau>-\beta$, one has the inequality

$$\tilde{d}_a<\tilde{d}_f\ . \tag{7.19}$$

As seen from the above scaling arguments, magnetic fractons should exist in diluted Heisenberg antiferromagnets as well as for the case of ferromagnets (Shender, 1978; Christou and Stinchcombe, 1986b; Orbach and Yu, 1987; Orbach *et al.*, 1988; Polatsek, Entin-Wohlman, and Orbach, 1988; Orbach, 1989c). The DOS of antiferromagnetic fractons is

$$\mathcal{D}_a(\omega)\propto\omega^{\tilde{d}_a-1}\ , \tag{7.20}$$

and its dispersion relation becomes

$$\Lambda(\omega)\propto\omega^{-1/z_a}\ , \tag{7.21}$$

where Λ is the characteristic length of fractons.

The relationship between τ and other known exponents has been investigated by Harris and Kirkpatrick (1977). They considered a system in which all the spins are directed initially along the z axis, dividing it into small cells v_m with volume ξ^d. The disorder of the system produces the unbalanced spins $S(v_m)=\sum_{\text{cell}}\langle S_i^z\rangle\propto\sqrt{N_m}$, where N_m is the number of spins in the cell v_m. Magnetic fields $H_0\hat{\mathbf{x}}$ on v_m are applied, where $\hat{\mathbf{x}}$ is a unit vector perpendicular to $\hat{\mathbf{z}}$. Provided that the spins on the boundary of each cell are fixed to be parallel to $\hat{\mathbf{z}}$, spins are tilted by the magnetic field and are expressed by

$$\mathbf{S}(\mathbf{r})=S_i^z\left[\left[1-\frac{\theta_r^2}{2}\right]\hat{\mathbf{z}}+\theta_r\hat{\mathbf{x}}\right]\ , \tag{7.22}$$

with

$$\theta_r = a_k \prod_{\alpha=1}^{d} \sin k x_\alpha ,$$

where x_α is the Cartesian coordinate of the α direction and $k = 2\pi/\xi$ is chosen so that θ_r vanishes on the boundary of v_m. The symbol a_k is a numerical constant. The change of the total energy $E(v_m)$ in v_m arises from the exchange energy of order $\xi^d a_k^2 k^2$ and the Zeeman energy of the unbalanced spins. As a result, one has

$$E(v_m) = c_1 \xi^d a_k^2 k^2 - c_2 S(v_m) a_k H_0 , \tag{7.23}$$

where c_1 and c_2 are numerical constants. Minimizing $E(v_m)$ with respect to a_k, one has

$$a_k \sim S(v_m) \xi^{2-d} H_0 ,$$

so that the transverse magnetization per site $m_\perp$ $[\sim \xi^{-d} \int S(v_m) \sin\theta_r d\mathbf{r}]$ is given by

$$m_\perp \sim S(v_m)^2 \xi^{2-2d} .$$

This is the result for the constrained spins on the boundary of a cell. We expect larger magnetization for unconstrained spins. Therefore the transverse susceptibility $\chi_\perp (= m_\perp / H_0)$ should be

$$\chi_\perp \geq S(v_m)^2 \xi^{2-2d} / H_0 .$$

The effective field $\sum_j J_{ij} \mathbf{S}_j$ for the ith spin plays the role of H_0 in this case, and this field is proportional to A ($\propto \xi^{-\mu/\nu}$) in Eq. (7.14). Using $S(v_m)^2 \propto N_m \propto \xi^{D_f}$, one obtains

$$\chi_\perp \geq \xi^{2+D_f-2d+\mu/\nu} , \tag{7.24}$$

and thus

$$\tau \geq \mu - \beta + (2-d)\nu . \tag{7.25}$$

There are several arguments on inequality (7.25) suggesting that this relation should be an equality (Harris and Kirkpatrick, 1977; Ziman, 1979; Kumar and Harris, 1985). Ziman (1979) has derived the same relation by considering the propagation of spin waves on a *nodes-links-blobs* picture of the percolating network. The mean-field calculation by Kumar and Harris (1985) also generates an equality for Eq. (7.25). Ziman (1985) has calculated numerically the value of the exponent τ for $d=3$ percolating antiferromagnets by employing the finite-size scaling technique for the transverse susceptibility *per occupied site,* $\bar{\chi}_\perp$ $[\propto (p - p_c)^{-\tau-\beta}]$. For a finite-size system, this quantity depends on system size L as $\bar{\chi}_\perp \propto L^{(\tau+\beta)/\nu}$ at $p = p_c$. Ziman (1985) calculated the size dependence of $\bar{\chi}_\perp$ for percolating systems formed on $d=3$ lattices of $10\times10\times10$ to $80\times80\times80$ available sites. The results suggest $\bar{\chi}_\perp \propto L^{1.4\pm0.1}$, corresponding to an exponent $\tau = 0.79\pm0.1$. The lower bound value of τ for $d=3$ percolating systems becomes 0.72, using known values of μ, β, and ν. The value $\tau = 0.79\pm0.1$ is larger than the value of the lower bound.

Using Eq. (7.18) and the inequality (7.24), we show that the fracton dimension $\tilde{d}_a$ is bounded by

$$\tilde{d}_a \leq \frac{2\nu D_f}{2\mu - \beta + (4-d)\nu} . \tag{7.26}$$

Yakubo, Terao, and Nakayama (1993) have found that if the Alexander-Orbach conjecture $\tilde{d} = 4/3$ is taken into account in inequality (7.25), i.e., $\mu = [\nu(3d-4) - \beta]/2$, the upper bound for $\tilde{d}_a$ becomes unity independent of the Euclidean dimension d. Thus

$$\tilde{d}_a \leq 1 \tag{7.27}$$

for all $d \geq 2$, a most surprising result.

2. Simulated results of the density of states

Several numerical calculations for the universality class of antiferromagnetic fractons have been reported so far. Hu and Huber (1986) have carried out numerical studies of the DOS of spin waves excited on percolating Heisenberg antiferromagnets using eigenvalue-counting techniques (Dean, 1960; Grassl and Huber, 1984). They obtained the averaged DOS over 65 configurations of $d=2$ percolating systems formed on 50×50 square lattices at p_c. Their results indicate $\mathcal{D}_a(\omega) \propto \omega^{-0.06}$, indicating $\tilde{d}_a = 0.94$. This value of $\tilde{d}_a$ is very close to the upper bound of inequality (7.27).

Large-scale and more accurate calculations have been performed by Yakubo, Terao, and Nakayama (1993; see also Nakayama, 1993, 1994). Their results show the clear existence of antiferromagnetic fractons for $d=2$, 3, and 4 percolating networks. They employed the equation-of-motion method (Alben and Thorpe, 1975; Thorpe and Alben, 1976), introduced in Sec. VII.A, to calculate the fracton DOS. In the case of $d=2$ systems, BP networks (11 realizations) are formed on 1000×1000 square lattices at p_c with periodic boundary conditions for both x and y directions. The largest BP network has 605 544 sites. The DOS and the integrated DOS for $d=2$ percolating antiferromagnets are shown by solid squares in Figs. 27 and 28, respectively. It is remarkable that an almost constant DOS for $\omega \ll 1$ is found in Fig. 27 for all three dimensions. The least-squares fitting for solid squares in Fig. 27 leads to $\mathcal{D}_a \propto \omega^{-0.03\pm0.03}$; so $\tilde{d}_a = 0.97\pm0.03$. It should be emphasized that the $\omega^{\tilde{d}_a - 1}$ law holds even in the very low-frequency region, as in the case of Fig. 3. We see from Fig. 27 that the DOS does not follow the power-law dependence $\omega^{\tilde{d}_a - 1}$ above $\omega \sim 1$. This is because the system is not fractal on a length scale shorter than the wavelength corresponding to $\omega \sim 1$. The value $\tilde{d}_a = 0.97$ agrees well with the upper bound given by inequality (7.27).

The DOS and the integrated DOS for $d=3$ percolating antiferromagnets at $p_c (= 0.2488)$ are shown in Figs. 27 and 28 by solid triangles, respectively. The BP networks of 13 realizations (the largest network has 177 886 spins) are formed on $96\times96\times96$ cubic lattices. The value of $\tilde{d}_a$ obtained by least-squares fitting takes $\tilde{d}_a = 0.97\pm0.03$.

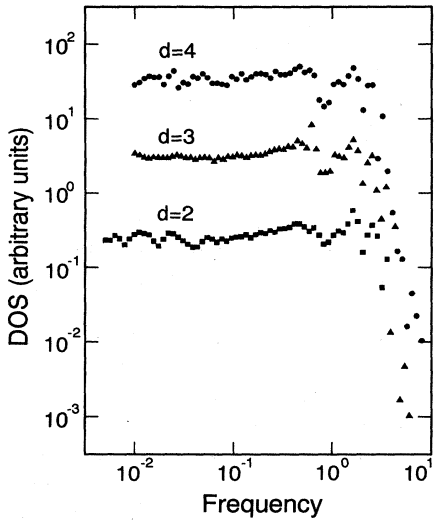

FIG. 27. Density of states (DOS) per spin for $d=2$ (squares), $d=3$ (triangles), and $d=4$ (circles) BP antiferromagnets at $p=p_c$. The results have been obtained by averaging over 11, 13, and 12 realizations of BP networks formed on 1000×1000, $96\times96\times96$, and $28\times28\times28\times28$ hypercubic lattices for $d=2$, $d=3$, and $d=4$, respectively. After Yakubo, Terao, and Nakayama (1993).

Solid circles in Figs. 27 and 28 indicate the DOS and the integrated DOS for $d=4$ BP networks at $p_c(=0.160)$, respectively. The BP networks of 12 realizations (the largest network has 26 060 spins) are formed on $28\times28\times28\times28$ hypercubic lattices. From the DOS data, we obtain $\tilde{d}_a=0.98\pm0.09$ for $d=4$ antiferromagnetic fractons. These values of $\tilde{d}_a$ do not depend on the Euclidean dimension d, but they agree with the upper bound of $\tilde{d}_a$ expressed through inequality (7.27); that is,

$$\tilde{d}_a=1 \quad \text{for all } d\ (\geq 2)\ .$$

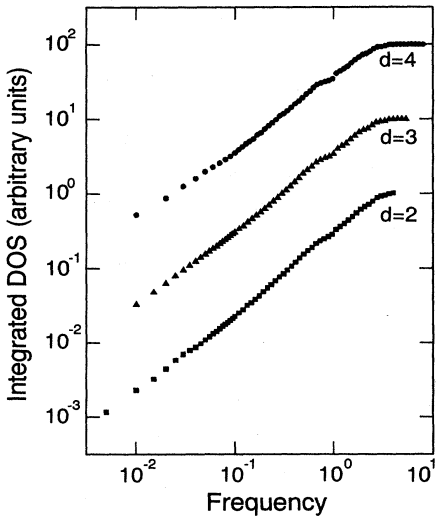

FIG. 28. Integrated DOSs per spin for $d=2$ (squares), $d=3$ (triangles), and $d=4$ (circles) BP antiferromagnets at $p=p_c$. After Yakubo, Terao, and Nakayama (1993).

Polatsek, Entin-Wohlman, and Orbach (1989) have calculated the DOS of percolating antiferromagnets in terms of the effective-medium approximation (EMA). They find a fracton dimension $\tilde{d}_a=\frac{2}{3}$ for antiferromagnetic fractons in any Euclidean dimensions d, in disagreement with the results of numerical simulations. This discrepancy is not surprising for the same reason as that found for ferromagnetic fractons. Pimentel and Stinchcombe (1989) have analytically calculated the values of z_a and $\tilde{d}_a$ using Nagatani's model (Nagatani, 1985) for BP networks. They obtained $z_a=\ln22/\ln9\simeq1.41$ and $\tilde{d}_a=2\ln8/\ln22\simeq1.35$, exceeding the upper bound expressed in Eq. (7.27).

C. Dynamical structure factor of antiferromagnets

1. Theories and numerical simulations

The dynamical structure factor of antiferromagnets has been analyzed with several theoretical treatments. Perturbation technique or coherent-potential-approximation (CPA) calculations of $S(q,\omega)$ for diluted antiferromagnets have been investigated so far by various authors (Jones and Edwards, 1971; Buyers, Pepper, and Elliott, 1972; Tahir-Kheli, 1972b; Elliott and Pepper, 1973; Holcomb, 1974, 1976). These calculations, however, do not suggest critical properties, such as the fracton DOS or the anomalous dispersion of spin-wave excitations in diluted antiferromagnets.

In order to describe fracton dynamics, an EMA calculation was performed by Yu and Orbach (1984; see also Orbach and Yu, 1987), Orbach *et al.* (1988), and Polatsek, Entin-Wohlman, and Orbach (1988, 1989). They treated the isotropic Heisenberg antiferromagnet formed on a bond-percolating network and obtained the dispersion relation, the DOS, and the dynamical structure factor $S(q,\omega)$ for percolating antiferromagnets slightly above p_c. The EMA leads to the fracton dimension $\tilde{d}_a=2/3$ and a cubic dispersion relation. The dynamical structure factor $S(q,\omega)$ within the EMA is expressed by a quasi-Lorentzian form which is characterized by an effective stiffness constant $C(\omega)$ and a linewidth $\tau^{-1}(\omega)$. The linewidth for magnon excitations ($\omega\ll\omega_c$) follows the Rayleigh law ($\tau^{-1}\propto\omega^{d+1}$), whereas the fracton excitation linewidth obeys the Ioffe-Regel condition for strong localization (Ioffe and Regel, 1960). Though the qualitative features of $S(q,\omega)$ appear consistent with the experimental results (see Fig. 31), the EMA results are not quantitatively correct because they ignore the spatial correlation of spin configurations.

The intrinsic properties of $S(q,\omega)$ for magnetic fractons and, similarly, for vibrational fractons, are given by the single-length-scale postulate (SLSP). The SLSP leads $S(q,\omega)$ to be expressed, by analogy with Eq. (6.2), by

$$S(q,\omega)=q^{-y_a}H[q\Lambda(\omega)]\ , \tag{7.28}$$

where $\Lambda(\omega)$ is the unique characteristic length of a spin-

wave fracton. Christou and Stinchcombe (1986a, 1986b) have presented an analytic expression of $S(q,\omega)$ for $q\xi \ll 1$ satisfying the dynamical scaling hypothesis. They employed a Green's-function technique and a dynamical scaling argument for hydrodynamic magnons. The dynamical structure factor they obtained takes a Lorentzian form with respect to frequency. It seems natural that the Lorentzian form of $S(q,\omega)$ keeps its profile even in the fracton regime. In this case, the dynamical structure factor $S(q,\omega)$ for antiferromagnetic fractons is written in the form (Terao, Yakubo, and Nakayama, 1994; Yakubo, Terao, and Nakayama, 1994)

$$S(q,\omega)=I(q)\frac{\Gamma(q)}{[\omega-\omega_p(q)]^2+\Gamma^2(q)} , \tag{7.29}$$

where ω_p is the frequency at which $S(q,\omega)$ takes its maximum value for fixed q. The symbols $\Gamma(q)$ and $I(q)$ represent the width of the line shape and q-dependent intensity, respectively. Terao, Yakubo, and Nakayama (1994; see also Yakubo, Terao, and Nakayama, 1994) have shown, using Eqs. (7.28) and (7.29), that the profile of $S(q,\omega)$ can be characterized by one unknown exponent y_a. The SLSP requires that both the peak frequency ω_p and the width Γ have the same wave-number dependence, i.e., $\omega_p(q)=\omega_0 q^{z_a}$ and $\Gamma(q)=\Gamma_0 q^{z_a}$, where z_a is the dynamical exponent given by Eq. (7.17). Thus the right-hand side of Eq. (7.29) is written in the form of $I(q)G[q\Lambda(\omega)]/\omega$, where G is a function of $q\Lambda(\omega)$. The scaling function $H[q\Lambda(\omega)]$ in Eq. (7.28) is then given by

$$H[q\Lambda(\omega)]=I(q)\frac{q^{y_a}G(q\Lambda)}{\omega} . \tag{7.30}$$

Because the right-hand side of Eq. (7.30) should be a function of the variable $q\Lambda$, the function $I(q)$ should be proportional to $q^{z_a-y_a}$. Therefore, from Eq. (7.29), one obtains $S(q,\omega)$ in the form

$$S(q,\omega)=S_0\frac{\Gamma_0 q^{2z_a-y_a}}{(\omega-\omega_0 q^{z_a})^2+\Gamma_0^2 q^{2z_a}} , \tag{7.31}$$

where S_0 is a numerical constant. The asymptotic behavior of frequency dependence of $S(q,\omega)$ given by Eq. (7.31) is ω^{-2} for $\omega \gg \omega_p(q)$, whereas the wave-number dependencies are $q^{2z_a-y_a}$ and q^{-y_a} for $q \ll q_p(\omega)$ $(=[\omega/\omega_0]^{1/z_a})$ and for $q \gg q_p(\omega)$, respectively. The validity of Eq. (7.31) can be checked by numerical simulations.

One can evaluate the upper and lower bounds of the new exponent y_a as follows. From Eq. (7.28), the equal-time correlation function $C(q)$ defined by the integration of $S(q,\omega)$ over the whole range of ω is given by

$$C(q)\propto q^{z_a-y_a} . \tag{7.32}$$

The correlation function $C(q)$ should not be zero at $q=0$. This leads to a lower bound of the exponent y_a: $y_a > z_a$. The Fourier transform $C(r)$ of Eq. (7.32) becomes proportional to $r^{y_a-z_a-d}$. Because the spatial correlation function $C(r)$ should decrease with increasing distance r between two spins, one has $y_a < z_a+d$, which generates an upper bound for y_a. Consequently, the value of the exponent y_a is bounded by

$$z_a < y_a < z_a+d . \tag{7.33}$$

The explicit value of the exponent y_a can be determined from numerical computations of $S(q,\omega)$ for magnetic fractons.

Terao, Yakubo, and Nakayama (1994) have performed numerical simulations on $S(q,\omega)$ of magnetic fractons on percolating Heisenberg antiferromagnets. They considered BP at $d=2$ networks at the percolation threshold ($p_c=0.5$) formed on 62×62 square lattices with periodic boundary conditions. The dynamical structure factor $S(\mathbf{q},\omega)$ of Heisenberg antiferromagnets is expressed by spin-wave eigenmodes $\chi_i(\lambda)$ as (Terao, Yakubo, and Nakayama, 1994)

$$S(\mathbf{q},\omega)=\frac{1}{V}\sum_{\lambda}\delta(\omega-\omega_\lambda)R_\lambda\left|\sum_i e^{-i\mathbf{q}\cdot\mathbf{R}_i}\chi_i(\lambda)\right|^2 , \tag{7.34}$$

where V is the volume of the system and $\mathbf{R}_i$ is the positional vector of the site i. The symbol R_λ is defined by $R_\lambda=\tilde{\chi}_i(\lambda)/\chi_i(\lambda)$, which is independent of i, where $\tilde{\chi}_i(\lambda)$ is related to $\chi_i(\lambda)$ as $\sum_i \sigma_i\tilde{\chi}_i(\lambda)\chi_i(\lambda')=\delta_{\lambda\lambda'}$. The direct diagonalization technique has been employed to obtain fracton eigenmodes $\chi_i(\lambda)$, and $S(\mathbf{q},\omega)$ has been calculated from the Fourier transforms of $\chi_i(\lambda)$, whose eigenfrequencies are close to ω. The dynamical structure factor $S(q,\omega)$ as a function of $q(=|\mathbf{q}|)$ and ω has been obtained by a directional average over vector $\mathbf{q}$ and an ensemble average over 54 realizations of percolating networks. Calculated results of q dependence of $S(q,\omega)$ for several values of ω are shown in Fig. 29. The value of the exponent y_a in Eq. (7.28) is evaluated by least-squares fitting for the q dependence of $S(q,\omega)$ with fixed values of $q\Lambda(\omega)$. They find $y_a=3.0\pm 0.3$. This value satisfies condition (7.33).

Figure 30 is a plot of the calculated value $H(q\Lambda(\omega))=q^{y_a}S(q,\omega)$, with the above value of y_a, as a function of $q\Lambda(\omega)$. Solid circles represent the average value over data within narrow range of the scaling variable $q\Lambda(\omega)$. The results show that $S(q,\omega)$ obeys Eq. (7.28), with the single scaling function $H(x)$ having a power-law asymptotic form both for $x \ll 1$ and for $x \gg 1$. From Fig. 30, Terao, Yakubo, and Nakayama (1994) obtained the wave-number dependence and the frequency dependence of $S(q,\omega)$ for these cases. For $\omega \gg \omega_p(q)$, the frequency dependence of $S(q,\omega)$ behaves as $S(q,\omega)\propto\omega^{-1.9\pm 0.1}$. The wave-number dependencies are $q^{0.5\pm 0.1}$ and $q^{-2.8\pm 0.8}$ for $q \ll q_p(\omega)$ and for $q \gg q_p(\omega)$, respectively. With the values of $z_a=1.83\pm 0.08$ and $y_a=3.0\pm 0.3$ taken into account, these results are consistent with Eq. (7.31).

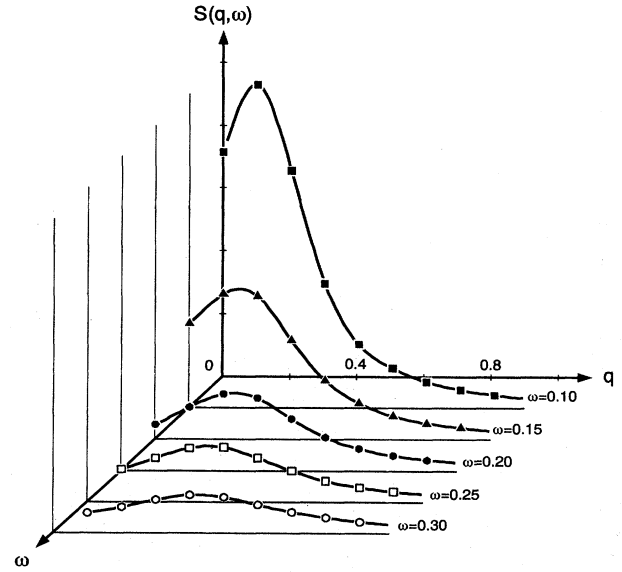

FIG. 29. Numerically obtained $S(q,\omega)$ of percolating antiferromagnets at p_c. The solid lines are only meant as guides to the eye. After Terao, Yakubo, and Nakayama (1994).

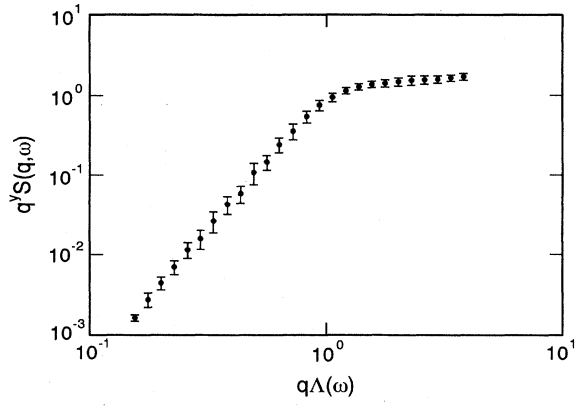

FIG. 30. Scaling function of the dynamical structure factor of $d=2$ percolating Heisenberg antiferromagnets at p_c as a function of the scaling variable $q\Lambda(\omega)$. Solid circles are plotted by averaging over a narrow range of $q\Lambda$. The ensemble average has been taken over 54 BP networks formed on 62×62 square lattices. Error bars indicate the statistical errors of the data. The asymptotes have the theoretical slopes $2z_a$ and 0 with $z_a=1.83$. After Terao, Yakubo, and Nakayama (1994).

2. Experiments

In this subsection we describe experimental work leading to the observation of fractons in antiferromagnets. Inelastic neutron-scattering experiments reveal the characteristic features of fracton excitations most easily, as mentioned in Sec. VI.[19] In order to compare experimental results with theoretical predictions of fracton excitations, one should prepare samples with the following properties: (i) The coupling between spins should be described by the Heisenberg interaction; (ii) the anisotropy of the system should be negligible; (iii) the spin interaction should be short range; (iv) the diluted magnetic ions should be distributed uniformly over the entire system so that the configuration of magnetic ions has a percolation structure; and (v) randomness should not introduce spin frustration. $Mn_xZn_{1-x}F_2$ is one material that satisfies most of these conditions [it does not satisfy property (ii)]. MnF_2 is a representative $d=3$ Heisenberg antiferromagnet with the rutile structure. Below the Néel temperature, $T_N=67.4$ K, the Mn spins align along the c axis because of the weak anisotropic Ising interaction between the Mn moments. The antiferromagnetic exchange interaction between the Mn moments located at the body center and the corner of the rutile crystal is much stronger than this anisotropy energy and the coupling between Mn spins on the same sublattice. Therefore the randomness introduced by diluting MnF_2 does not give rise to frustration. Diffuse scattering measurements (Birgeneau *et al.*, 1980; Uemura and Birgeneau, 1986, 1987) suggest that this material can be regarded as a $d=3$ site-percolating spin network on the body-centered-cubic lattice. Because the threshold concentration of the bcc site-percolation network is 0.245, one can expect spin-wave excitations above 25% Mn concentration.

Coombs *et al.* (1976) performed inelastic neutron-scattering experiments on $Mn_{0.78}Zn_{0.22}F_2$ and $Mn_{0.32}Zn_{0.68}F_2$. For high-density Mn samples, they observed a well-defined magnon spectrum with the energy width broadened with increasing wave vector. Such weakly damped spin-wave excitations supported the validity of the hydrodynamic theory of Harris and Kirkpatrick (1977). In contrast, for the $Mn_{0.32}Zn_{0.68}F_2$ sample, a very broad spin-wave response has been observed. This is a sign of nonpropagating spin waves in antiferromagnets. Takahashi and Ikeda (1993) have performed inelastic neutron-scattering experiments on $d=3$ diluted antiferromagnets $RbMn_xMg_{1-x}F_3$ with $x=0.74$ and 0.63.

Uemura and Birgeneau (1986, 1987) performed high-resolution inelastic neutron-scattering studies on $Mn_xZn_{1-x}F_2$ with $x=0.75$ and 0.50. High-quality and quite large (~10 cm^3) single crystals made it possible to perform detailed measurements with an energy resolution much better than that of previous scattering experiments. Their results for $Mn_{0.75}Zn_{0.25}F_2$ at $T=5$ K (the Néel temperature of this sample is $T_N=46.2$ K) indicate that the magnon peak is still sharp (well defined) even at high energies. This feature agrees well with the result of

[19]There is an experiment other than inelastic-scattering measurements that observes antiferromagnetic fracton excitations. Ito and Yasuoka (1990) have investigated magnetic excitations in antiferromagnets $Mn_xZn_{1-x}F_2$ using NMR techniques. They observed the temperature dependence of the ^{19}F resonance frequency $\nu(T)$, which follows the relation $\nu(T)=\nu(0)(1-aT^2)$ for extended spin waves. They found that $\nu(T)/\nu(0)$ of this sample deviated slightly from the T^2 law, and attributed this deviation to fractons.

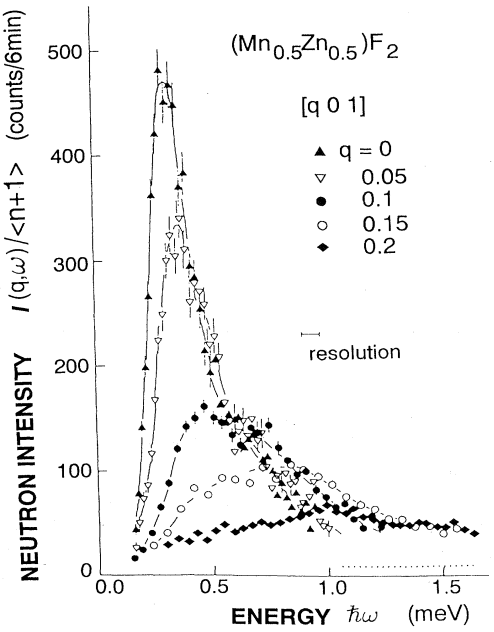

FIG. 31. Energy spectra of spin waves in $Mn_{0.5}Zn_{0.5}F_2$ measured at $T=5$ K along the $[q01]$ (in reciprocal-lattice unit) direction by use of cold neutrons with $E_f=3.5$ meV. The solid lines are guides to the eye; the dotted line shows the background level. After Uemura and Birgeneau (1987).

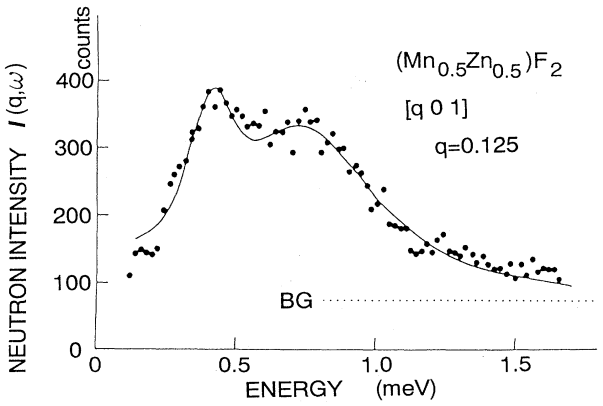

FIG. 32. Energy spectra from $Mn_{0.5}Zn_{0.5}F_2$ observed at wave vector $q=0.125$ r.l.u. in the $[q01]$ direction at $T=5$ K. The solid line represents the fit to the sum of a sharp Gaussian and a broad Lorentzian; the dotted line shows the background level. A double-peak feature characteristic of the wave vector around $q_c\sim0.15$ r.l.u. is demonstrated. After Uemura and Birgeneau (1987).

Coombs *et al.* (1976) for $Mn_{0.78}Zn_{0.22}F_2$. The results obtained for $Mn_{0.5}Zn_{0.5}F_2$ at $T=5$ K (the Néel temperature is $T_N=21.0$ K) are shown in Fig. 31, which displays the energy dependence of the reduced intensity. Peaks at higher energies are extremely broad, whereas responses at the lower energies continue to have sharp peaks. They identified the sharp and broad peaks with extended magnons and localized fractons, respectively. Line shapes of neutron intensities at small q are highly asymmetric. This is because the spectrum for $q<1/\xi$ may be described as the sum of a sharp component at low energies (magnons) and a broad component extending to high energies (fractons). Such a two-component shape of neutron intensity was predicted by Aharony, Entin-Wohlman, and Orbach (1988). At $q\approx q_c$ (crossover wave vector), the amplitudes of these two components become comparable.

Uemura and Birgeneau (1987) observed a double-peak structure in $S(\mathbf{q},\omega)$ near q_c, as shown in Fig. 32. They fitted their data from $Mn_{0.5}Zn_{0.5}F_2$ with a line shape composed of the sum of a sharp Gaussian (magnon spectrum) and a broad Lorentzian (fracton spectrum). Three distinct energies—the peak energies of the Gaussian ω_G and of the Lorentzian ω_L and the energy width of the Lorentzian Γ_L—are plotted in Fig. 33 as a function of wave vector. The diamond symbols (ω_G) in Fig. 33 show the dispersion relation of the magnons. The value of ω_G at $q=0$ indicates the anisotropy gap energy. Solid circles (ω_L) and open circles (Γ_L) above $q\sim0.2$ (r.l.u., reciprocal-lattice units) show the fracton dispersion relation. Both of them have the same q dependence, indicating that magnetic fractons satisfy the SLSP. The value of ω_L at $q=0$ exhibits a crossover energy ω_c. In the case of $Mn_{0.5}Zn_{0.5}F_2$, the gap energy is about a half of the crossover energy. In order to obtain precise information about magnetic fractons, it is important to perform experiments on more isotropic antiferromagnets such as $RbMn_xMg_{1-x}F_3$ (Ikeda *et al.*, 1994).

VIII. TRANSPORT ON A VIBRATING FRACTAL NETWORK

In this section, we introduce the process of phonon-assisted fracton hopping through the effects of vibrational anharmonicity and calculate the characteristic hop-

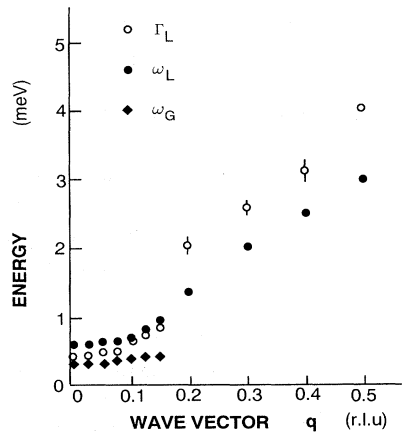

FIG. 33. Best-fit values of the peak energy ω_L (ω_G) and the energy width Γ_L for the Lorentzian (Gaussian) part of the energy spectra of $Mn_xZn_{1-x}F_2$ at $T=5$ K. The data at $q\lesssim0.15$ r.l.u. are fitted to the sum of the two parts, while those at $q>0.2$ r.l.u. are fitted to the Lorentzian alone. After Uemura and Birgeneau (1987).

ping distance and the contribution to the thermal conductivity κ. We also calculate the change in the velocity of sound coming from the same microscopic process and compare it with the results with the two-level-system model of amorphous materials.

A. Anharmonicity

The thermal conductivity at temperature T is given by

$$\kappa=\frac{1}{V}\sum_{\alpha'} C_{\alpha'}(T)D_{\alpha'}(T)\ , \tag{8.1}$$

where $C_{\alpha'}$ is the specific heat and $D_{\alpha'}$ the diffusion constant associated with the mode α'. However, in the absence of diffusion, $D_{\alpha'}$ is zero and κ vanishes. This is a strong condition, for it implies that whenever the condition for localization in the Anderson sense occurs (Anderson, 1958), thermal transport is forbidden. Thus thermal conductivity approaches zero where the mean-free path becomes of the order of, or even worse, less than the wavelength for vibrational excitations. Unfortunately, the literature abounds with use of the above expression for κ under conditions where the vibrational states are strongly localized. Transport on structures where the geometry allows a crossover from phonon to fracton vibrational excitations faces this problem directly. Fractons are known to be strongly localized (see Sec. V.B), so that thermal transport can only be accomplished by the (extended) phonon normal modes.

It is interesting to calculate κ under these conditions. Clearly, that part of κ associated with the phonons, $\kappa_{\rm ph}$, will increase with increasing temperature for two reasons. The first is associated with increasing mode density occupied as T increases; the second is associated with the increase in the Bose factor as T increases. This increase will continue until one exhausts all of the extended phonon states with increasing temperature. The thermal conductivity from phonon sources will then saturate in the Dulong-Petit regime with regard to the extended phonon states ($k_BT\gg\hbar\omega_{\rm ph}$). However, this is not the case for aerogels, as κ continues to increase above the value where the phonon contribution saturates. The question presents itself: why? We shall show that the introduction of anharmonicity into the phonon-fracton excitation spectrum allows for fracton contributions to thermal transport. Indeed, the form for this increase in thermal conductivity is reminiscent of the universal features of amorphous structures. Just why is currently a matter of speculation, to which we shall return.

The introduction of anharmonicity is essential for thermal transport in the fracton regime (Alexander, Entin-Wohlman, and Orbach, 1986). As we shall see, its introduction allows for fracton "hopping" in much the same sense as the "phonon-assisted electronic hopping" of Mott for localized electronic states (Mott, 1967, 1969). In fact, our treatment will follow Mott's arguments closely. That the introduction of vibrational anharmonicity allows for thermal transport is an interesting feature of random structures. In ordered structures, anharmonicity (through, e.g., umklapp processes) *reduces* thermal transport. In random structures, what thermal transport there is *results* from anharmonicity. Thus randomness causes anharmonicity to "stand on its head": whereas in ordered structures, anharmonicity serves to reduce heat flow, in disordered structures anharmonicity is the cause of heat flow. This is but another example of the complexity of random structures and how their properties are consequences of sometimes quite counterintuitive ideas.

1. Phonon-assisted fracton hopping

The introduction of vibrational anharmonicity results in two important vertices exhibited in Fig. 34. The second vertex, (b), is relevant to phonon-assisted fracton hopping (Alexander, Entin-Wohlman, and Orbach, 1986; Jagannathan, Orbach, and Entin-Wohlman, 1989). We introduce the corresponding Hamiltonian,

$$\mathcal{H}_{\rm hop}=C_{\rm eff}\sum_{\alpha,\alpha',\alpha''}(A_{\alpha,\alpha',\alpha''}b^{\dagger}_{\alpha'}b_{\alpha''}b_{\alpha}+\text{H.c.})\ , \tag{8.2}$$

where the b_α ($b^{\dagger}_\alpha$) operators annihilate (create) phonons or fractons depending on whether the index α refers to modes with frequencies less than or greater than the crossover frequency ω_c.

a. Characteristic hopping distance

Because the fractons are strongly localized, the two fractons in Fig. 34 are, in general, located at different spatial positions. To determine how far they are separated spatially, we invoke the *most probable hopping distance* of Mott (1969). The region of volume ξ^{D_f} contains $\mathcal{D}_{\rm fr}(\omega'_\alpha)\Delta\omega_{\alpha'}$ fractons of energy in the interval $[\omega'_\alpha,\omega_{\alpha'}+\Delta\omega_{\alpha'}]$. The differential probability of finding these fractons in a volume element $r^{D_f-1}dr$ (assuming a uniform random distribution of the fractons) is then

$$dP(\mathbf{r},\omega_{\alpha'})=\left[\frac{1}{\xi^{D_f}}\right]\mathcal{D}_{\rm fr}(\omega_{\alpha'})\Delta\omega_{\alpha'}r^{D_f-1}dr\ . \tag{8.3}$$

Take the first fracton in Fig. 34(b) (index α'') to lie at the origin. Then, to obtain the most probable hopping

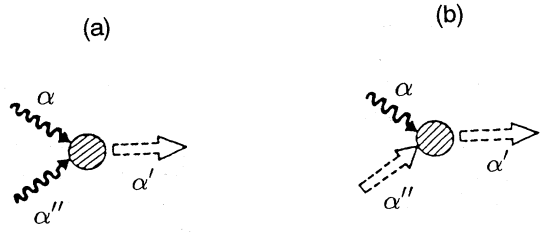

FIG. 34. Schematics of the anharmonic process: (a) phonon+phonon↔fracton; (b) phonon+fracton↔fracton. The wavy lines denote phonon states; the dashed arrows, fracton states.

distance, we integrate Eq. (8.3) up to that distance $R(\alpha')$ which would give us a second fracton within the volume with probability 1. Integrating up to the maximum distance ξ would give us $\mathcal{D}_{\rm fr}(\omega_{\alpha'})\Delta\omega_{\alpha'}$, i.e., the total number of fractons inside the volume ξ^{D_f}. One finds that

$$R(\alpha')=\Lambda(\omega_{\alpha'})\left[\frac{\omega_{\alpha'}}{\omega_c}\right]^{1/D_f}, \tag{8.4}$$

where the energy uncertainty $\Delta\omega_{\alpha'}$ has been taken to be ω_c (Alexander *et al.*, 1983). Note that this results in a hopping distance $R_{\alpha'}>\Lambda(\omega_{\alpha'})$, so that in fact the fracton hops a significant distance relative to its localization length scale. The diffusion constant associated with the hopping of the α' fracton then becomes

$$D_{\alpha'}=\frac{R^2(\omega_{\alpha'})}{\tau_{\rm fr}(\omega_{\alpha'},T)}, \tag{8.5}$$

where $\tau_{\rm fr}(\omega_{\alpha'},T)$ is the lifetime of the fracton of energy $\omega_{\alpha'}$ at temperature T associated with its hopping a distance $R_{\alpha'}$.

b. Contribution to the thermal conductivity

These relationships allow direct calculation of the thermal transport associated with fracton hopping. At temperatures greater than the crossover energy, inserting Eq. (8.5) into Eq. (8.1) yields the contribution to the thermal conductivity from fracton hopping (Jagannathan, Orbach, and Entin-Wohlman, 1989):

$$\kappa_{\rm hop}(T)=\frac{2^4G\pi^3C_{\rm eff}^2\bar{d}^{\,2}\omega_D}{8\rho^3v_s^2\xi^8\omega_c^3}k_B^2T. \tag{8.6}$$

This equation has very few undetermined constants (e.g., G arises from an integral over frequencies and has a value close to 1.4). The other terms appearing include ω_D, which is the Debye frequency *associated with* the phonon velocity of sound v_s, and ρ, the mass density. Thus it represents a quantitative contribution to the thermal conductivity, which, apart from the coupling constant, can be determined quite accurately. In reverse, knowing $\kappa_{\rm hop}$, one can determine $C_{\rm eff}$ directly.

Another feature of Eq. (8.6) is the absence of any dependence upon the fracton density of states above the crossover frequency ω_c. This is because the dispersion relation for fractons (Sec. IV.B.2) leads to a rapid spatial diminution of the fracton size with increasing fracton energy. As a consequence, the fracton overlap associated with vertex (b) in Fig. 34 falls off so rapidly with increasing fracton energy, that the principal contribution to $\kappa_{\rm hop}$ arises from fractons in the immediate vicinity of ω_c. Hence only the lowest energy fractons contribute to the thermal conductivity via phonon-assisted fracton hopping. We shall argue below that this can explain the rather universal form found for thermal transport above the plateau temperature for amorphous materials. That is, the thermal conductivity appears to increase linearly with temperature *independent* of the precise nature of the density of states for temperatures above the plateau temperature.

The vertex (b) in Fig. 34 not only determines the fracton hopping rate, but also the phonon lifetime associated with fracton hopping. Because the same vertex is involved for both processes, one can express $\kappa_{\rm hop}$ in terms of the inelastic lifetime $\tau_{\rm ph}(\omega_{\rm ph},T)$ for a phonon of frequency $\omega_{\rm ph}$ at temperature T. Now there are almost no adjustable parameters. Jagannathan, Orbach, and Entin-Wohlman (1989) find

$$\kappa_{\rm hop}=\frac{ad_\phi I2^{D_f}\omega_D}{8D_f\Gamma(D_f/d_\phi)}\frac{k_B\omega_c^2}{\xi}\frac{1}{\omega_{\rm ph}^2\tau_{\rm ph}(\omega_{\rm ph},T)}. \tag{8.7}$$

This remarkable formula involves only the constant $a=5-\tilde{d}-4\tilde{d}/D_f$; I, an integral of order unity [Eq. (17) of Jagannathan, Orbach, and Entin-Wohlman (1989)]; and the Γ function with argument D_f/d_ϕ.

2. Temperature dependence of the sound velocity

Even more remarkably, use of the Kramers-Kronig relation allows for the extraction of the velocity of sound change caused by the (b) vertex above in terms of the fracton hopping contribution to the thermal conductivity. Jagannathan and Orbach (1990) find

$$\frac{\delta v_s}{v_s}=-0.1\frac{\xi^2}{2\pi^2v_s}\frac{\kappa_{\rm hop}(T)}{T}\frac{T}{k_B}. \tag{8.8}$$

The term $\kappa(T)/T$ is independent of temperature for phonon-assisted fracton hopping, so that Eq. (8.8) is linear in the temperature but *independent* of the frequency of the sound wave. This result differs substantially from that generated by two-level systems (TLS) in amorphous materials. Such models generate (Jäckle, 1972; Tielburger *et al.*, 1992)

$$\frac{\delta v_s}{v_s}=\frac{Ck_BT}{E_0}\ln(\omega\tau_0), \tag{8.9}$$

where C is a constant proportional to the product of the tunneling parameter $\bar{P}$ and the square of the coupling constant between the phonons and the TLS; E_0 is the ground-state energy of the tunneling particle; ω is the sound wave frequency; and τ_0 is a few times the vibrational frequency of the tunneling particle in a single well. Whereas this quantity has not been measured in the aerogels at temperatures in the vicinity of the phonon-fracton crossover, it has been extensively studied in amorphous materials. We shall discuss the relevance of Eqs. (8.8) and (8.9) to experiments in Sec. VIII.D.

In conclusion, all three quantities,

$$\kappa_{\rm hop},\quad \tau_{\rm ph}(\omega_{\rm ph},T),\quad \frac{\delta v_s}{v_s},$$

are closely linked within the phonon-fracton model. They are all consequences of the vibrational anharmonic

vertex (b) of Fig. 34, so that knowledge of any one of them determines the other two. The phonon-fracton theory overdetermines the quantities that can be measured experimentally, and therefore it can be stringently tested.

B. Thermal conductivity of the aerogels

The specific heat and thermal conductivity of aerogels were first measured by Calemczuk *et al.* (1987) and de Goer *et al.* (1989). These measurements were carried out for unrelated samples and over a restricted temperature range which did not cover the phonon-fracton crossover energy. More recently, specific-heat and thermal-conductivity measurements by Sleator *et al.* (1991) and Posselt *et al.* (1991), respectively, and by Bernasconi *et al.* (1992) were carried out on the same materials that were characterized by small-angle neutron scattering (SANS; see Posselt, 1991), and over a temperature range that included the phonon-fracton crossover energy.

The arguments at the beginning of Sec. VIII.A suggest that the thermal conductivity for fractal structures should increase in the phonon regime up to a saturation value when one reaches a temperature such that vibrational excitations of energy greater than $\hbar\omega_c$ are populated. At such temperatures (and higher), there are no further phonon states to thermally excite, and the only additional excitations are fractons. But fractons are localized and so cannot contribute to the heat current by themselves. Hence $k_B T$ exceeds the phonon energies, and one is in the Dulong-Petit regime where the thermal conductivity from the phonons saturates at a constant value. However, as shown and calculated earlier, the presence of vibrational anharmonicity, Eq. (8.2), profoundly affects the subsequent form of κ. An additional transport channel opens up, with a contribution $\kappa_{\rm hop}$ that is linear in temperature and that does not depend upon the specific nature of the density of states at energies $k_B T$. The strength of this contribution will depend upon the anharmonic coupling constant, $C_{\rm eff}$, from Eq. (8.6).

We display the experimental observations of Posselt *et al.* (1991) for the thermal conductivity of two aerogels of density 0.145 g/cm^3 (low density, LD) and 0.275 g/cm^3 (high density, HD) in Fig. 35. These are the first measurements ever to explore κ for aerogels in the temperature range $T_c=\hbar\omega_c/k_B$. For the HD sample, $T_c=0.37$ K, and a strong break in slope occurs around $T=0.13$ K, as can be seen in Fig. 36. This is interpreted by Posselt *et al.* (1991) as evidence of a crossover from phonon-dominated to fracton-dominated thermal transport. The sharp increases in κ above about 3 K is ascribed to particle modes, caused by the approximately 20 Å spheres that make up the fractal network in the aerogels. For the LD sample, $T_c=0.10$ K, and the accessible measurement temperatures were too high to observe the crossover from phonon- to fracton-dominated transport.

The phonon-fracton model predicts the following form for the thermal conductivity:

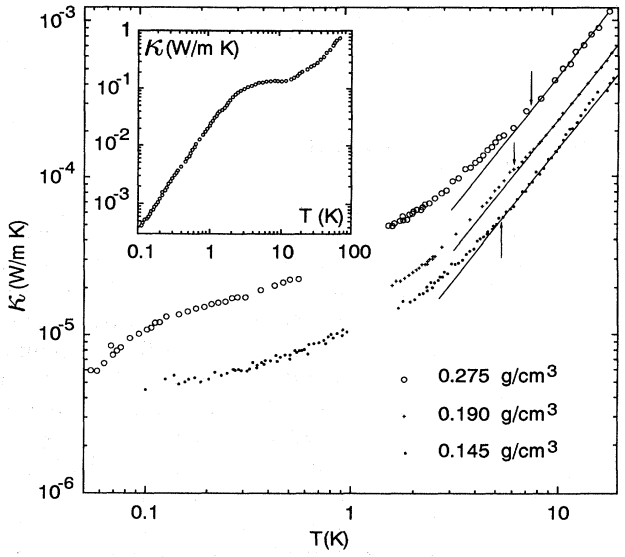

FIG. 35. Temperature dependence of the thermal conductivity for silica aerogels of different densities. The three parallel straight lines indicate that at high temperatures the T dependence of κ is the same for different densities. The inset shows $\kappa(T)$ for vitreous silica by Zeller and Pohl (1971). After Bernasconi *et al.* (1992).

$$\kappa=\kappa_{\rm ph}+\kappa_{\rm hop}\ , \tag{8.10}$$

which can be written, for $T > T_c$,

$$\kappa= A+BT\ , \tag{8.11}$$

in an obvious notation. Posselt *et al.* (1991) find that A scales with ξ in a consistent manner for the HD and LD samples, the limiting phonon mean free path being of order ξ (see Aharony *et al.*, 1987). Using the form for $\kappa_{\rm hop}$ given by Eq. (8.7), they find that the ratio $B^{\rm HD}/B^{\rm LD}$ from the fit is in fair agreement with calculations based on Eq.

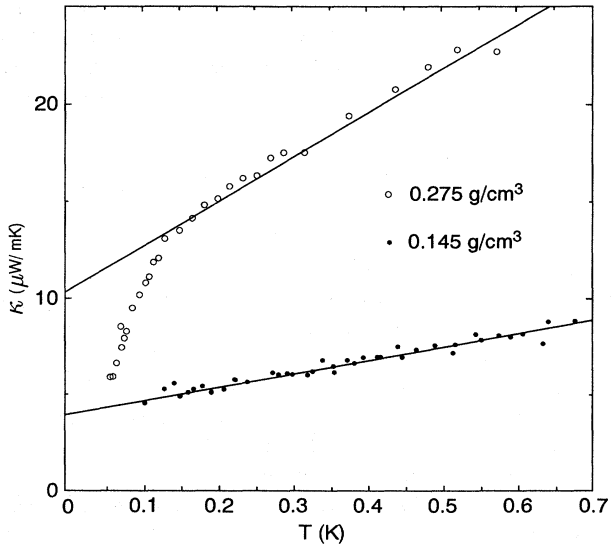

FIG. 36. $\kappa(T)$ between 0.05 and 0.7 K. The solid lines are fits to Eq. (8.11). After Bernasconi *et al.* (1992).

(8.8). Thus the predictions for thermal transport based on phonon-assisted fracton hopping appear to be quantitatively verified in the aerogels.

C. Transport properties of glassy and amorphous materials

The lessons we have learned from the phonon-fracton concept are attractive because of the simplicity of the model and the tractability of the equations. We are able to execute quantitative calculations for quantities as complex as thermal transport associated with the hopping of localized excitations. In addition, the actual results for the quantities calculated often bear a striking similarity to the more or less universal properties of glasses and amorphous materials. We are not saying that such substances are fractal, nor that they exhibit dynamic properties that mimic fractal structures, e.g., phonon-fracton crossover. What we are saying is that there may be properties of glassy and amorphous materials that might obey the same kinetics as those that we have explored for fractal structures. In this subsection, we shall focus on two of those properties that have been extensively explored: the thermal conductivity and the temperature and frequency dependence of the velocity of sound. We shall suggest that the internal structure of lattice vibrations in glasses and amorphous materials is such that a mobility edge exists, which we term ω_c, above which energy the vibrational excitations are localized. The energy width of the crossover region is unknown to us, but undoubtedly it is connected with the temperature width of the plateau in the thermal conductivity, exhibited by nearly every glass or amorphous material. At the high-temperature end of the plateau, the thermal conductivity κ is known to rise with increasing temperature. Examples for five amorphous solids are given in Fig. 37. In addition, similar behavior is exhibited by the epoxy resins, as shown in Fig. 38. To our eyes at least, the rise of κ above the plateau value is certainly at least initially linear with increasing temperature, reminiscent of the linear increase in the thermal conductivity manifest in $\kappa_{\rm hop}$ of the previous subsection.

1. Thermal conductivity

Many authors have observed (Dreyfus *et al.*, 1968; Blanc *et al.*, 1971; Lasjaunias and Maynard, 1971; Lasjaunias, 1973; Alexander *et al.*, 1983; Karpov *et al.*, 1983; Karpov and Parshin, 1983, 1985; Akkermans and Maynard, 1985; Buchenau *et al.*, 1988, 1991; Buchenau, Galperin, *et al.*, 1992; Sheng and Zhou, 1991; Buchenau, Galperin, *et al.*, 1992) that the plateau in the thermal conductivity, κ, for amorphous materials can be explained if one assumes the existence of a mobility edge for phonons in the medium. Evidence for localization can be obtained from the extraction of the phonon mean free path as a function of phonon frequency from the thermal conductivity. We exhibit in Fig. 39 the analysis of Zeller and Pohl (1971) as an example. The phonon mean free path is seen to plunge precipitously for phonon frequencies just below the plateau frequency (temperature) to a few atomic spacings, suggesting that a Ioffe-Regel limit (1960) for phonons is reached at this vibra-

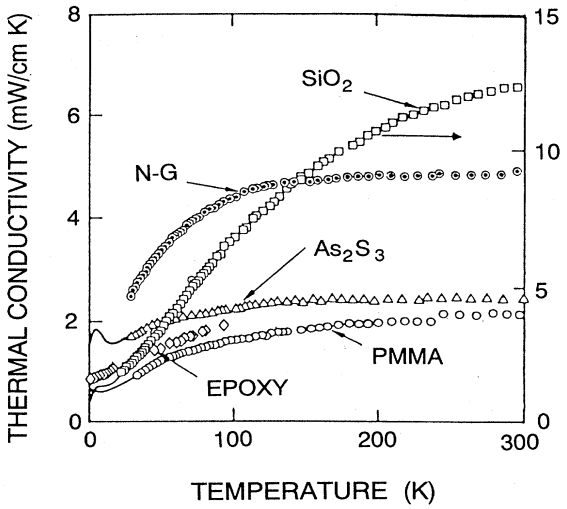

FIG. 37. Thermal conductivity for temperatures above the plateau temperature for five amorphous solids. The data for vitreous silica are plotted according to the scale on the right. After Cahill and Pohl (1987).

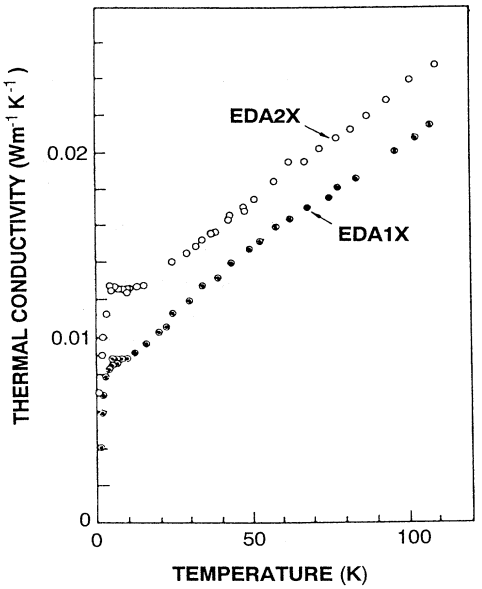

FIG. 38. $\kappa(T)$ for temperatures above the plateau temperature for different samples of epoxy resin. EDA2X contains twice the stoichiometric quantity of hardener EDA (thylene diamine), while EDA1X contains the stoichiometric amount. The greater than amount of hardener, the shorter the value of the crossover length scale (corresponding to a greater crossover frequency). After de Oliveira, Page, and Rosenberg (1989).

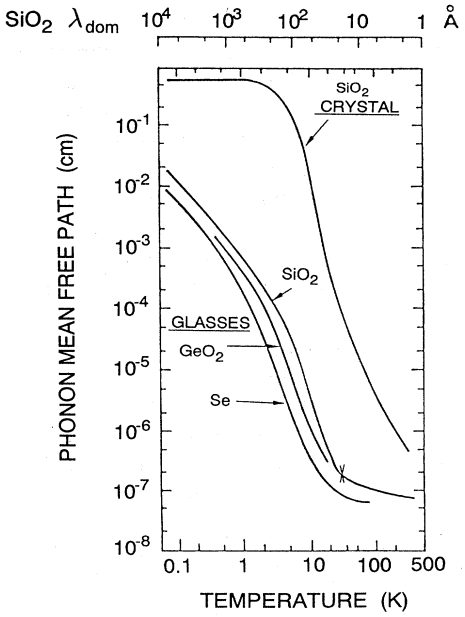

FIG. 39. The average phonon mean free path $\Lambda(T)$ extracted from thermal-conductivity measurements for various glasses using the kinetic formula $\kappa=\frac{1}{3}C_v v_s \Lambda(T)$, where κ is the thermal conductivity, C_v is the phonon specific heat, and v_s is the Debye sound velocity, respectively. The phonon wavelengths are indicated at the top of the figure in the dominant-phonon approximation for vitreous silica. The $\times$ drawn on the SiO_2 curve denotes the length scale at which crossover takes place between extended and localized vibrational states. After Zeller and Pohl (1971).

tional energy.[20] As shown by John, Sompolinsky, and Stephen (1983), John (1984), and Aharony *et al.* (1987), this implies phonon localization. With an assigned phonon localization frequency, say, ω_c, then, for temperatures above $\hbar\omega_c/k_B$, conventional heat transport can only occur via the already excited phonons. We have argued that such behavior leads to a saturation in κ; for glasses and amorphous materials, it is referred to as the *plateau* in the thermal conductivity.

The general argument we have presented for the occurrence of the plateau in the thermal conductivity was first made by Dreyfus, Fernandes, and Maynard (1968). Akkermans and Maynard (1985) suggested that Rayleigh scattering of phonons could lead to a mobility edge in the phonon spectrum. However, there are strong experimental indications that the mean-free-path dependence may be inelastic in character for phonon frequencies approaching ω_c (Dietsche and Kinder, 1979), and therefore non-Rayleigh-like.

We interpret the increase in κ at temperatures higher than that marking the onset of the plateau to be caused by an additional heat conduction channel, namely, phonon-assisted hopping of the strongly localized vibrational states with energies larger than ω_c. This is different from the "resonance" interpretation of others (Karpov and Parshin, 1983, 1985), where the increase in κ above the plateau temperature is caused by a return to extended character for the phonon states. There is clearly a point here where the competing theories can be tested: are there extended phonon states above ω_c? Some preliminary answers are now available. Experiments by Cahill *et al.* (1991) and Love and Anderson (1990) have shown that there is no contribution to thermal conductivity from phonons at room temperature.

There is an additional complication. Glancing at Fig. 37, one sees that the increase in κ does not continue linearly with temperature indefinitely, that there is a "roll-over" in the vicinity of 100 K. Jagannathan, Orbach, and Entin-Wohlman (1989) have hypothesized that this is caused by the condition $\omega_{\rm ph}\tau_{\rm loc}<1$ brought about by anharmonicity. Here, $\omega_{\rm ph}$ is the phonon that assists the vibrational state hopping, and $\tau_{\rm loc}$ is the anharmonic-induced lifetime for the localized vibrational state that is doing the hopping. This quench of the phonon-assisted localized vibrational state hopping is quite analogous to the Simons (1964) calculation of the breakdown of three-phonon anharmonic scattering.

Our approach to the calculation of the increase of κ above the plateau temperature will follow closely the results of Sec. VIII.A.1, except that we shall substitute the localized vibrational excitations above ω_c for the fractons. The mathematical machinery will be comparable for the two calculations, leading to some interesting quantitative conclusions. This approach has recently been criticized by Bernasconi *et al.* (1992), who argue, "We conclude that the κ plateau of amorphous SiO_2 is most likely not the result of fractal behavior at short length scales, because a similar feature is not observed for aerogels in the regime dominated by particle modes." While there is a serious criticism it is possible that *the small 20 Å particles may not possess the same structure as conventional vitreous silica.* Further, the existence of a plateau in κ means that the crossover region cannot be sharp, but must be extended in energy. Neither we nor anyone else possesses a satisfactory microscopic theory for dynamics in this energy range for glasses. Rather, we wish to focus on those aspects that are amenable to calculation, and see if the consequences warrant consideration.

To be specific, we use Eq. (8.7) for vitreous silica, taking $\tau_{\rm ph}(\omega_{\rm ph},T)$ from Fig. 39 at the value of $\omega_{\rm ph}$ where the Ioffe-Regal condition is satisfied. We have marked this point by an $\times$ on Fig. 39. Reading from the axes, we find $\xi=20$ Å. The average sound velocity v_s in vitreous silica in 4.4×10^5 cm/s. The crossover frequency is then obtained from $\omega_c=2\pi v_s/\xi$, so that $\omega_c=1.4\times10^{13}$ s^{-1}. The dominant phonon approximation sets $\omega_{\rm dom}(T)=3.83k_BT/\hbar$, giving a crossover temperature $T_c=28$ K. To choose the phonon whose frequency and lifetime we

[20]See also the detailed analysis of Graebner, Golding, and Allen (1986).

shall insert into Eq. (8.7), we select an equivalent temperature (dominant phonon approximation) of 10 K. One extracts from Fig. 39 $\omega_{ph}=5.3\times10^{12}$ s^{-1}, and a mean free path of Λ(10 K) of approximately 200 Å. We use conventional exponents for the fractal parameters which appear in Eq. (8.7), but they do not affect the numerical results very much.

Inserting these values into Eq. (8.7), we find at 50 K for vitreous silica

$$\kappa_{hop}(T=50\text{ K})=5\times10^{4}\text{ ergs/cm K s}\ .$$

This is clearly an upper bound for κ_{hop} because of our assumption that $1/\tau_{ph}$ as extracted from Fig. 39 is entirely inelastic. Nevertheless, comparison with experiment is remarkable, remembering that no adjustable parameters have been introduced. From Fig. 37, we find

$$\kappa_{exp}(T=50\text{ K})=2\times10^{4}\text{ ergs/cm K s}\ .$$

The quantitative agreement between the calculation of $\kappa_{hop}(T)$ and the increase of κ for temperatures greater than the plateau temperature for vitreous silica is suggestive. When combined with increasing evidence for vibrational localization in glasses at low energies (Laird and Schober, 1991), it may be that vibrational localization, which leads to the plateau, and phonon-assisted hopping of localized states above the plateau are the fundamental mechanisms that generate the near-universal behavior of $\kappa(T)$ found for glasses and amorphous solids.

A test of the correctness of the hopping model can be found by inverting Eq. (8.6), using the experimental value of $\kappa(T)$ above the plateau for vitreous silica, to find the anharmonic coupling coefficient C_{eff}. We obtain (Jagannathan, Orbach, and Entin-Wohlman, 1989)

$$C_{eff}=10^{14}\text{ ergs/cm}^3\ . \tag{8.12}$$

Using measurements of the pressure derivative of the elastic stiffness moduli (Andreatch and McSkimin, 1976), we find C_{eff} to be about an order of magnitude larger than the third-order elastic constant found at long length scales. A recent experimental realization of a Cantor-like structure (Alippi *et al.*, 1992) finds an enhancement of the nonlinear vibrational interaction of about the same magnitude. This is discussed in Sec. VIII.E.

2. Sound velocity

As derived in Sec. VIII.A.2, the vertex (b) of Fig. 34 also leads to a change in the velocity of sound with increasing temperature. We found from phonon-assisted fracton hopping that $\delta v_s/v_s$ varied linearly with T and was independent of sound frequency [see Eq. (8.8)]. Making the argument that an analogous process involving localized vibrational states takes place in glasses and amorphous materials, is such a dependence found? And if so, what would be its predicted magnitude in vitreous silica using C_{eff} as extracted from thermal-conductivity measurements, Eq. (8.12)?

The velocity of sound in glasses and amorphous materials exhibits a temperature dependence that is very different from crystalline materials. The change in the sound velocity is nonmonotonic at low temperatures, involving resonance scattering of the sound waves off the TLS (Hunklinger and Arnold, 1976). In the vicinity of 1 K and above, relaxational scattering leads to a decrease in the sound velocity with increasing temperature as the logarithm of the temperature (Dreyfus, Fernandes, and Maynard, 1968; Blanc *et al.*, 1971; Lasjaunias and Maynard, 1971; Lasjaunias, 1973). With increasing temperature, the sound velocity exhibits a stronger temperature dependence. It is in this regime, above 10 K or so, that we suggest that localized vibration hopping accounts for the temperature dependence of the velocity of sound. The temperature scale for this regime is set by the experimental observation of the plateau in the thermal conductivity.

The experimental work of Bellessa (1978) demonstrates that the frequency and temperature dependence of the sound velocity in amorphous materials can be broken into two parts,

$$\frac{\delta v_s}{v_s}=AT+B\ln\omega\ . \tag{8.13}$$

The two constants A and B are independent of temperature and frequency, respectively. This behavior is inconsistent with the TLS result quoted in Eq. (8.9). Examples of the first term are exhibited in Fig. 40, and that of the second in Fig. 41 for vitreous soda-silica. More recent measurements of Duquesne and Bellessa (1986) on amorphous Se, Ge, and Se-Ge compounds show identical behavior, as exhibited in Fig. 42. These figures suggest that the temperature dependence of the velocity of sound in this temperature range can be associated with sound-wave–assisted localized vibrational hopping, whereas the temperature-independent term arises from the TLS (Bellessa, 1978).

The magnitude of the velocity change can be calculated immediately from Eq. (8.8). We find for vitreous silica

$$\frac{(\delta v_s)_{hop}}{v_s}=-(1.0\times10^{-3}\text{ K}^{-1})T\ ,$$

while experimentally, from Hunklinger and Arnold (1976), we extract

$$\frac{(\delta v_s)_{exp}}{v_s}=-(0.3\times10^{-3}\text{ K}^{-1})T\ .$$

Our calculated value somewhat overestimates the slope. However, the numerical prefactors that led to Eq. (8.13) were only approximate, and so the agreement with experiment can be considered quite reasonable. The more important point is the *consistency* between all calculated quantities. We find that the magnitude of the thermal conductivity and the temperature-dependent part of the velocity of sound all are related to the phonon lifetime which we have extracted from experiment. There are no

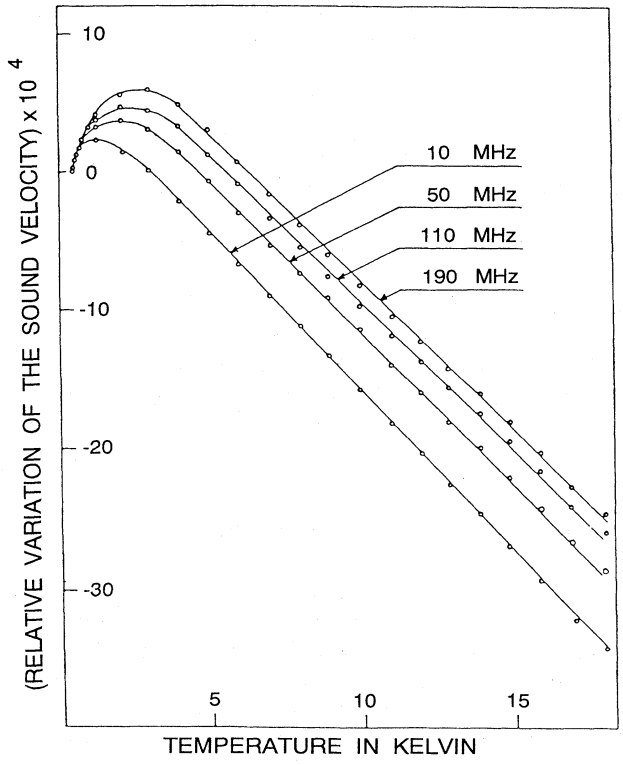

FIG. 40. Variation in the velocity of longitudinal sound waves as a function of temperature for different frequencies in vitreous soda-silica. The velocity variation is relative to the value at 0.4 K. The longitudinal sound velocity is 5.8×10^5 cm/s. After Bellessa (1978).

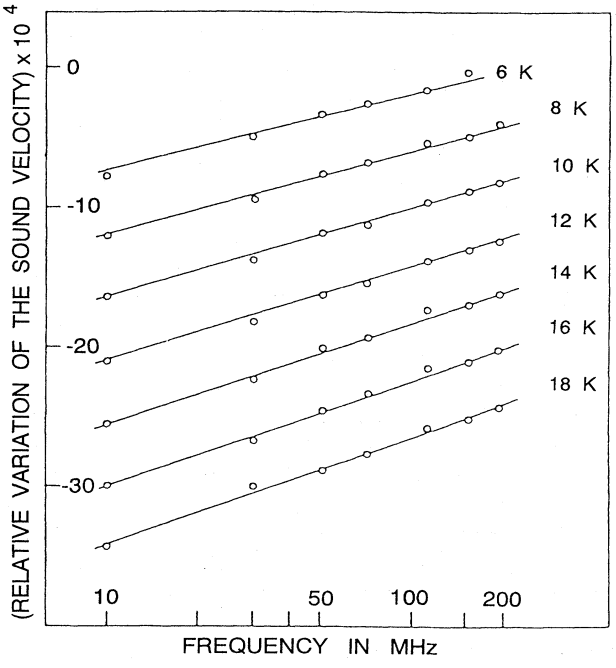

FIG. 41. Variation in the velocity of longitudinal sound as a function of frequency for different temperatures in vitreous soda-silica. The velocity variation is relative to the value at 0.4 K. After Bellessa (1978).

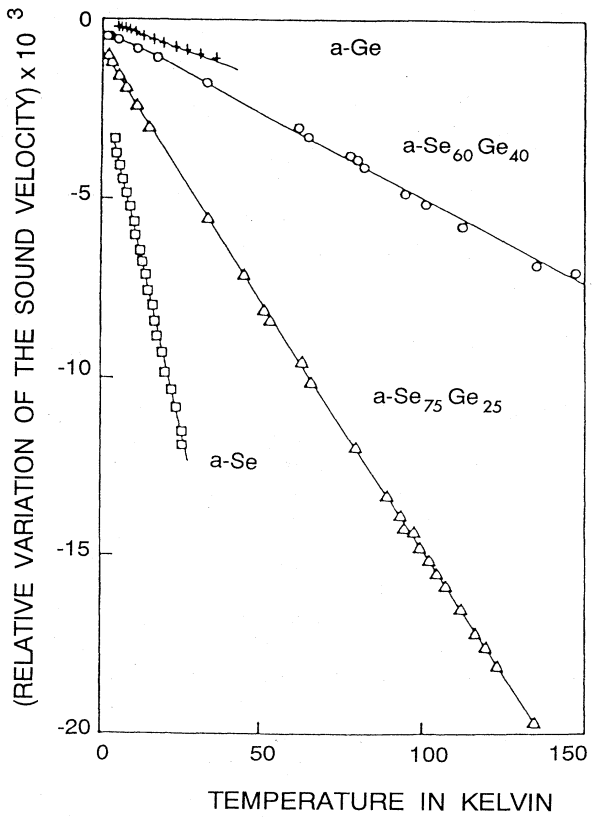

FIG. 42. Variation in the velocity of ultrasonic waves in *a*-Se (164 MHz), *a*-$Se_{75}Ge_{25}$ (150 MHz), *a*-$Se_{60}Ge_{40}$ (450 MHz; shear waves), and *a*-Ge (220 MHz; Rayleigh wave) as a function of temperature. The curves are arbitrarily shifted along the velocity axis. After Duquesne and Bellessa (1986).

undetermined parameters. This is strongly suggestive that our basic picture of vibrational transport at temperatures above the plateau temperature has relevance to glasses and amorphous materials.

Very recent experiments of Tielburger *et al.* (1992) on vitreous silica agree with neither the form of Eq. (8.13) nor the analysis of Bellessa (1978). They find, in the temperature range between 5 and 15 K, that the coefficient A depends upon frequency as the logarithm, in accord with the results of the TLS model quoted in Eq. (8.9). It is difficult to know how to reconcile the results from the two groups, except to note that the energy characteristic of the plateau for vitreous silica is 28 K [see the analysis for $\kappa(T)$ above]. The temperature range of Tielburger *et al.* (1992) is therefore too low to have present significantly many thermally excited localized vibrational states. Our model would predict a change in the frequency dependence found by Tielburger *et al.* (1992) in the vicinity of the energy characteristic of the plateau. Indeed, the experiments of Bellessa (1978) are all at or above this characteristic energy, consistent with the assumptions of our model.

Above about 50 K for vitreous silica, Jagannathan and Orbach (1990) estimated that there would be substantial

deviations from the simple perturbative results that led to Eq. (8.8). Finite lifetimes for the localized vibrational states arising from anharmonicity will inhibit the full strength of the vertices in Fig. 34, leading to a diminution in our calculated value for δv_s. This will allow the increase in coupling with density inhomogeneities to dominate, leading to a minimum in $\delta v_s / v_s$, as observed around 60 K, and then to a subsequent linear rise up to the highest temperatures measured, as observed for vitreous silica.

D. Magnitude of the anharmonic coupling constant

An important point of phonon-assisted localized vibrational state hopping is the large value of anharmonicity required to explain agreement between theory and experiment. The value of $C_{\rm eff}$ extracted from comparison with the absolute values for $\kappa(T)$ [and, concomitantly, $\delta v_s(T)$] observed experimentally are too large by roughly an order of magnitude when compared with the values found for the anharmonicity at long length scales.

Very recently, Alippi *et al.* (1992) found experimental evidence of extremely low thresholds for subharmonic generation of ultrasonic waves in one-dimensional artificial piezoelectric plates with Cantor-like structures, as compared to the corresponding homogeneous and periodic plates. A theoretical analysis demonstrated that the enhancement of the interaction between the localized vibrational states (in their case, true fractons) and the extended phonon states was caused by favorable frequency and spatial matching of the coupled modes in the Cantor-like structure, "wish no need to invoke anomalous modifications of the nonlinear elastic constants." Whereas the driving voltage for subharmonic generation for the homogeneous and periodic structures was around 25 V, typical values of the lowest threshold voltages observed for the Cantor-like sample were 3–5 V.

The frequency and spatial matching arose from the nature of the fracton states. Rather than being completely overdamped, they were found to possess two or three oscillations before the envelope fell to zero. This allowed substantial overlap with the square of the subharmonic modes. An example is shown in Fig. 43. Our results for the structure factor, as given in Sec. VI (Fig. 22), exhibit structure similar to that in Fig. 43—a few wavelike oscillations within a narrow (superlocalized) envelope.

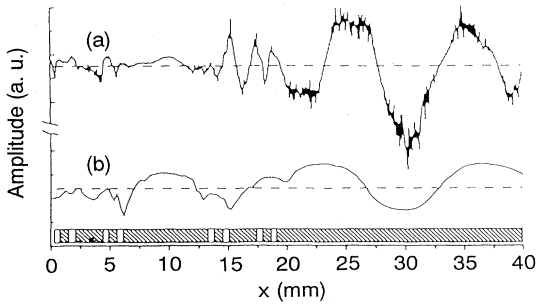

FIG. 43. Experimental displacement profiles of the normal modes (a) $\omega_n = 385.5$ kHz, a fracton mode, and (b) $\omega_m = \omega_n/2$, a phonon mode, of the Cantor-like sample. The anharmonic coupling between these two modes, which is responsible for the subharmonic generation, is favored by the relatively large spatial overlap between the square of the subharmonic displacement (b) and the displacement of the fundamental mode (a) in the region where the fracton mode (a) extends. Ater Alippi *et al.* (1992).

The lessons from fractal structures may carry over to glasses and amorphous materials. Anharmonic couplings on length scales of the order of the localized vibrational modes may be much larger (an order of magnitude) than those conventionally measured at large length scales. This amplification would be all that is necessary to quantitatively match the strength of phonon-assisted localized vibrational hopping processes to experimental observations.

IX. SUMMARY AND CONCLUSIONS

This review has attempted to present a complete picture of the dynamical properties of fractal networks as of this point in time. Its size and scope reflect the great activity in this field since the review by Orbach (1986) and Vacher, Courtens, and Pelous (1990). It is fair to say that theory and experiment, especially in relation to the silica aerogels, agree remarkably. True, but perhaps surprising, scaling based upon a single length scale has yet to fail. We have reviewed the properties of a percolating network, defining the nature of excitations on this model structure and displaying the crossover between extended (phonon, magnon) and strongly localized (fracton) excitations. Scaling theory has been introduced which freed us from these specific examples and enabled an analysis of excitations on any self-similar (fractal) structure. The advent of modern, large, and fast computers has allowed numerical simulations of sufficient size to shed light on and to test the scaling theories through explicit simulations. Two physical systems with fractal geometry over a rather significant length scale have yielded extensive excitation spectrum data from light- and neutron-scattering experiments: the silica aerogels (vibrational excitations) and site-diluted antiferromagnets (magnetic excitations).

Finally, the transport properties of fractal networks were examined, addressing the disturbing question of how a strongly localized fracton could transport heat. A calculation of the thermal diffusivity was described which involved phonon-assisted fracton hopping. This is the vibration analog of Mott's variable range phonon-assisted localized electronic state hopping. The theory that has been developed couples together the assisting phonon lifetime, the fracton contribution to the thermal conductivity, and the temperature dependence of the velocity of sound. Knowledge of any one of these quantities determines the other two with no adjustable parameters. Very recent thermal-conductivity experiments on the silica aerogels have exhibited results consistent with the theory and have shown that the results scale as the theory would require.

The transport results for fractal networks appear to be similar to those found universally for (nonfractal) glasses and amorphous materials at and above the temperature region of the plateau in the thermal conductivity. This led to speculation that the plateau was a consequence of a crossover from extended to localized vibrational excitations in these materials. If so, and if the localized character of the vibrational excitations continued well above the plateau energy (temperature), phonon-assisted localized vibrational state hopping might well be an important mechanism for thermal transport. Calculations were performed for the thermal conductivity arising from this mechanism for vitreous silica, using phonon lifetimes extracted from lower temperature thermal-conductivity measurements. Agreement was found with experiment with nearly no adjustable parameters, but it was found that the anharmonic coupling constant extracted from the fit to experiment was about an order of magnitude larger than that for long (continuum) length scales. This has now been shown to be the case for an artificially constructed one-dimensional (Cantor) fractal, suggesting that by analogy random structures may exhibit similar properties (Alippi *et al.*, 1992; Craciun *et al.*, 1992).

These considerations point to continued activity in this field for some time to come. Numerical simulations for $d=3$ percolating networks can shed further light on the structure factor and on the reasons why single length scaling works so well. As interesting is the question of the effects of anharmonicity. So far only one-dimensional Cantor-like structures have been analyzed to show how phonons and fractons interact. It is very important to know whether the resonances in frequency and space which are crucial for the enhancement of anharmonicity for $d=1$ are still present for $d=3$. Preliminary evidence, through the form of the structure factor, suggests that this may be the case (the fracton exhibits a few spatial oscillations within its superlocalized envelope).

The recent low-temperature measurements of the thermal conductivity and the specific heat for the silica aerogels suggest further work. Lower measurement temperatures would enable comparative measurements of the phonon-fracton crossover as exhibited through these measures, enabling systematic information to be extracted. In addition, the relationship between phonon lifetime, thermal transport, and variations in the velocity of sound can be directly tested in the aerogels. It is important to measure v_s at temperatures near and above the crossover temperature to determine if the phonon-assisted fracton hopping relationship predicted between κ and v_s is, in fact, observed.

Another area of interest is site-diluted magnets. So far, excitations in $d=3$ antiferromagnets have been measured through neutron scattering for the highly anisotropic antiferromagnet $Mn_xZn_{1-x}F_2$. Lower anisotropy would allow a greater energy range for magnon excitations for materials with p closer to p_c. It would also be very interesting to measure the magnetic excitation spectrum of $d=2$ site-diluted magnets, for which numerical simulations of $S(\mathbf{q},\omega)$ have been performed. New results from simulations and scaling theory suggest that $\tilde{d}_a$ is close to unity for all d greater than 2. This is a strong prediction for the fracton DOS and dispersion law and cries out for experimental examination. And, of course, it would be welcome to have numerical simulations to serve as a test of scaling theories and to match with experiment. For example, is it possible to obtain two peaks in $S(\mathbf{q}_{\text{fixed}},\omega)$ as a function of ω, one for magnons, the other for fracton excitations, as has been observed for $Mn_{0.5}Zn_{0.5}F_2$ (Uemura and Birgeneau, 1986, 1987), but which fail to show up in effective-medium calculations?

Finally, are the vibrational excitations in glasses and amorphous materials strongly localized above energies of the magnitude of the plateau temperatures? This is a crucial question to test the applicability of the ideas generated by fractal lattices to these nonfractal but disordered structures.

Surprises will continue to abound in this field. We hope that this review will serve as a basis for further exploration of the dynamics of random structures.

ACKNOWLEDGMENTS

We are grateful to Shlomo Alexander and Eric Courtens for many valuable discussions and useful suggestions. We thank S. Feng, S. Havlin, J. K. Kjems, M. Matsushita, A. Petri, S. Russ, E. F. Shender, Y. Tsujimi, R. Vacher, and O. Wright for fruitful discussions. The work was supported in part by a grant-in-aid for scientific research in the international joint research program from the Japan Ministry of Education, Science, and Culture (MESC), which has made our collaboration possible. This work was also supported by a grant-in-aid for scientific research in priority areas, computational physics as new frontiers in condensed matter research from the MESC. This work was also supported in part by the U.S. National Science Foundation through grants DMR 90-23107 and DMR 91-12830; the U.S. Office of Naval Research through contract number Nonr-N00014-88-K-0058; and the University of California, Los Angeles and Riverside.

REFERENCES

Abrahams, E., P. W. Anderson, D. C. Licciardello, and T. V. Rama-Krishnan, 1979, Phys. Rev. Lett. **42**, 673.
Adler, J., 1984, Z. Phys. B **55**, 227.
Adler, J., 1985, J. Phys. A **18**, 307.
Adler, J., A. Aharony, and A. B. Harris, 1984, Phys. Rev. B **30**, 2832.
Adler, J., A. Aharony, Y. Meir, and A. B. Harris, 1986a, Phys. Rev. B **34**, 3469.
Adler, J., A. Aharony, Y. Meir, and A. B. Harris, 1986b, J. Phys. A **19**, 3631.
Adler, J., A. Aharony, Y. Meir, and A. B. Harris, 1986b, J. Phys. A **19**, 3631.
Adler, J., Y. Meir, A. Aharony, and A. B. Harris, 1990, Phys.

Rev. B **41**, 9183.
Aharony, A., 1986, in *Directions in Condensed Matter Physics,* edited by G. Grinstein and G. Mazenko (World Scientific, Singapore), p. 1.
Aharony, A., S. Alexander, O. Entin-Wohlman, and R. Orbach, 1985a, Phys. Rev. Lett. **31**, 2565.
Aharony, A., S. Alexander, O. Entin-Wohlman, and R. Orbach, 1985b, Phys. Rev. B **31**, 2565.
Aharony, A., S. Alexander, O. Entin-Wohlman, and R. Orbach, 1987a, Phys. Rev. Lett. **58**, 132.
Aharony, A., O. Entin-Wohlman, S. Alexander, and R. Orbach, 1987b, Philos. Mag. B **56**, 949.
Aharony, A., O. Entin-Wohlman, and R. Orbach, 1988, in *Time Dependent Effects in Disordered Materials,* edited by T. Riste and R. Pynn (Plenum, New York), p. 233.
Aharony, A., and A. B. Harris, 1992, Physica A **191**, 365.
Akkermans, E., and R. Maynard, 1985, Phys. Rev. B **32**, 7850.
Alben, R., and M. F. Thorpe, 1975, J. Phys. C **8**, L275.
Alexander, S., 1983, in *Percolation, Structure and Process,* edited by G. Deutscher, J. Adler, and R. Zallen (Hilger, Bristol); Ann. Isr. Phys. Soc. (Israel) **5**, 149.
Alexander, S., 1984, J. Phys. (Paris) **45**, 1939.
Alexander, S., 1986, Physica **140A**, 397.
Alexander, S., 1989, Phys. Rev. B **40**, 7953.
Alexander, S., J. Bernasconi, W. R. Schneider, and R. Orbach, 1981, Rev. Mod. Phys. **53**, 175.
Alexander, S., E. Courtens, and R. Vacher, 1993, Physica A **195**, 286.
Alexander, S., O. Entin-Wohlman, and R. Orbach, 1985a, J. Phys. (Paris) Lett. **46**, L549.
Alexander, S., O. Entin-Wohlman, and R. Orbach, 1985b, J. Phys. (Paris) Lett. **46**, L555.
Alexander, S., O. Entin-Wohlman, and R. Orbach, 1985c, Phys. Rev. B **32**, 6447.
Alexander, S., O. Entin-Wohlman, and R. Orbach, 1986a, Phys. Rev. B **33**, 3935.
Alexander, S., O. Entin-Wohlman, and R. Orbach, 1986b, Phys. Rev. B **34**, 2726.
Alexander, S., O. Entin-Wohlman, and R. Orbach, 1987, Phys. Rev. B **35**, 1166.
Alexander, S., C. Laermans, R. Orbach, and H. M. Rosenberg, 1983, Phys. Rev. B **28**, 4615.
Alexander, S., and R. Orbach, 1982, J. Phys. (Paris) Lett. **43**, L625.
Alexandrowicz, Z., 1980, Phys. Lett. A **80**, 284.
Alippi, A., G. Shkerdin, A. Bettucci, F. Craciun, E. Molinari, and A. Petri, 1992, Phys. Rev. Lett. **69**, 3318.
Allen, J. P., J. T. Colvin, D. G. Stinson, C. P. Flynn, and H. J. Stapleton, 1982, Biophys. J. **38**, 299.
Anderson, P. W., 1958, Phys. Rev. **109**, 1492.
Andreatch, P., Jr., and H. J. McSkimin, 1976, J. Appl. Phys. **47**, 1299.
Arai, M., and J. E. Jørgensen, 1988, Phys. Lett. A **133**, 70.
Arbabi, S., and M. Sahimi, 1988, Phys. Rev. B **38**, 7173.
Argyrakis, P., L. W. Anacker, and R. Kopelman, 1984, J. Stat. Phys. **36**, 579.
Argyrakis, P., S. N. Evangelou, and K. Magoutis, 1992, Z. Phys. B **87**, 257.
Argyrakis, P., and R. Kopelman, 1984, Phys. Rev. B **29**, 511.
Argyrakis, P., and R. Kopelman, 1985, Phys. Rev. B **31**, 6008.
Ashraff, J. A., and B. W. Southern, 1988, J. Phys. A **21**, 2431.
Baltes, H. P., and E. R. Hilf, 1973, Solid State Commun. **12**, 483.
Barnsley, M., 1988, *Fractal Everywhere* (Academic, San Diego).
Beck, A., O. Gelsen, P. Wang, and J. Fricke, 1989, Rev. Phys. Appl. C **4**, 203.
Bellessa, G., 1978, Phys. Rev. Lett. **40**, 1456.
Ben-Avraham, D., and S. Havlin, 1982, J. Phys. A **15**, L691.
Ben-Avraham, D., and S. Havlin, 1983, J. Phys. A **16**, L559.
Benguigui, L., 1984, Phys. Rev. Lett. **53**, 2028.
Benguigui, L., P. Ron, and D. J. Bergman, 1987, J. Phys. (Paris) **48**, 1547.
Benoit, C., G. Poussigue, and A. Assaf, 1992, J. Phys. Condens. Matter **4**, 3153.
Bergman, D. J., 1985, Phys. Rev. B **31**, 1691.
Bergman, D. J., and Y. Kantor, 1984, Phys. Rev. Lett. **53**, 511.
Bernasconi, A., 1978a, Phys. Rev. B **18**, 2185.
Bernasconi, A., 1978b, Phys. Rev. B **18**, 3577.
Bernasconi, A., T. Sleator, D. Posselt, J. K. Kjems, and H. R. Ott, 1992, Phys. Rev. B **45**, 10 363.
Birgeneau, R. J., R. A. Cowley, G. Shirane, J. A. Tarvin, and H. J. Guggenheim, 1980, Phys. Rev. B **21**, 317.
Blanc, J., D. Brochier, J. C. Lasjaunias, R. Maynard, and A. Ribeyron, 1971, in *Proceedings of the Twelfth International Conference on Low Temperature Physics,* Kyoto, Japan, September, 1970, edited by E. Kanda (Academic Press of Japan, Tokyo), p. 827.
Bloch, F., 1932, Z. Phys. **74**, 295.
Blumenfeld, R., and A. Aharony, 1990, Phys. Rev. Lett. **64**, 1843.
Börjesson, L., 1989, in *Dynamics of Disordered Materials,* Springer Proceedings in Physics Vol. 37, edited by D. Richter, A. J. Dianoux, W. Petry, and J. Teixeira (Springer-Verlag, Berlin), p. 316.
Born, M., and K. Huang, 1954, *Dynamical Theory of Crystal Lattices* (Clarendon, Oxford), Chap. IV.
Böttger, H., A. Freyberg, and D. Wegener, 1990, Z. Phys. B **79**, 415.
Bouchaud, J. P., and A. Georges, 1990, Phys. Rep. **195**, 127.
Boukenter, A., B. Champagnon, J. Dumas, E. Duval, J. F. Quinson, and J. Serughetti, 1987, J. Non-Cryst. Solids **95&96**, 1189.
Boukenter, A., B. Champagnon, E. Duval, J. Dumas, J. F. Quinson, and J. Serughetti, 1986, Phys. Rev. Lett. **57**, 2391.
Boukenter, A., E. Duval, and H. M. Rosenberg, 1988, J. Phys. C **21**, 541.
Bourbonnais, R., R. Maynard, and A. Benoit, 1989, J. Phys. (Paris) **50**, 3331.
Bourret, A., 1988, Europhys. Lett. **6**, 731.
Breed, D. J., K. Gilijamse, J. W. E. Sterkenberg, and A. R. Miedema, 1970, J. Appl. Phys. **41**, 1267.
Breed, D. J., K. Gilijamse, J. W. E. Sterkenberg, and A. R. Miedema, 1973, Physica **68**, 303.
Brenig, W., G. Döhler, and P. Wölfle, 1971, Z. Phys. **246**, 1.
Brinker, C. J., K. D. Keefer, D. W. Schaeffer, and C. S. Ashley, 1982, J. Non-Cryst. Solids **48**, 47.
Brinker, C. J., and G. W. Scherer, 1990, *The Physics and Chemistry of Sol-Gel Processing* (Academic, San Diego).
Broadbent, S. R., 1954, J. R. Stat. Soc. B **16**, 68.
Broadbent, S. R., and J. M. Hammersley, 1957, Proc. Cambridge Philos. Soc. **53**, 629.
Buchenau, U., 1989, in *Dynamics of Disordered Materials,* Springer Proceedings in Physics Vol. 37, edited by D. Richter, A. J. Dianoux, W. Petry, and J. Teixeira (Springer-Verlag, Berlin), p. 172.
Buchenau, U., Yu. M. Galperin, V. L. Gurevich, D. A. Parshin, M. A. Ramos, and H. R. Schober, 1992, Phys. Rev. B **46**, 2798.
Buchenau, U., Yu. M. Galperin, V. L. Gurevich, and H. R.

Schober, 1991, Phys. Rev. B **43**, 5039.
Buchenau, U., M. Morkenbusch, G. Reichenauer, and B. Frick, 1992, J. Non-Cryst. Solids **145**, 121.
Buchenau, U., N. Nücker, and A. J. Dianoux, 1984, Phys. Rev. Lett. **53**, 2316.
Buchenau, U., M. Prager, N. Nücker, A. J. Dianoux, N. Ahmad, and W. A. Phillips, 1986, Phys. Rev. B **34**, 5665.
Buchenau, U., H. M. Zhou, N. Nuecker, K. S. Gilroy, and W. A. Phillips, 1988, Phys. Rev. Lett. **60**, 1318.
Buckley, A. M., and M. Greenblatt, 1992, J. Non-Cryst. Solids **143**, 1.
Bunde, A., and S. Havlin, 1991, in *Fractals and Disordered Systems,* edited by A. Bunde and S. Havlin (Springer-Verlag, Berlin), p. 51.
Bunde, A., S. Havlin, and H. E. Roman, 1990, Phys. Rev. A **42**, 6274.
Bunde, A., and H. E. Roman, 1992, Philos. Mag. B **65**, 191.
Bunde, A., H. E. Roman, S. Russ, A. Aharony, and A. B. Harris, 1992, Phys. Rev. Lett. **69**, 3189.
Buyers, W. J. L., D. E. Pepper, and R. J. Elliott, 1972, J. Phys. C **5**, 2611.
Cahill, D. G., and R. O. Pohl, 1987, Phys. Rev. B **35**, 4067.
Cahill, D. G., R. B. Stephens, R. H. Tait, S. K. Watson, and R. O. Pohl, 1991, in *Proceedings of the 21st International Conference on Thermal Conductivity,* edited by C. J. Cremers and H. A. Fine (Plenum, New York), p. 3.
Calemczuk, R., A. M. De Goer, B. Salce, R. Maynard, and A. Zarembowitch, 1987, Europhys. Lett. **3**, 1205.
Cardey, J. L., and P. Grassberger, 1985, J. Phys. A **18**, L267.
Careri, G., A. Giansanti, and J. A. Rupley, 1988, Phys. Rev. A **37**, 2703.
Castellani, C., and L. Peliti, 1986, J. Phys. A **19**, L429.
Chan, M. H. W., K. I. Blum, S. Q. Murphy, G. K. S. Wong, and J. D. Reppy, 1988, Phys. Rev. Lett. **61**, 1950.
Chayes, J. T., L. Chayes, D. S. Fisher, and T. Spencer, 1986, Phys. Rev. Lett. **57**, 2999.
Christou, A., and R. B. Stinchcombe, 1986a, J. Phys. C **19**, 5895.
Christou, A., and R. B. Stinchcombe, 1986b, J. Phys. C **19**, 5917.
Clerc, J. P., G. Giraud, J. M. Laugier, and J. M. Luck, 1990, Adv. Phys. **39**, 191.
Coddens, G., J. Pelous, T. Woignier, R. Vacher, E. Courtens, and J. Williams, 1990, in *Phonons 89,* Proceedings of the Third International Conference on Phonon Physics and the Sixth International Conference on Phonon Scattering in Condensed Matter, Heidelberg, August 1989, edited by S. Hunklinger, W. Ludwig, and G. Weiss (World Scientific, Singapore), p. 697.
Coniglio, A., 1982a, J. Phys. A **15**, 3829.
Coniglio, A., 1982b, Phys. Rev. Lett. **46**, 250.
Coniglio, A., 1987, Philos. Mag. B **56**, 785.
Conrad, H., U. Buchenau, R. Schaetzler, G. Reichenauer, and J. Fricke, 1990, Phys. Rev. B **41**, 2753.
Conrad, H., J. Fricke, and G. Reichenauer, 1989, Rev. Phys. Appl. Colloq. C **4**, 157.
Conrad, H., G. Reichenauer, and J. Fricke, 1989, in *Dynamics of Disordered Materials,* Springer Proceedings in Physics Vol. 37, edited by D. Richter, A. J. Dianoux, W. Petry, and J. Teixeira (Springer-Verlag, Berlin), p. 304.
Coombs, G. J., R. A. Coweley, W. J. L. Buyers, E. C. Svensson, T. M. Holden, and D. A. Jones, 1976, J. Phys. C **9**, 2167.
Courtens, E., C. Lartigue, F. Mezei, R. Vacher, G. Coddens, M. Foret, J. Pelous, and T. Woignier, 1990, Z. Phys. B **79**, 1.
Courtens, E., J. Pelous, J. Phalippou, R. Vacher, and T. Woignier, 1987a, Phys. Rev. Lett. **58**, 128.
Courtens, E., J. Pelous, J. Phalippou, R. Vacher, and T. Woignier, 1987b, J. Non-Cryst. Solids **95&96**, 1175.
Courtens, E., J. Pelous, R. Vacher, and T. Woignier, 1987c, in *Time-Dependent Effects in Disordered Materials,* NATO ASI Series B, Vol. 167, edited by R. Pynn and T. Riste (Plenum, New York), p. 255.
Courtens, E., and R. Vacher, 1987, Z. Phys. B **68**, 355.
Courtens, E., and R. Vacher, 1988, in *Random Fluctuations and Pattern Growth: Experiments and Models,* NATO ASI Series E, Vol. 157, edited by H. E. Stanley and N. Ostrowsky (Kluwer, Utrecht), p. 20.
Courtens, E., and R. Vacher, 1989, Proc. R. Soc. London Ser. A **423**, 55.
Courtens, E., and R. Vacher, 1992, Philos. Mag. B **65**, 347.
Courtens, E., R. Vacher, and J. Pelous, 1990, in *Fractal's Physical Origin and Properties,* edited by L. Pietronero (Plenum, London), p. 285.
Courtens, E., R. Vacher, J. Pelous, and T. Woignier, 1988, Europhys. Lett. **6**, 245.
Courtens, E., R. Vacher, and E. Stoll, 1989, Physica D **38**, 41.
Craciun, F., A. Bettucci, E. Molinari, A. Petri, and A. Alippi, 1992, Phys. Rev. Lett. **68**, 1555.
Daoud, M., 1983, J. Phys. (Paris) **44**, L925.
Day, A. R., and M. F. Thorpe, 1988, Phys. Rev. Lett. **61**, 2502.
Day, A. R., R. Tremblay, and A.-M. S. Tremblay, 1985, J. Non-Cryst. Solids **75**, 245.
de Alcantara Bonfim, O. F., J. E. Kirkham, and A. J. McKane, 1980, J. Phys. A **13**, L247.
de Alcantara Bonfim, O. F., J. E. Kirkham, and A. J. McKane, 1981, J. Phys. A **14**, 2391.
Dean, P., 1960, Proc. R. Soc. London Ser. A **254**, 507.
de Arcangelis, L., S. Redner, and A. Coniglio, 1985, Phys. Rev. B **31**, 4725.
de Arcangelis, L., S. Redner, and A. Coniglio, 1986, Phys. Rev. B **34**, 4656.
de Gennes, P. G., 1976a, J. Phys. (Paris) Lett. **37**, L1.
de Gennes, P. G., 1976b, La Recherche **7**, 919.
de Gennes, P. G., 1979, *Scaling Concepts in Polymer Physics* (Cornell University Press, Ithaca).
de Gennes, P. G., 1984, in *Percolation, Localization, and Superconductivity,* NATO ASI Series B, Vol. 109, edited by A. M. Goldman and S. A. Wolf (Plenum, New York), p. 83.
de Gennes, P. G., P. Lafore, and J. D. Millot, 1959a, J. Phys. Radium **20**, 624.
de Gennes, P. G., P. Lafore, and J. D. Millot, 1959b, J. Phys. Chem. Solids **11**, 105.
de Goer, A. M., R. Calemczuk, B. Salce, J. Bon, E. Bonjour, and R. Maynard, 1989, Phys. Rev. B **40**, 8327.
den Nijs, M. P. M., 1979, J. Phys. A **12**, 1857.
de Oliveira, J. E., J. N. Page, and H. M. Rosenberg, 1989, Phys. Rev. Lett. **62**, 780.
Deptuck, D., J. P. Harrison, and P. Zawadzki, 1985, Phys. Rev. Lett. **54**, 913.
Derrida, B., 1984, Phys. Rev. B **29**, 6645.
Derrida, B., and L. de Seze, 1982, J. Phys. (Paris) **43**, 475.
Derrida, B., R. Orbach, and K. W. Yu, 1984, Phys. Rev. B **29**, 6645.
Derrida, B., and J. Vannimenus, 1982, J. Phys. A **15**, L557.
Deutscher, G., 1987, in *Chance and Matter,* edited by J. Souletie, J. Vannimenus, and R. Stora (North-Holland, Amsterdam), p. 1.
Deutscher, G., R. Zallen, and J. Adler, 1983, Eds., *Percolation Structures and Processes;* Ann. Isr. Phys. Soc. (Israel) **5**.

de Vries, P., H. de Raedt, and A. Lagendijk, 1989, Phys. Rev. Lett. **62**, 2515.
Dhar, D., 1977, J. Math. Phys. **18**, 577.
Dianoux, A. J., 1989, Philos. Mag. B **59**, 17.
Dianoux, A. J., U. Buchenau, M. Prager, and N. Nücker, 1986, Physica **138B**, 264.
Dianoux, A. J., J. N. Page, and H. M. Rosenberg, 1987, Phys. Rev. Lett. **58**, 886.
Dietler, G., C. Aubert, D. S. Cannell, and P. Wiltzius, 1986, Phys. Rev. Lett. **57**, 3117.
Dietler, G., C. Aubert, D. S. Cannell, and P. Wiltzius, 1987, Phys. Rev. Lett. **59**, 246.
Dietsche, W., and H. Kinder, 1979, Phys. Rev. Lett. **43**, 1413.
Domb, C., 1966, Proc. Phys. Soc. London **89**, 859.
Domb, C., and M. F. Sykes, 1960, Phys. Rev. **122**, 77.
Domes, H., R. Leyrer, D. Haarer, and A. Blumen, 1987, Phys. Rev. B **36**, 4522.
Dreyfus, B., N. C. Fernandes, and R. Maynard, 1968, Phys. Lett. **26A**, 647.
Duering, E., and H. E. Roman, 1991, J. Stat. Phys. **64**, 851.
Duquesne, J.-Y., and G. Bellessa, 1986, J. Non-Cryst. Solids **81**, 319.
Duval, E., A. Boukenter, T. Achibat, B. Champagnon, J. Serugetti, and J. Dumas, 1992, Philos. Mag. B **65**, 181.
Duval, E., G. Mariott, M. Montegna, O. Pilla, G. Villiani, and M. Barland, 1987, Europhys. Lett. **3**, 333.
Edwards, S. F., and R. C. Jones, 1971, J. Phys. C **4**, 2109.
Efros, A. L., 1986, *Physics and Geometry of Disorder: Percolation Theory* (Mir, Moscow).
Elliott, R. J., and D. E. Pepper, 1973, Phys. Rev. B **8**, 2374.
Entin-Wohlman, O., S. Alexander, and R. Orbach, 1985, Phys. Rev. B **32**, 8007.
Entin-Wohlman, O., S. Alexander, R. Orbach, and K.-W. Yu, 1984, Phys. Rev. B **29**, 4588.
Entin-Wohlman, O., R. Orbach, and G. Polatsek, 1989, in *Dynamics of Disordered Materials,* Springer Proceedings in Physics, Vol. 137, edited by D. Richter, A. J. Dianoux, W. Petry, and J. Teixeira (Springer-Verlag, Berlin), p. 288.
Entin-Wohlman, O., U. Sivan, R. Blumenfeld, and Y. Meir, 1989, Physica D **38**, 93.
Essam, J. W., 1980, Rep. Prog. Phys. **43**, 843.
Essam, J. W., and F. M. Bhatti, 1985, J. Phys. A **18**, 3577.
Evangelou, S. N., 1986a, Phys. Rev. B **33**, 3602.
Evangelou, S. N., 1986b, J. Phys. C **19**, 4291.
Evangelou, S. N., 1990, J. Phys. A **23**, L317.
Evangelou, S. N., 1991, in *Fractals in the Fundamental and Applied Sciences,* edited by H. O. Peiten, J. M. Heinriques, and L. F. Penedo (North-Holland, Amsterdam), p. 123.
Evangelou, S. N., N. I. Papanicolaou, and E. N. Economou, 1991, Phys. Rev. B **43**, 11 171.
Family, F., and D. P. Landau, 1984, *Kinetics of Aggregation and Gelation* (North-Holland, Amsterdam).
Family, F., and T. Vicsek, 1991, *Dynamics of Fractal Surfaces* (World Scientific, Singapore).
Farmer, J. D., E. Ott, and J. A. Yorke, 1983, Physica **7D**, 153.
Feder, J., 1988, *Fractals* (Plenum, New York).
Feder, J., and A. Aharony, 1990, *Fractals in Physics* (North-Holland, Amsterdam).
Feng, S., 1985a, Phys. Rev. B **32**, 510.
Feng, S., 1985b, Phys. Rev. B **32**, 5793.
Feng, S., and M. Sahimi, 1985, Phys. Rev. B **31**, 1671.
Feng, S., and P. N. Sen, 1984, Phys. Rev. Lett. **52**, 216.
Feng, S., P. N. Sen, B. I. Halperin, and C. J. Lobb, 1984, Phys. Rev. B **30**, 5386.
Ferri, B., J. Frisken, and D. S. Cannell, 1991, Phys. Rev. Lett. **67**, 3626.
Fisch, R., and A. B. Harris, 1978, Phys. Rev. B **18**, 416.
Fischer, U., C. von Borczyshowski, and N. Schwentner, 1990, Phys. Rev. B **41**, 9126.
Flory, P. J., 1941a, J. Am. Chem. Soc. **63**, 3083.
Flory, P. J., 1941b, J. Am. Chem. Soc. **63**, 3091.
Flory, P. J., 1941c, J. Am. Chem. Soc. **63**, 3096.
Fogelholm, R., 1980, J. Phys. C **13**, L571.
Fontana, A., F. Rocca, and M. P. Fontana, 1987, Phys. Rev. Lett. **58**, 503.
Fontana, A., F. Rocca, M. P. Fontana, B. Rosi, and A. J. Dianoux, 1990, Phys. Rev. B **41**, 3778.
Forsman, J., J. P. Harrison, and A. Rutenberg, 1987, Can. J. Phys. **65**, 767.
Frank, D. J., and C. J. Lobb, 1988, Phys. Rev. B **37**, 302.
Freltoft, T., J. K. Kjems, and D. Richter, 1987, Phys. Rev. Lett. **59**, 1212.
Fricke, J., 1986, *Aerogels* (Springer-Verlag, Berlin).
Fricke, J., 1988, Sci. Am. **258**, No. 5, 68.
Fricke, J., 1992, Ed., *Proceedings of the 3rd International Symposium on Aerogels;* J. Non-Cryst. Solids **145**, No. 1–3.
Frisken, B. J., F. Ferri, and D. S. Cannell, 1991, Phys. Rev. Lett. **66**, 2754.
Fucito, F., and E. Marinari, 1981, J. Phys. A **14**, L85.
Garcia-Molina, R., F. Guinea, and E. Louis, 1988, Phys. Rev. Lett. **60**, 124.
Gaunt, D. S., 1977, J. Phys. A **10**, 807.
Gaunt, D. S., and H. Ruskin, 1978, J. Phys. A **11**, 1369.
Gaunt, D. S., and M. F. Sykes, 1983, J. Phys. A **16**, 783.
Gaunt, D. S., M. F. Sykes, and H. Ruskin, 1976, J. Phys. A **9**, L43.
Gaunt, D. S., S. G. Whittington, and M. F. Sykes, 1981, J. Phys. A **14**, L247.
Gefen, Y., A. Aharony, and S. Alexander, 1983, Phys. Rev. Lett. **50**, 77.
Gingold, D. G., and C. J. Lobb, 1990, Phys. Rev. B **42**, 8220.
Given, J. A., 1984, Phys. Rev. Lett. **52**, 1853.
Goldman, A. M., and S. A. Wolf, 1983, Eds., *Percolation, Localization, and Superconductivity,* NATO ASI Series B, Vol. 109 (Plenum, New York).
Gordon, J. M., and A. M. Goldman, 1987, Phys. Rev. B **35**, 4909.
Gordon, J. M., and A. M. Goldman, 1988a, Phys. Rev. B **38**, 12019.
Gordon, J. M., and A. M. Goldman, 1988b, Physica B **152**, 125.
Gordon, J. M., A. M. Goldman, J. Maps, D. Costello, R. Tiberio, and B. Whitehead, 1986, Phys. Rev. Lett. **56**, 2280.
Gordon, J. M., A. M. Goldman, and B. Whitehead, 1987, Phys. Rev. Lett. **59**, 2311.
Graebner, J. E., B. Golding, and L. C. Allen, 1986, Phys. Rev. B **34**, 5696.
Grassberger, P., 1986, J. Phys. A **19**, 1681.
Grassl, C. M., and D. L. Huber, 1984, Phys. Rev. B **30**, 1366.
Grest, G. S., and I. Webman, 1984, J. Phys. (Paris) Lett. **45**, L1155.
Halperin, B. I., and P. C. Hohenberg, 1967, Phys. Rev. Lett. **19**, 700.
Halperin, B. I., and P. C. Hohenberg, 1969, Phys. Rev. **177**, 952.
Hammersley, J. M., 1983, in *Percolation, Structure and Process,* edited by G. Deutscher, J. Adler, and R. Zallen (Hilger, Bristol); Ann. Isr. Phys. Soc. **5**, 47.
Harder, H., A. Bunde, and W. Dietrich, 1986, J. Chem. Phys. **85**, 4123.

Harris, A. B., 1987, Philos. Mag. B **56**, 833.
Harris, A. B., and A. Aharony, 1987, Europhys. Lett. **4**, 1355.
Harris, A. B., S. Kim, and T. C. Lubensky, 1984, Phys. Rev. Lett. **53**, 743.
Harris, A. B., and K. Kirkpatrick, 1977, Phys. Rev. B **16**, 542.
Harris, A. B., and T. C. Lubensky, 1984, J. Phys. A **17**, L609.
Harris, A. B., and T. C. Lubensky, 1987, Phys. Rev. B **35**, 6987.
Harris, A. B., Y. Meir, and A. Aharony, 1987, Phys. Rev. B **36**, 8752.
Hattori, K., and T. Hattori, 1988, J. Phys. A **21**, 3117.
Hattori, K., T. Hattori, and H. Watanabe, 1985, Phys. Rev. A **32**, 3730.
Hattori, K., T. Hattori, and H. Watanabe, 1986, Phys. Lett. A **15**, 207.
Havlin, S., 1988, in *Random Fluctuations and Pattern Growth: Experiments and Models,* NATO ASI Series E, Vol. 157, edited by H. E. Stanley and N. Ostrowsky (Kluwer, Utrecht), p. 15.
Havlin, S., and D. Ben-Avraham, 1983, J. Phys. A **16**, L483.
Havlin, S., and D. Ben-Avraham, 1987, Adv. Phys. **36**, 695.
Havlin, S., D. Ben-Avraham, and D. Movshovitz, 1984, J. Stat. Phys. **36**, 831.
Havlin, S., D. Ben-Avraham, and H. Sompolinsky, 1983, Phys. Rev. A **27**, 1730.
Havlin, S., and S. Bunde, 1989, Physica D **38**, 184.
Havlin, S., and S. Bunde, 1991, in *Fractals and Disordered Systems,* edited by A. Bunde and S. Havlin (Springer-Verlag, Berlin), p. 97.
Havlin, S., and R. Nossal, 1984, J. Phys. A **17**, L427.
Havlin, S., B. Trus, G. H. Weiss, and D. Ben-Avraham, 1985, J. Phys. A **18**, L247.
Hayashi, M., E. Gerkema, A. M. van der Kraan, and I. Tamura, 1990, Phys. Rev. B **42**, 9771.
Heermann, D. W., and D. Stauffer, 1981, Z. Phys. B **44**, 339.
Helman, J. S., A. Coniglio, and C. Tsallis, 1984, Phys. Rev. Lett. **53**, 1195.
Herrmann, H. J., 1986, Phys. Rev. Lett. **56**, 2432.
Herrmann, H. J., B. Derrida, and J. Vannimenus, 1984, Phys. Rev. B **30**, 4080.
Herrmann, H. J., and H. E. Stanley, 1988, J. Phys. A **21**, L829.
Holcomb, W. K., 1974, J. Phys. C **7**, 4299.
Holcomb, W. K., 1976, J. Phys. C **9**, 1771.
Hong, D. C., S. Havlin, H. J. Herrmann, and H. E. Stanley, 1984, Phys. Rev. B **30**, 4083.
Hu, G. J., and D. L. Huber, 1986, Phys. Rev. B **33**, 3599.
Hunklinger, S., and W. Arnold, 1976, in *Physical Acoustics Vol. XII,* edited by W. P. Mason and R. N. Thurston (Academic, New York), p. 155.
Ikeda, H., J. A. Fernandez-Baca, R. M. Nicklow, M. Takahashi, and K. Iwasa, 1994, private communication.
Ingram, M. D., 1987, Phys. Chem. Glasses **28**, 215.
Ioffe, A. F., and A. R. Regel, 1960, Prog. Semicond. **4**, 237.
Isichenko, M. B., 1992, Rev. Mod. Phys. **64**, 961.
Itoh, M., and H. Yasuoka, 1990, J. Magn. Magn. Mater. **90&91**, 359.
Jäckle, J., 1972, Z. Phys. **257**, 212.
Jagannathan, A., and R. Orbach, 1990, Phys. Rev. B **41**, 3153.
Jagannathan, A., R. Orbach, and O. Entin-Wohlman, 1989, Phys. Rev. B **39**, 13 465.
Jan, N., D. C. Hong, and H. E. Stanley, 1985, J. Phys. A **18**, L935.
Jaynes, E. T., 1957a, Phys. Rev. **106**, 620.
Jaynes, E. T., 1957b, Phys. Rev. **108**, 171.
John, S., 1984, Phys. Rev. Lett. **53**, 2169.
John, S., H. Sompolinsky, and M. J. Stephen, 1983, Phys. Rev. B **27**, 5592.
Jones, R. C., and S. F. Edwards, 1971, J. Phys. C **6**, L194.
Kantor, Y., and I. Webman, 1984, Phys. Rev. Lett. **52**, 1891.
Kapitulnik, A., A. Aharony, G. Deutscher, and D. Stauffer, 1983, J. Phys. A **16**, L269.
Karpov, V. G., M. I. Klinger, and F. N. Ignatév, 1983, Zh. Eksp. Teor. Fiz. **84**, 760 [Sov. Phys. JETP **57**, 439 (1983)].
Karpov, V. G., and D. A. Parshin, 1983, Pis'ma Zh. Eksp. Teor. Fiz. **38**, 536 [JETP Lett. **38**, 648 (1983)].
Karpov, V. G., and D. A. Parshin, 1985, Zh. Eksp. Teor. Fiz. **88**, 2212 [Sov. Phys. JETP **61**, 1308 (1985)].
Keating, P. N., 1966, Phys. Rev. B **152**, 774.
Keffer, F., 1966, in *Handbuch der Physik,* edited by S. Flugge (Springer-Verlag, Berlin), Vol. 18, p. 1.
Keramiotis, A., P. Argyrakis, and R. Kopelman, 1985, Phys. Rev. B **31**, 4617.
Keys, T., and T. Ohtsuki, 1987, Phys. Rev. Lett. **59**, 603.
Kim, D. Y., H. J. Heermann, and D. P. Landau, 1987, Phys. Rev. B **35**, 3661.
Kirkpatrick, S., 1973a, Rev. Mod. Phys. **45**, 574.
Kirkpatrick, S., 1973b, Solid State Commun. **12**, 2109.
Kirkpatrick, S., 1979, in *Ill Condensed Matter,* edited by R. Balian, R. Maynard, and G. Toulouse (North-Holland, Amsterdam), p. 323.
Kistler, S. S., 1932, J. Phys. Chem. **36**, 52.
Kjems, J. K., 1991, in *Fractals and Disordered Systems,* edited by A. Bunde and S. Havlin (Springer-Verlag, Heidelberg), p. 263.
Kjems, J. K., 1993, Physica A **191**, 328.
Kopelman, R., S. Parus, and J. Prasad, 1986, Phys. Rev. Lett. **56**, 1742.
Korzhenevskiĭ, and A. A. Luzhkov, 1991, Zh. Eksp. Teor. Fiz. **99**, 530 [Sov. Phys. JETP **72**, 295 (1991)].
Krumhansl, J. A., 1986, Phys. Rev. Lett. **56**, 2696.
Kumar, D., 1984, Phys. Rev. B **30**, 2960.
Kumar, D., and A. B. Harris, 1985, Phys. Rev. B **32**, 3251.
Laird, B. B., and H. R. Schober, 1991, Phys. Rev. Lett. **66**, 636.
Lam, P. M., and W. Bao, 1985, Z. Phys. B **59**, 333.
Lam, P. M., W. Bao, and Z. Zheng, 1985, Z. Phys B **59**, 63.
Lambert, C. J., and G. D. Hughes, 1991, Phys. Rev. Lett. **66**, 1074.
Lasjaunias, L. C., 1973, thesis (University of Grenoble, Grenoble, France).
Lasjaunias, L. C., and R. Maynard, 1971, J. Non-Cryst. Solids **6**, 101.
Last, B. J., and D. J. Thouless, 1971, Phys. Rev. Lett. **27**, 1719.
Levy, Y. E., and B. Souillard, 1987, Europhys. Lett. **4**, 233.
Lewis, S., and R. B. Stinchcombe, 1984, Phys. Rev. Lett. **52**, 1021.
Leyvraz, F., and H. E. Stanley, 1983, Phys. Rev. Lett. **51**, 2048.
Li, P., and W. Strieder, 1982, J. Phys. C **15**, 6591.
Li, Q., C. M. Soukoulis, and G. S. Grest, 1990, Phys. Rev. B **41**, 11 713.
Lin, J. J., 1991, Phys. Rev. B **44**, 789.
Liu, S. H., 1984, Phys. Rev. B **30**, 4045.
Liu, S. H., and A. J. Liu, 1985, Phys. Rev. B **32**, 4753.
Lobb, C. J., and D. J. Frank, 1984, Phys. Rev. B **30**, 4090.
Lobb, C. J., and K. R. Karasek, 1982, Phys. Rev. B **25**, 492.
Loring, R. F., and S. Mukamel, 1986, Phys. Rev. B **34**, 6582.
Lottici, P. P., 1988, Phys. Status Solidi B **146**, K18.
Love, M. S., and A. C. Anderson, 1990, Phys. Rev. B **42**, 1845.
MacDonald, M., and N. Jan, 1986, Can. J. Phys. **64**, 1353.
Majid, I., D. Ben-Avraham, S. Havlin, and H. E. Stanley, 1984,

Phys. Rev. B **30**, 1626.
Malieppard, M. C., J. H. Page, J. P. Harrison, and R. J. Stubbs, 1985, Phys. Rev. B **32**, 6261.
Malinovskiĭ, V. K., V. N. Novikov, A. P. Sokolov, and V. A. Bagryansky, 1988, Chem. Phys. Lett. **143**, 111.
Mandelbrot, B. B., 1975, *Les Objets Fractals: Forme, Hasard et Dimension* (Flammarion, Paris).
Mandelbrot, B. B., 1977, *Fractals: Form, Chance and Dimension* (Freeman, San Francisco).
Mandelbrot, B. B., 1978, in *Proceedings of the Thirteenth International Union of Pure and Applied Physics Conference on Statistical Physics,* edited by D. Cabib, C. G. Kuper, and I. Reiss (Hilger, Bristol), p. 225.
Mandelbrot, B. B., 1982, *The Fractal Geometry of Nature* (Freeman, San Francisco).
Mandelbrot, B. B., 1989, *Les Objets Fractals: Forme, Hasard et Dimension* (Flammarion, Paris).
Mandelbrot, B. B., and C. J. G. Evertsz, 1990, Nature **348**, 143.
Margolina, A., H. J. Herrmann, and D. Stauffer, 1982, Phys. Lett. **93A**, 73.
Margolina, A., H. Nakanishi, D. Stauffer, and H. E. Stanley, 1984, J. Phys. A **17**, 1683.
Mariotto, G., M. Montagna, G. Viliani, R. Campostrini, and G. Carturan, 1988a, J. Phys. C **21**, L797.
Mariotto, G., M. Montagna, G. Viliani, R. Campostrini, and G. Carturan, 1988b, J. Non-Cryst. Solids **106**, 384.
Mazzacurati, V., M. Montagna, O. Pilla, G. Viliani, G. Ruocco, and G. Signorelli, 1992, Phys. Rev. B **45**, 2126.
McCarthy, J. F., 1988, J. Phys. A **21**, 3379.
Mead, L. R., and N. Papanicolaou, 1984, J. Math. Phys. **25**, 2404.
Meakin, P., 1986, Phys. Rev. A **34**, 710.
Meyer, R., J. L. Gavilano, B. Jeanneret, R. Theron, C. Leemann, H. Beck, and P. Martinoli, 1991, Phys. Rev. Lett. **67**, 3622.
Meyer, R., P. Martinoli, J. L. Gavilano, and B. Jeanneret, 1992, Helv. Phys. Acta **65**, 391.
Meyer, R., R. C. Nussbaum, J. L. Gavilano, B. Jeanneret, C. Leemann, and P. Martinoli, 1992, Physica A **191**, 458.
Middlemiss, K. M., S. G. Whittingston, and D. C. Gaunt, 1980, J. Phys. A **13**, 1835.
Mitescu, C. D., and M. J. Musolf, 1983, J. Phys. (Paris) **44**, L679.
Montagna, M., O. Pilla, and G. Viliani, 1989, Philos. Mag. B **59**, 49.
Montagna, M., O. Pilla, G. Viliani, V. Mazzacurati, G. Ruocco, and G. Signorelli, 1990, Phys. Rev. Lett. **65**, 1136.
Montroll, E. W., and R. B. Potts, 1955, Phys. Rev. **100**, 525.
Mott, N. F., 1967, Adv. Phys. **16**, 49.
Mott, N. F., 1969, Philos. Mag. **19**, 835.
Movshovitz, D., and S. Havlin, 1988, J. Phys. A **21**, 2761.
Mulders, N., R. Mehrotra, L. S. Goldner, and G. Ahlers, 1991, Phys. Rev. Lett. **67**, 695.
Murray, G. A., 1966, Proc. Phys. Soc. London **89**, 87.
Nagatani, T., 1985, J. Phys. A **18**, L1149.
Nakanishi, H., and H. E. Stanley, 1980, Phys. Rev. B **22**, 2466.
Nakayama, T., 1989, in *Progress in Low Temperature Physics,* Vol. XII, edited by D. F. Brewer (North-Holland, Amsterdam), p. 115.
Nakayama, T., 1990, in *Phonons 89,* Proceedings of the Third International Conference on Phonon Physics and the Sixth International Conference on Phonon Scattering in Condensed Matter, Heidelberg, August, 1989, edited by S. Hunklinger, W. Ludwig, and G. Weiss (World Scientific, Singapore), p. 646.
Nakayama, T., 1992, Physica A **191**, 386.
Nakayama, T., 1993, Fractals **1**, 806.
Nakayama, T., 1994, in *Soft Order in Physical Systems,* Proceedings of NATO Advanced Research Workshop, edited by R. Bruinsma and Y. Rabin (Plenum, New York), p. 181.
Nakayama, T., and K. Yakubo, 1990, Proc. Indian Acad. Sci. **102**, 575.
Nakayama, T., and K. Yakubo, 1992a, in *Slow Dynamics in Condensed Matter,* edited by K. Kawasaki, M. Tokuyama, and T. Kawakatsu (AIP, New York), p. 279.
Nakayama, T., and K. Yakubo, 1992b, J. Phys. Soc. Jpn. **61**, 2601.
Nakayama, T., K. Yakubo, and R. Orbach, 1989, J. Phys. Soc. Jpn. **58**, 1891.
Neumann, U. A., and S. Havlin, 1988, J. Stat. Phys. **52**, 203.
Nienhuis, B., 1982, J. Phys. A **15**, 199.
Nienhuis, B., E. K. Riedel, and M. Schick, 1980, J. Phys. A **13**, 189.
Normand, J. M., H. J. Herrmann, and M. Hajjar, 1988, J. Stat. Phys. **52**, 441.
Octavio, M., and C. J. Lobb, 1991, Phys. Rev. B **43**, 8233.
Odagaki, T., 1993, *Percolation-no-kagaku (Science of Percolation)* (Shokabo, Tokyo).
Odagaki, T., N. Ogita, and H. Matsuda, 1980, J. Phys. C **13**, 189.
Orbach, R., 1984, J. Stat. Phys. **36**, 735.
Orbach, R., 1986, Science **231**, 814.
Orbach, R., 1989a, Physica D **38**, 226.
Orbach, R., 1989b, Annu. Rev. Mater. Sci. **19**, 497.
Orbach, R., 1989c, Hyperfine Interact. **49**, 325.
Orbach, R., A. Aharony, S. Alexander, and O. Entin-Wohlman, 1988, in *Competing Interactions and Microstructures: Statics and Dynamics,* Springer Proceedings in Physics, Vol. 27, edited by R. LeSar, A. Bishop, and R. Heffner (Springer-Verlag, Berlin), p. 212.
Orbach, R., and H. M. Rosenberg, 1984, in *Proceedings of the 17th International Conference on Low Temperature Physics,* edited by U. Eckern, A. Schmid, W. Weber, and H. Wuhl (Elsevier, Amsterdam), p. 375.
Orbach, R., and K.-W. Yu, 1987, J. Appl. Phys. **61**, 3689.
Page, J. H., W. J. L. Buyers, G. Dolling, P. Gerlach, and J. P. Harrison, 1989, Phys. Rev. B **39**, 6180.
Page, J. H., and R. D. McCulloch, 1986, Phys. Rev. Lett. **57**, 1324.
Page, J. H., D. W. Schaefer, J. H. Root, W. J. L. Buyers, and C. J. Brinker, 1990, in *Phonons 89,* Proceedings of the Third International Conference on Phonon Physics and the Sixth International Conference on Phonon Scattering in Condensed Matter, Heidelberg, August, 1989, edited by S. Hunklinger, W. Ludwig, and G. Weiss (World Scientific, Singapore), p. 667.
Paladin, G., and A. Vulpiani, 1987, Phys. Rep. **156**, 147.
Pandey, R. B., D. Stauffer, A. Margolina, and J. G. Zabolitzky, 1984, J. Stat. Phys. **34**, 427.
Pandey, R. B., D. Stauffer, and J. G. Zabolitzky, 1987, J. Stat. Phys. **49**, 849.
Pearson, R. B., 1980, Phys. Rev. B **22**, 2579.
Peitgen, H. O., and D. Saupe, 1988, *Fractal Images* (Springer-Verlag, Berlin).
Pelous, J., R. Vacher, T. Woignier, J. L. Sauvajol, and E. Courtens, 1989, Philos. Mag. B **59**, 65.
Petri, A., 1991, Physica A **185**, 166.
Petri, A., and L. Pietronero, 1992, Phys. Rev. B **45**, 12 864.
Phalippou, J., A. Ayral, T. Woignier, J. F. Quinson, M. Pauthe, and M. Chatelut, 1991, Europhys. Lett. **14**, 249.

Pietronero, L., and E. Tosatti, 1988, *Fractals in Physics* (North-Holland, Amsterdam).
Pike, R. B., and H. E. Stanley, 1981, J. Phys. A **14**, L169.
Pilla, O., G. Vilani, M. Montagna, V. Mazzacurati, G. Ruocco, and G. Signorelli, 1992, Philos. Mag. B **65**, 243.
Pimentel, I. L., and R. B. Stinchcombe, 1989, J. Phys. A **22**, 3959.
Polatsek, G., and O. Entin-Wohlman, 1988, Phys. Rev. B **37**, 7726.
Polatsek, G., O. Entin-Wohlman, and R. Orbach, 1988, J. Phys. (Paris) Colloq. **49**, 1191.
Polatsek, G., O. Entin-Wohlman, and R. Orbach, 1989, Phys. Rev. B **39**, 9353.
Posselt, D., 1991, Ph.D. thesis (Riso National Laboratory, Roskilde, Denmark).
Posselt, D., J. K. Kjems, A. Bernasconi, T. Sleator, and H. R. Ott, 1991, Europhys. Lett. **16**, 59.
Posselt, D., J. K. Kjems, A. Bernasconi, T. Sleator, and H. R. Ott, 1992, in *Slow Dynamics in Condensed Matter,* AIP Conference Proceedings No. 256, edited by K. Kawasaki, M. Tokuyama, and T. Kawakatsu (AIP, New York), p. 207.
Posselt, D., J. S. Pedersen, and K. Mortensen, 1992, J. Non-Cryst. Solids **145**, 128.
Prassas, M., J. Phalippou, and J. Zarzycki, 1984, J. Mater. Sci. **19**, 1656.
Pynn, R., and T. Riste, 1987, *Time-Dependent Effects in Disordered Materials* (Plenum, New York).
Pynn, R., and A. Skjeltorp, 1985, *Scaling Phenomena in Disordered Systems* (Plenum, New York).
Rahmani, A., C. Benoit, E. Royer-Vilanova, and G. Poussigue, 1993, J. Phys. Condens. Matter **5**, 7941.
Rammal, R., 1983, Phys. Rev. B **28**, 4871.
Rammal, R., 1984a, J. Phys. (Paris) **45**, 191.
Rammal, R., 1984b, Phys. Rep. **103**, 151.
Rammal, R., J. C. Angels d'Auriac, and A. Benoit, 1984, Phys. Rev. B **30**, 4087.
Rammal, R., C. Tannous, P. Breton, and A. M. S. Tremblay, 1985, Phys. Rev. Lett. **54**, 1718.
Rammal, R., C. Tannous, and A. M. S. Tremblay, 1985, Phys. Rev. A **31**, 2662.
Rammal, R., and G. Toulouse, 1983, J. Phys. (Paris) **44**, L13.
Rapaport, D. C., 1985, J. Phys. A **18**, L175.
Reeve, J. S., 1982, J. Phys. A **15**, L521.
Reeve, J. S., A. J. Guttmann, and B. Keck, 1982, Phys. Rev. B **26**, 3923.
Reichenauer, G., J. Fricke, and U. Buchenau, 1989, Europhys. Lett. **8**, 415.
Richter, D., T. Freltoft, and J. K. Kjems, 1987, in *Time-Dependent Effects in Disordered Materials,* NATO ASI Series B, Vol. 167, edited by R. Pynn and T. Riste (Plenum, New York), p. 251.
Richter, D., and L. Passell, 1980, Phys. Rev. Lett. **44**, 1593.
Rocca, F., and A. Fontana, 1989, Philos. Mag. B **59**, 57.
Roman, H. E., 1990, J. Stat. Phys. **58**, 375.
Roman, H. E., 1992a, Phys. Rev. Lett. **68**, 2856.
Roman, H. E., 1992b, Physica A **191**, 379.
Roman, H. E., S. Russ, and A. Bunde, 1991, Phys. Rev. Lett. **66**, 1643.
Rosenberg, H. M., 1985, Phys. Rev. Lett. **54**, 704.
Rousset, J. L., A. Boukenter, B. Champagnon, J. Dumas, E. Duval, J. F. Quinson, and J. Serughetti, 1990, J. Phys. Condens. Matter **2**, 8445.
Roux, S., 1986, J. Phys. A **19**, L351.
Roux, S., A. Hansen, and E. Guyon, 1988, Phys. Rev. Lett. **61**, 2501.
Royer, E., C. Benoit, and G. Poussigue, 1991, in *High Performance Computing II,* Proceedings of the Second Symposium, edited by M. Durand and F. El Dabaghi (North-Holland, Amsterdam), p. 513.
Royer, E., C. Benoit, and G. Poussigue, 1992, J. Phys. Condens. Matter **4**, 561.
Russ, S., 1992, Physica A **191**, 335.
Russ, S., H. E. Roman, and A. Bunde, 1990, in *Phonons 89,* Proceedings of the Third International Conference on Phonon Physics and the Sixth International Conference on Phonon Scattering in Condensed Matter, Heidelberg, August, 1989, edited by S. Hunklinger, W. Ludwig, and G. Weiss (World Scientific, Singapore), p. 685.
Russ, S., H. E. Roman, and A. Bunde, 1991, J. Phys. Condens. Matter **3**, 4797.
Sahimi, M., 1984, J. Phys. C **17**, 3957.
Sahimi, M., 1986, J. Phys. C **19**, L79.
Sahimi, M., 1993, *Applications of Percolation Theory* (Taylor&Francis, London).
Sahimi, M., and S. Arbabi, 1991, J. Stat. Phys. **62**, 453.
Sahimi, M., B. D. Hughes, L. E. Scriven, and H. T. Davis, 1983, J. Phys. C **16**, L521.
Saikan, S., T. Kishida, Y. Kanematsu, H. Aota, A. Harada, and M. Kamachi, 1990, Chem. Phys. Lett. **166**, 358.
Sakamoto, S., F. Yonezawa, K. Aoki, S. Nosé, and M. Hori, 1989, J. Phys. A **22**, L705.
Sakamoto, S., F. Yonezawa, and M. Hori, 1989, J. Phys. A **22**, L699.
Salamon, M. B., and Y. Yeshurun, 1987, Phys. Rev. B **36**, 5643.
Saleur, H., and B. Derrida, 1985, J. Phys. (Paris) **46**, 1043.
Sapoval, B., 1990, *Les Fractals* (Editions Aditech, Paris).
Sarychev, A. K., A. P. Vinogradoff, and A. M. Karimov, 1985, J. Phys. C **18**, L105.
Schaefer, D. W., C. J. Brinker, D. Richter, B. Farago, and B. Frick, 1990, Phys. Rev. Lett. **64**, 2316.
Schaefer, D. W., and K. D. Keefer, 1984, Phys. Rev. Lett. **53**, 1383.
Schaefer, D. W., and K. D. Keefer, 1986, Phys. Rev. Lett. **56**, 2199.
Schaefer, D. W., D. Richter, B. Farago, C. J. Brinker, C. S. Ashley, B. J. Olivier, and P. Seeger, 1990, in *Neutron Scattering for Materials Science,* edited by S. M. Shapiro, S. C. Moss, and J. D. Jørgensen (Materials Research Society, Pittsburgh), p. 355.
Schober, H. R., and B. B. Laird, 1991, Phys. Rev. B **44**, 6746.
Schreiber, M., and H. Grussbach, 1991, Phys. Rev. Lett. **67**, 607.
Schreiber, M., and H. Grussbach, 1992, Phys. Rev. Lett. **68**, 2857.
Schwarzer, S., J. Lee, A. Bunde, S. Havlin, and H. E. Stanley, 1990, Phys. Rev. Lett. **65**, 603.
Seaton, N. A., and E. D. Glandt, 1987, J. Phys. A **20**, 3029.
Senning, B., P. Erhart, P. Martinoli, R. Meyer, and F. Waldner, 1991, Physica C **185-189**, 2701.
Shante, V. K. S., and S. Kirkpatrick, 1971, Adv. Phys. **20**, 325.
Shender, E. F., 1976a, J. Phys. C **9**, L309.
Shender, E. F., 1976b, Zh. Eksp. Teor. Fiz. **70**, 2251 [Sov. Phys. JETP **43**, 1174 (1976)].
Shender, E. F., 1978, Zh. Eksp. Teor. Fiz. **75**, 352 [Sov. Phys. JETP **48**, 175 (1978)].
Sheng, P., and M. Zhou, 1991, Science **253**, 539.
Shklovskii, B. I., and A. L. Efros, 1984, *Electronic Properties of Doped Semiconductors* (Springer-Verlag, Berlin).

Shrivastava, K. N., 1986, Phys. Status Solidi B **138**, 699.
Shrivastava, K. N., 1989a, Phys. Status Solidi B **153**, 547.
Shrivastava, K. N., 1989b, Solid State Commun. **69**, 301.
Simons, S., 1964, Proc. Phys. Soc. London **83**, 749.
Sivan, U., R. Blumenfeld, Y. Meir, and O. Entin-Wohlman, 1988, Europhys. Lett. **7**, 249.
Skal, A. S., and B. I. Shklovskii, 1974, Fiz. Tekh. Poluprovodn. **8**, 1586 [Sov. Phys. Semicond. **8**, 1029 (1975)].
Sleator, T., A. Bernasconi, D. Posselt, J. K. Kjems, and H. R. Ott, 1991, Phys. Rev. Lett. **66**, 1070.
Sofo, J., J. Lorenzana, and E. N. Martinez, 1987, Phys. Rev. B **36**, 3960.
Sokolov, I. M., 1986, Usp. Fiz. Nauk **150**, 221 [Sov. Phys. Usp. **29**, 924 (1986)].
Song, Yi, Taw Won Noh, Sung-Ik Lee, and J. R. Gaines, 1986, Phys. Rev. B **33**, 904.
Southern, B. W., and A. R. Douchant, 1985, Phys. Rev. Lett. **55**, 966.
Stanley, H. E., 1977, J. Phys. A **10**, L211.
Stanley, H. E., 1984, J. Stat. Phys. **36**, 843.
Stanley, H. E., and A. Coniglio, 1983, in *Percolation, Structure and Process,* edited by G. Deutscher, J. Adler, and R. Zallen (Hilger, Bristol); Ann. Isr. Phys. Soc. **5**, 101.
Stanley, H. E., and N. Ostrowsky, 1986, Eds., *On Growth and Form: Fractal and Non-Fractal Patterns in Physics,* NATO ASI Series E, No. 100 (Martinus Nijhoff, Dordrecht).
Stapleton, H. J., J. P. Allen, C. P. Flynn, D. G. Stinson, and S. R. Kurtz, 1980, Phys. Rev. Lett. **45**, 1456.
Stapleton, H. J., J. S. Helman, A. Coniglio, and C. Tsallis, 1985, Phys. Rev. Lett. **54**, 1734.
Stauffer, D., 1979, Phys. Rep. **54**, 1.
Stauffer, D., 1985, *Introduction to Percolation Theory* (Taylor&Francis, London/Philadelphia).
Stauffer, D., and A. Aharony, 1992, *Introduction to Percolation Theory,* 2nd ed. (Taylor&Francis, London/Philadelphia).
Stinchcombe, R. B., 1989, Proc. R. Soc. London Ser. A **423**, 17.
Stinchcombe, R. B., and C. K. Harris, 1983, J. Phys. A **16**, 4083.
Stinchcombe, R. B., and I. R. Pimentel, 1988, J. Phys. A **21**, L807.
Stockmayer, W. H., 1943, J. Chem. Phys. **11**, 45.
Stoll, E., and E. Courtens, 1990, Z. Phys. B **81**, 1.
Stoll, E., M. Kolb, and E. Courtens, 1992, Phys. Rev. Lett. **68**, 2472.
Strenski, P. N., R. M. Bradley, and J. M. Debierre, 1991, Phys. Rev. Lett. **66**, 133.
Sykes, M. F., and J. W. Essam, 1963, Phys. Rev. Lett. **10**, 3.
Sykes, M. F., and J. W. Essam, 1964, J. Math. Phys. **5**, 1117.
Sykes, M. F., D. S. Gaunt, and M. Glen, 1976a, J. Phys. A **9**, 725.
Sykes, M. F., D. S. Gaunt, and M. Glen, 1976b, J. Phys. A **9**, 1705.
Sykes, M. F., and M. K. Wilkinson, 1986, J. Phys. A **19**, 3415.
Tahir-Kheli, R. A., 1972a, Phys. Rev. B **6**, 2808.
Tahir-Kheli, R. A., 1972b, Phys. Rev. B **6**, 2826.
Takahashi, M., and H. Ikeda, 1993, Phys. Rev. B **47**, 9132.
Takayasu, H., 1990, *Fractals in Physical Sciences* (Manchester University, Manchester).
Takayasu, M., and H. Takayasu, 1988, Phys. Lett. A **128**, 45.
Teixeira, J., 1986, in *On Growth and Form: Fractal and Non-Fractal Patterns in Physics,* NATO ASI Series E, No. 100, edited by H. E. Stanley and N. Ostrowsky (Martinus Nijhoff, Dordrecht), p. 145.
Terao, T., K. Yakubo, and T. Nakayama, 1992, J. Phys. Soc. Jpn. **61**, 2173.
Terao, T., K. Yakubo, and T. Nakayama, 1994, Phys. Rev. B **49**, 12 281.
Thorpe, M. F., and R. Alben, 1976, J. Phys. C **9**, 2555.
Thouless, D. J., 1974, Phys. Rep. **13**, 93.
Thouless, D. J., 1979, in *Ill-Condensed Matter,* edited by R. Balian, R. Maynard, and G. Toulouse (North-Holland, Amsterdam), p. 1.
Tielburger, D., R. Merz, R. Ehrenfels, and S. Hunklinger, 1992, Phys. Rev. B **45**, 2750.
Tsujimi, Y., E. Courtens, J. Pelous, and R. Vacher, 1988, Phys. Rev. Lett. **60**, 2757.
Tua, P. F., and S. J. Putterman, 1986, Phys. Rev. B **33**, 2855.
Tua, P. F., S. J. Putterman, and R. Orbach, 1983, Phys. Lett. **98A**, 357.
Tyc, S., 1988, Phys. Rev. Lett. **61**, 2500.
Uemura, Y. J., and R. J. Birgeneau, 1986, Phys. Rev. Lett. **57**, 1947.
Uemura, Y. J., and R. J. Birgeneau, 1987, Phys. Rev. B **36**, 7024.
Vacher, R., and E. Courtens, 1989a, Phys. Scr. T **29**, 239.
Vacher, R., and E. Courtens, 1989b, IEEE 1989 Ultrasonics Symposium Proceedings, **1248**, 1237.
Vacher, R., E. Courtens, G. Coddens, A. Heidemann, Y. Tsujimi, J. Pelous, and M. Foret, 1990, Phys. Rev. Lett. **65**, 1008.
Vacher, R., E. Courtens, and J. Pelous, 1990, La Recherche **21**, 426.
Vacher, R., E. Courtens, J. Pelous, G. Coddens, and T. Woignier, 1989, Phys. Rev. B **39**, 7384.
Vacher, R., E. Courtens, E. Stoll, M. Boffgen, and H. Rothuizen, 1991, J. Phys. Condens. Matter **3**, 653.
Vacher, R., T. Woignier, J. Pelous, G. Coddens, and E. Courtens, 1989, Europhys. Lett. **8**, 161.
Vacher, R., T. Woignier, J. Pelous, and E. Courtens, 1988, Phys. Rev. B **37**, 6500.
Vacher, R., T. Woignier, J. Phalippou, J. Pelous, and E. Courtens, 1988, J. Non-Cryst. Solids **106**, 161.
Vacher, R., T. Woignier, J. Phalippou, J. Pelous, and E. Courtens, 1989, in *Proceedings of the 2nd International Conference on Aerogels;* Rev. Phys. Appl. **24-C4**, 127.
van der Putten, D., J. T. Moonen, H. B. Brom, J. C. M. Brooken-Zijp, and M. A. J. Michels, 1992, Phys. Rev. Lett. **69**, 494.
Vicsek, T., 1989, *Fractal Growth Phenomena* (World Scientific, Singapore).
Wada, K., N. Watanabe, and T. Uchida, 1991, J. Phys. Soc. Jpn. **60**, 3289.
Wagner, N., and I. Balberg, 1987, J. Stat. Phys. **49**, 369.
Wang, J., and T. C. Lubensky, 1986, Phys. Rev. B **33**, 4998.
Wang, Z., and C. Gong, 1989, Commun. Theor. Phys. (China) **11**, 225.
Watson, B. P., and P. Leath, 1974, Phys. Rev. B **9**, 1719.
Webman, I., and G. S. Grest, 1985, Phys. Rev. B **31**, 1689.
Webman, I., and Y. Kantor, 1984, in *Kinetics of Aggregation and Gelation,* Proceedings of the International Topical Conference on Kinetics of Aggregation and Gelation, April, 1984, Athens, Georgia, U.S.A., edited by F. Family and D. Landau (North-Holland, New York), p. 133.
Wegner, F. J., 1980, Z. Phys. B **36**, 209.
Williams, M. L., and H. J. Maris, 1985, Phys. Rev. B **31**, 4508.
Wodzki, R., 1986, Eur. Polym. J. **22**, 845.
Woignier, T., J. Pelous, J. Phalippou, R. Vacher, and E. Courtens, 1987, J. Non-Cryst. Solids **95&96**, 1197.

Woignier, T., J. Phalippou, R. Vacher, J. Pelous, and E. Courtens, 1990, J. Non-Cryst. Solids **121**, 198.
Wong, A. P. Y., and M. H. W. Chan, 1990, Phys. Rev. Lett. **65**, 2567.
Wong, G. K. S., P. A. Crowell, H. A. Cho, and J. D. Reppy, 1990, Phys. Rev. Lett. **65**, 2410.
Wu, J., E. Guyon, A. Palevski, S. Roux, and I. Rudnick, 1987, C. R. Acad. Sci. **305**, 323.
Xhonneux, P., E. Courtens, J. Pelous, and R. Vacher, 1989, Europhys. Lett. **10**, 733.
Yakubo, K., E. Courtens, and T. Nakayama, 1990, Phys. Rev. B **42**, 1078.
Yakubo, K., and T. Nakayama, 1987a, Phys. Rev. B **36**, 8933.
Yakubo, K., and T. Nakayama, 1987b, Jpn. J. Appl. Phys. Suppl. **26-3**, 883.
Yakubo, K., and T. Nakayama, 1989a, Phys. Rev. B **40**, 517.
Yakubo, K., and T. Nakayama, 1989b, J. Phys. Soc. Jpn. **58**, 1504.
Yakubo, K., and T. Nakayama, 1989c, in *Cooperative Dynamics in Complex Physical Systems,* edited by H. Takayama (Springer-Verlag, Berlin), p. 217.
Yakubo, K., and T. Nakayama, 1990, Proc. Indian Acad. Sci. **102**, 581.
Yakubo, K., T. Nakayama, and H. J. Maris, 1991, J. Phys. Soc. Jpn. **60**, 3249.
Yakubo, K., K. Takasugi, and T. Nakayama, 1990, J. Phys. Soc. Jpn. **59**, 1909.
Yakubo, K., T. Terao, and T. Nakayama, 1993, J. Phys. Soc. Jpn. **62**, 2196.
Yakubo, K., T. Terao, and T. Nakayama, 1994, J. Phys. Soc. Jpn., in press.
Yeshurun, Y., and M. B. Salamon, 1987, Philos. Mag. B **56**, 957.
Yu, F., A. M. Goldman, and R. Bojko, 1990, Physica B **165&166**, 1639.
Yu, F., A. M. Goldman, R. Bojko, C. M. Soukoulis, L. Qiming, and G. S. Grest, 1990, Phys. Rev. B **42**, 10 536.
Yu, K.-W., 1984, Phys. Rev. B **29**, 4065.
Yu, K.-W., 1986, Phys. Rev. B **33**, 7748.
Yu, K.-W., and R. Orbach, 1984, Phys. Rev. B **30**, 2760.
Yugami, H., S. Matsuo, and M. Ishigame, 1992, Solid State Ionics **53-56**, 1264.
Yup Kim, 1988, J. Korean Phys. Soc. **21**, 332.
Zabolitzky, J. G., 1984, Phys. Rev. B **30**, 4077.
Zallen, R., 1983, *The Physics of Amorphous Solids* (Wiley, New York).
Zeller, R. C., and R. O. Pohl, 1971, Phys. Rev. B **4**, 2029.
Zemlyanov, M. G., V. K. Malinovskiĭ, V. N. Novikov, P. P. Parshin, and A. P. Sokolov, 1992, Zh. Eksp. Teor. Fiz. **101**, 284 [Sov. Phys. JETP **74**, 151 (1992)].
Ziff, R. M., 1992, Phys. Rev. Lett. **69**, 2670.
Ziman, T. A. L., 1979, J. Phys. C **12**, 2645.
Ziman, T. A. L., 1985, in *Scaling Phenomena in Disordered Systems,* NATO ASI Series B, Vol. 133, edited by R. Pynn and T. Riste (Plenum, New York), p. 361.